The University of Sheffield

Handover Control Parameters Optimisation in LTE Networks

By

Mr. Baoling Zhang

Department of Electronic and Electrical Engineering

This thesis is submitted to the University of Sheffield for the degree of Doctor of Philosophy, April 2018

UNIVERSITY OF SHEFFIELD

RESEARCH AND INNOVATION SERVICES

Abstract

In the past few years, the demand for data traffic has increased explosively, in order to meet such a demand in traffic volume, small cell networks have been introduced. With the wide adoption of small cells, the densification of small cell deployment has become an unavoidable trend. However, such density in small cell deployment brings various problems for the network operators, among which the handover issue is one of the most critical. In order to tackle the handover problem in heterogeneous networks (HetNets), this thesis was mainly concerned with the system-level handover control parameters optimisation.

The research work of this thesis is divided into three parts. The first part introduced two self-optimisation handover algorithms, which aimed to optimise the average system performance in terms of signal to interference and noise ratio (SINR), energy efficiency, and ping-pong handover ratio. Through a simulation of a HetNets scenario, the proposed two handover optimisation algorithms significantly enhanced the system performance. The second part of the research was a performance evaluation of handover control parameters combined with cell range expansion (CRE), through the modelling of a HetNets handover scenario in a Markov chain process (MCP). By establishing the mathematical method to model the relationship of the hysteresis margin (HM), CRE, and time-to-trigger (TTT), the coordination of these three parameters was achieved, which further optimised the network performance. The last part of this thesis proposed an adaptive HM and TTT selection scheme based on the individual user equipment's (UE's) mobility states. Based on the target of minimising unnecessary handover probability and maintaining a certain radio-link-

failure (RLF) ratio, a pair of appropriate handover control parameters were assigned for individual pieces of UE.

Acknowledgements

Firstly, I would like to thank my family, my parents Mr. Jinzhang Gao and Ms. Lili Jia, my wife Dr. Lukai Zheng, my parents-in-law Mr. Jie Zheng and Ms. Shuangfeng Li, without your love and support, I wouldn't be who I am today.

I would like to take this special opportunity to appreciate my supervisor Prof. Jie Zhang, for his encouragement, patient guidance and respected advices in my reserch work in the past four years. Without his continuous guidance I wouldn't finish my PhD research. I would also thank my second supervisor Dr. Xiaoli Chu for her kindness support in my entire study.

I would like to thank all my colleagues, Mr. Qi Hong, Mr. Hao Li, Mr. Weijie Qi, Mr. Haonan Hu, Ms. Hui Zheng, Mr. Kan Lin, Mr. Yuan Gao and Mr. Bozhong Chen, for all the help in my research work, for the working time we spend together, for all the fun that we had in the past four years.

I would like to thank my friends, Dr. Nan E, Dr. Tian Feng, Mr. Shuaida Ji, for the countless happy memories in my leisure time.

Last but not least, I would like to thank all the friends, colleagues and families, for the support, accompany in the past four years.

List of Publications

[1] **B. Zhang,** W. Qi, and J. Zhang. "An energy efficiency and ping-pong handover ratio optimization in two-tier heterogeneous networks." *IEEE, Computing and Communication Workshop and Conference*, 2018, pp.532-536.

[2] **B. Zhang,** W. Qi, and J. Zhang, "A Markov Based Performance Analysis of Handover and Load Balancing in HetNets," *Int. J. Commun. Netw. Syst. Sci*., vol. 10, no. 10, 2017,pp. 223.

[3] H. Hu, **B. Zhang**, Q. Hong, X. Chu, and J. Zhang, "Coverage Analysis of Reduced Power Subframes Applied in Heterogeneous Networks with Subframe Misalignment Interference," *IEEE Wireless Communications Letters*, 2018. pp.99

[4] W. Qi, **B. Zhang**, B. Chen, and J. Zhang, "A user-based K-means clustering offloading algorithm for heterogeneous network," *IEEE, Computing and Communication Workshop and Conference*, 2018, pp. 307–312.

[5] Q. Hong, J. Zhang, H. Zheng, H. Li, H. Hu, **B. Zhang**, Z. Lai, and J. Zhang, "The Impact of Antenna Height on 3D Channel: A Ray Launching Based Analysis," *Electronics*, vol. 7, no. 1, 2018.

Content

List of Figure

List of Figure

List of Figure

List of Table

Abbreviations

AP -Access Points

BB -Baseband

BBC -Break Before Connect

CBB-Connect Before Break

CIO -Cell Individual Offset

CRE -Cell Range Expansion

C-RAN -Cloud RAN

CDF -Cumulative Distribution Function

C_HI -Current Timeslot Handover Indicator

CoMP -Coordinated Multiple Points

CSG -Closed Subscriber Group

DC -Direct Current

DSL -Digital Subscriber Line

DTMC -Discrete Time Markov Chain

eNB -Evolved Node B

erf -Error Function

ERG -Energy Reduction Gain

ECR -Energy Consumption Ratio

ECG -Energy Consumption Gain

E-UTRAN -Evolved-Universal Terrestrial Radio Access Network

EPC -Evolved Packet Core

FPGA -Field Programmable Gate Array

GPS- Global Positioning System

Abbreviation

HetNets -Heterogeneous Networks

HeNB -Home e Node B

HO -Handover

HOF -Handover Failure

HI-Handover Indicator

HM-Hysteresis Margin

HOPP -Ping-pong Handover Ratio

HOR-Handover Rate

HPI -Handover Performance Indicator

HPP -Handover Performance Parameter

HRPD -High Rate Packet Data

IMT -International Mobile Telecommunications

IRAT –Inter Radio Access Technology

LGW -Local Gateway

LTE –Long Term Evolution

LTE-A –Long Term Evolution Advanced

MCP -Markov Chain Process

MME -Mobility Management Entity

MP -Microprocessor

O&M -Operations and Maintenance

PA -Power Amplifier

PCI -Personal Cell ID

PLMN -Public Land Mobile Network

QoS -Quality of Service

QoE -Quality of Experience

Abbreviation

RAN -Radio Access Network

RF-Radio Frequency

RNC -Radio Network Controller

RLF –Radio Link Failure

RSS -Reference Signal Strength

RSRP -Reference Signal Receiving Power

RSRQ -Reference Signal Receiving Quality

SCN -Small Cell Networks

SGW -Serving Gateway

SINR -Signal to Interference plus Noise Ratio

TTI -Transmission Time Interval

TTT –Time to Trigger

UE -User Equipment

WCDMA -Wideband Code Division Multiple Access

3D-Three Dimensional

3GPP -the third Generation Partnerships

Chapter 1. Introduction

Overview

In this chapter, first, the background knowledge of this thesis is introduced. The explosion in data traffic demand has led to a densification in cell deployment which caused various problems, and, as handover is one of the most critical issues, the motivation of this thesis is to investigate the optimisation of handover control parameters. Next, the main objectives of this thesis will be proposed, followed by the structure and main contribution of the thesis.

1.1. Background

The first mobile phone was manufactured by Motorola in 1973 [1], and, after several decades of developing communication technologies, mobile phones have become an indispensable part of our lives. The mobile networks not only shorten the distance between people, but also makes people's lives colourful. The function diversification of mobile terminals is no longer just designed for voice services, but also for different data services; for example, mobile games and live video steaming. According to [2], the mobile data traffic has grown dramatically in the past few years; the data traffic in 2016 is 18 times that of 2011, and in 2021 it is expected to have a seven-fold growth compared with 2016, which is a 128-fold increase in only ten years. Therefore, major enhancements are expected in the capacity of future networks to reasonably accommodate the increasing traffic volume[3]. In order to support the rapidly increasing data demands, the network operators are also dedicated to updating the network from 2G to 3G, then 4G, and then 5G. In order to meet the expected traffic demands and relieve the pressure on macro cells, small cell networks have been introduced.

The adoption of small cells succeeded in solving the conflict between limited radio resources and the data traffic demands [4], [5]. In the Cisco VNI report of 2017 [2], 60% of the data traffic has been successfully offloaded through the small cells or Wi-Fi. The system's total capacity and user quality of service (QoS) has been significantly promoted via the employment of small-sized base stations; the deployment of small cells will improve the existing network capacity as these low-power base stations overlap the existing macrocell networks, such a multi-tier network structure is known as heterogeneous networks (HetNets). The HetNets

scenario is an important concept that has been widely used in the Long-Term Evolution Advanced (LTE-A) networks. Small cells are normally understood to be microcells, picocells, or femtocells. The range of small cells can be from ten to several dozen meters. With the interference issues being well addressed, the number of small cells can even linearly increase the network capacity. As a trend, the densification of small cells deployment will become popular in future network planning.

1.2. Motivation

The growing density of cell numbers and the shortening in the cell radius has created various communications problems, among which the handover issue is one of the most challenging issues. In a traditional network, the main function of handover is to maintain the connected user equipment's (UE's) quality without interruption, which aims to guarantee the connectivity of the service; this circumstance is triggered by the problem that a single base station cannot provide good coverage in its whole service area [6]. With the introduction of overlaid HetNets, the function of handover has evolved, from not only maintaining connectivity but also enhancing the entire network's performance and quality of service (QoS). Furthermore, due to the small coverage and low transmission power, the handover procedure in HetNets is much more complicated and needs to be more intelligent.

Thus, this thesis mainly focuses on the optimisation of the system-level handover control parameters. Interference management, system energy efficiency, and frequent handovers are hot issues under the premise of small cell deployment. Taking these constraints into consideration, two self-optimisation algorithms based on dynamically changing handover control parameters have been proposed and

investigated. In order to simplify the model for the HetNets scenario and evaluate the handover performance affected by the control parameters combined with cell range expansion (CRE), the Markov chain process (MCP) is utilized. To resolve the inappropriate arrangement of handover control parameters for UE, a selection scheme for adaptive control parameters was studied, based on individual UE's mobility states.

1.3. Objective of the Thesis

As a result of the motivation for this study, the main objectives of this thesis can be summarized into the following points:

- To review the state of the art of small cell networks; handover procedures, especially the handover procedure in LTE network; handover control parameters; and handover decision algorithms, and to discuss and evaluate the status of current research.
- To develop new handover decision algorithms aimed at optimizing the average SINR and ping-pong handover ratio.
- To implement system energy efficiency and optimisation of the ping-pong handover ratio through dynamically adjusting the handover control parameters.
- To map the HetNets scenario into an MCP, in order to represent the handover process in a statistical method and investigate the handover performance affected by the hysteresis margin (HM) and CRE.
- To create a new selection scheme for handover control parameters, such that all UEs in the network no longer share the same handover parameters; the selection of new parameters should be based on individual UE's mobility states.

1.4. Main Contributions and Structure of the Thesis

The structure of this thesis is organized as follows:

- **Chapter 2: Literature review**

In chapter 2, first, basic knowledge of small cell networks and detailed handover procedures are introduced, followed by the introduction of two important handover control parameters. Moreover, five different categories of handover decision algorithms are classified, and a literature review of the corresponding research is summarized and evaluated.

- **Chapter 3: Two self-optimisation handover decision algorithms**

In chapter 3, two mechanisms for handover self-optimisation are introduced. The first self-optimisation mechanism is based on the system's average SINR and ping-pong handover ratio. Through detecting system performance in every time slot, the system will automatically optimise the selection of handover control parameters. Similarly, the second self-optimisation mechanism is based on the feedback from the system's energy efficiency states and ping-pong handover ratio.

Contributions: 1) The interference-aware handover decision algorithm is investigated and implemented through SINR control in HetNets, as interference is one of the key issues of concern in the HetNets scenario. 2) The energy-efficiency-aware algorithm is currently lacking in the handover decision algorithm, especially taking UE power consumption into consideration; most handover decision algorithms only consider from the operators' perspective, but the UE actually is an important part that consumes power over the whole network.

- **Chapter 4: An MCP based performance analysis of handover and load balancing in HetNets**

In chapter 4, an MCP-based handover performance analysis is proposed. The main idea is to analyze the impact of HM and CRE through modelling HetNets in an MCP. Through mapping the HetNets handover process in an MCP, all the phases of the handover can be calculated and analyzed through a probability calculation, so that further predictions and simulations can be realized. By establishing the mathematical method to model the relationships among HM, CRE, and time-to-trigger (TTT) in HetNets, the coordination of these three important parameters is achieved to obtain system optimisation.

Contributions: 1) How handover performance is affected by both HM and CRE is modelled and analyzed. 2) The HetNets handover scenario into MCP is mapped to statistically analyze handover performance. 3) The total network throughput is optimised by the coordination through HM and CRE.

- **Chapter 5: Adaptive HM and TTT selection scheme**

In chapter 5, an adaptive HM and TTT selection scheme is proposed. The main idea of this chapter is to assign a pair of the most suitable handover control parameters for arbitrary UE inside the network. Based on the target of minimising unnecessary handovers while maintaining ideal cell coverage, an adaptive HM selection scheme is proposed. Through detecting the UE distance to the serving cell, the adaptive HM is selected based on the user-location information. As any UE mobility model consists of two parameters, location and velocity, based on the UE velocity status, the other handover control parameter TTT can be determined. While ensuring a certain radio-link-failure (RLF) threshold, the maximum TTT is selected.

After deciding the criteria in adaptive HM and TTT, a joint self-optimisation mechanism is proposed for the optimisation of system-level handover performance.

Contributions: 1) An adaptive HM selection scheme is proposed based on the UE location in the network. 2) An adaptive TTT selection scheme is proposed based on the UE velocity. 3) An entirely new selection scheme for handover control parameters is created because in the traditional network the HM and TTT assigned for all UEs are the same value, but in this work an arbitrary UE is assigned along with the most appropriate individual HM and TTT. 4) A new self-optimisation mechanism is proposed.

- **Chapter 6: Conclusion and future works**

In this chapter, the conclusion of this thesis is presented, followed by research directions for future works.

Chapter 2. Literature Review

Overview

This chapter firstly provides a review of small cells in HetNets and the fundamental concept of a detailed handover procedure. Secondly, To explain the handover mechanism more specifically, two handover control parameters, HM and TTT, are presented. The third section provides an overview of the handover decision algorithms with respect to received-signal-strength-based handover, speed-based handover, cost-function-based handover, interference-based handover, and energy-efficiency-based handover decision algorithms.

2.1. Review of Small Cell Networks

Nearly two thirds of calls and 90% of data services happen indoors. This has led to the issue of how to provide high quality voice, video, and high-speed data services [7]. Small cells are expected to be one of the most important technologies in 5G and will help satisfy the traffic demand through spatial reuse [8]. Although there has been a rapid increase in mobile data traffic, in the short term, a large proportion of indoor mobile data traffic can be offloaded from cellular networks through the adoption of small cells. As we all know, the reduction of cell size is the most effective and easiest way to improve system capacity. Small cell networks (SCN) are a new network design concept that can provide different cost- and energy-efficient solutions to cope with the forecast traffic growth [9].

2.1.1. Review of Small Cells

Small cells refer to low power radio access nodes that can operate in either a licensed or unlicensed spectrum. As mentioned previously, the types of small cells can be divided into femtocell, picocell, and microcell depending on the cell's range. In [10], the third-generation partnerships (3GPP) introduced a new small range and low power base station that is known as Home eNB (HeNB). This small base station is used for providing indoor and outdoor broadband services [7], and in users' offices and houses they act like a common Wi-Fi access point that connects to the operator network through a digital subscriber line (DSL).

Through small cell deployment, several benefits can be achieved. Firstly, network capacity can be increased. According to [11], an effective way to enhance the capacity of a single wireless link is to reduce the distance between the transmitter and the receiver, as in the rationale of LTE small cells. In this context, it is also possible to

efficiently offload from macrocells since the small cells are expected to provide a relevant quota of traffic. Secondly, from an economic perspective, as an operator can accurately identify the traffic generated/received in each small cell, it can offer personalized fees and discounts that would be very attractive to consumers. The support of small cell is an integral part of existing International Mobile Telecommunications (IMT) advanced standards and would play an increasingly important role in their wider usage on a broad scale.

With the deployment of small cells, several problems inevitably appear. Firstly, with the deployment of a large number and high density of small cells, this is unlikely to be scalable to the broadcasting of small cell information in the network. This increases the network signalling overhead. Secondly, compared with macrocells, the neighbouring cell list of the small cell is dynamic as the small cell is dynamically powered on or off at any location depending on consumers' needs. Thirdly, variant access methods are used in small cells that result in different authorization. Finally, user/operator preferences can lead to different priorities for the utilization of small cells [12].

Handover refers to the transfer of a UE's connection from one radio channel to another (this can be within the same cell or between different cells) while maintaining QoS [13]. In a conventional network, UE typically uses the same set of handover parameters (e.g. HM and TTT) through the network. In a HetNet, however, using the same set of parameters may degrade mobility performance. Moreover, high-mobility macrocell UE may run deep into small cell coverage areas before the TTT timer is expired for this handover, thus incurring handover failures due to degradation in signal to interference plus noise ratio (SINR)[14].

In [15], handover from a non-closed subscriber group (CSG) cell to an allowed CSG cell is not within the scope of Release 8, but this changed in 3GPP Release 9 [16]. Release 9 proposed three new aspects of the UE handover to an eNB/HeNB compared to the normal handover procedure: proximity estimation, PSC/PCI (personal cell ID) confusion, and access control. More changes were made in Release 12 [17], where the public land mobile network (PLMN) report was added as the fourth aspect that is different from normal handover procedure.

In [18], the specification lists the basic mobility functionality (including access control, cell selection/ reselection) for the support to HeNB and HeNB. Whereas [15] covers the specification of the functions for UE that does not support CSG and UE that does supports CSG. It also covers Home NodeB specific requirements for operations and maintenance (O&M). Two critical modifications were made in terms of in-bound mobility and HeNB-to-HeNB mobility in Release 9 [8]. Furthermore, a new element, the local gateway (LGW), is proposed in the network structure [19].

In [7], we can find the benefits of small cell listed as follows:

1. Assuming that good isolation can be achieved, small cells can significantly improve the total network capacity by reusing radio spectrum indoors.
2. The demand for higher and higher data rates.
3. Small cells can provide effective power saving for UE.
4. Small cells are ‘greener’ than macrocells from the perspective of energy consumption.
5. Users will pay to install small cells, which indicates a new direction for operators when building or updating networks.

According to [9], the challenges of small cells can be summarized as follows:

1. Coverage and performance prediction: Dense and unplanned deployment of small cells in SCNs will result in unpredictable interference patterns and possibly patchy coverage.
2. Interference management: With public access, due to full frequency reuse and the increasing density of small cell deployments, the interference between small cells, as well as the interference between small cells and macrocells, dramatically increases and needs to be well addressed.
3. Mobility: Due to the range of small cells, it can be difficult to solve user mobility problems in SCNs.

2.1.2. Two-Tier Evolved-Universal Terrestrial Radio Access Network (E-UTRAN) Architecture

LTE is a new radio access technology that was proposed by the 3GPP. The aim of the LTE network is to provide a peak downlink rate of at least 100 Mbps and an uplink rate of at least 50 Mbps [20]. The main purpose of LTE is to improve the capacity, speed, and coverage of mobile networks [21]. The two main components of the LTE system are: 1) the air interface (i.e. the E-UTRAN), and 2) the packet switched core network, also known as the Evolved Packet Core (EPC).

The E-UTRAN consists of eNBs, which can provide the user plane and the control plane protocol terminations to the UE. Through the X2 interface, the eNBs can connect to each other and can also interconnect to the Evolved Packet Core (EPC) through the S1 interface. More specifically, the eNBs can communicate to the Mobility Management Entity (MME) by means of the S1-MME interface and to the SGW (Serving Gateway) via the S1-U interface.

As we can see from Figure 2-1, two of the EPC network entities are involved in supporting the HeNBs with respect to the SGW and the MME. The MME is used for the implementation of the functions of the core network signalling for system mobility management between 3GPP access networks, i.e. idle state mobility handling, tracking area list management, roaming, bearer control, security control, and authentication. Meanwhile, the SGW can provide the following functions: charging, accounting, packet routing, forwarding, and even mobility anchoring for inter and intra core network mobility management.

To introduce the small cells, the eNBs, HeNBs, and HeNB gateways (HeNB GW) are included inside the E-UTRAN architecture. The eNBs not only provide the UE with control plane protocols, they also support the modules for radio resource management, admission control, the scheduling and transmission of broadcast messages, and the measurement configuration for the mobility and routing of user plane data towards the SGW. The HeNBs support the same functions as those supported by eNBs, while the same procedures are applied between the HeNBs and the EPC. The function of the HeNB GW is to support a large number of HeNBs at the same level. The deployment of the HeNB GW is optional, but if it is deployed, it acts as an MME for the EPC, similar to an MME for the eNBs [22].

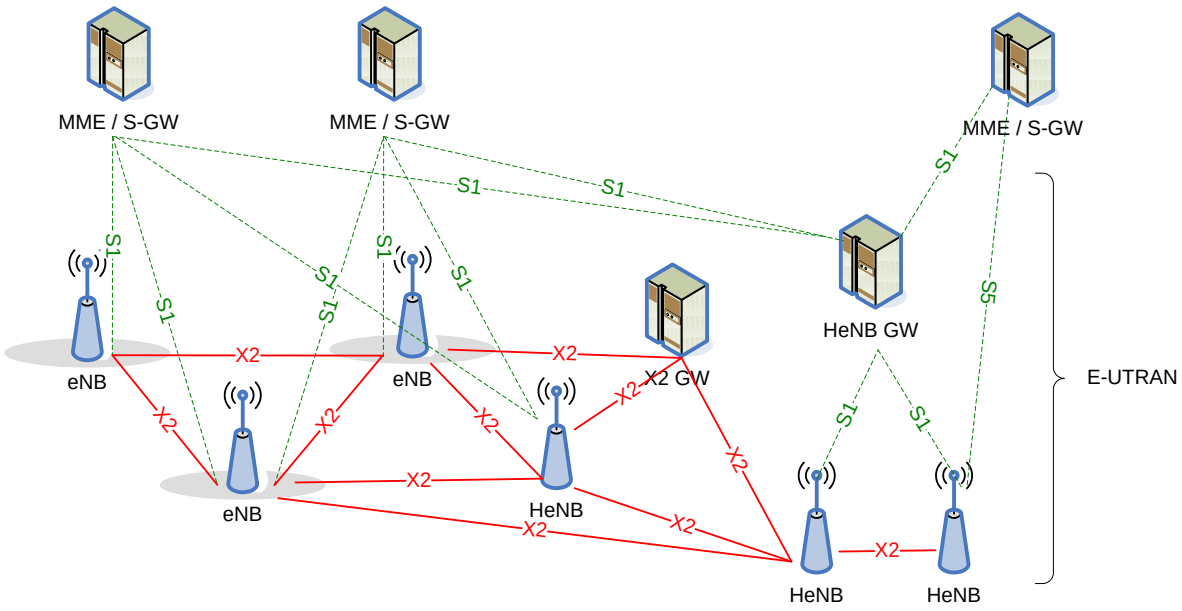

Figure 2-1 Overall E-UTRAN architecture with deployed HeNB GW and X2 GW [23]**.**

2.2. Review of Handover Procedures

Handovers can be divided into two categories: hard handovers, also known as break before connect (BBC), and soft handovers, also known as connect before break (CBB) [24]. In the following three subsections, soft and hard handovers and handovers in LTE are introduced.

2.2.1. Soft Handovers: Connect-Before-Break

A soft handover is a type of handover model where the radio links are added and abandoned in such a manner that the UE will always keep at least one radio link to the network [13]. Soft and softer handovers were introduced in WCDMA architecture. The centralized controller, which is called the radio network controller (RNC), is used to perform handover control for each UE in the architecture of WCDMA. It is possible for one piece of UE to connect to two or more cells or

different cell sectors during one data transmission session simultaneously [25]. A softer handover refers to the UE, which is connected from the same physical site. A soft handover is suitable for preventing voice call dropping, maintaining an active session, and resetting a packet session. However, the soft handover will result in more complicated signalling procedures and system architecture, , e.g. WCDMA networks.

2.2.2. Hard Handover: Break-Before-Connect

A hard handover refers to new radio links being established after all the old radio links in the UE are disconnected [26]. Hard handovers are widely used in traditional wireless communication systems. They require users to abandon the existing links with the current serving cell (the source cell) and establish a new connection to the target cell.

2.2.3. Handovers in LTE

A handover inside the LTE system can be summarized as three steps: measurement, handover decision, and handover execution (Figure 2-2). The measurement step is completed on the UE side with the UE needing to periodically report measurement ID, serving eNB measurement results (including Reference Signal Received Power (RSRP), Reference Signal Received Quality (RSRQ), path loss, etc.), and neighbouring eNBs measurement results (optional). eNBs control their measurements through the notification of measurement objects, cell lists, report modes, measurement metrics, measurement parameters, etc. When the measurement condition changes the eNB should notify the UE of the new measurement conditions. Table 2-1 shows the measurement report events. The events starting with A are used for intra-LTE systems and those starting with B are events that happen under IRAT (Inter-Radio Access Technology) conditions.

Table 2-1 Event entry conditions [27].

Event	Definition
A1	Serving cell better than threshold (can stop IF/IRAT measurement).
A2	Serving cell worse than threshold (can start IF/IRAT measurement).
A3	Neighbor cell better than serving cell + offset (used for handover).
A4	Neighbor cell better than threshold (Used for load balancing).
A5	Neighbor cell worse than threshold (used for load balancing).
A6	Neighbor cell better than secondary serving cell + offset.
B1	Neighbor cell better than threshold (used for IRAT).
B2	Serving cell worse than threshold (used for IRAT).

The handover decision and handover execution are based on the measurements, which include the relocation of the EPC node and the UE handover process. The relocation of the EPC also means the relocation of the MME and the SGW. The handover process is always initiated by the source eNB through the evaluation and control of the source eNB and UE measurement report results. The decision whether or not to make the handover will take the area restrictions of the UE into consideration. The reservation resource should be allocated by the target eNB after receiving the handover execution command. After the UE synchronizes to the target eNB, the network will release resources in the source eNB.

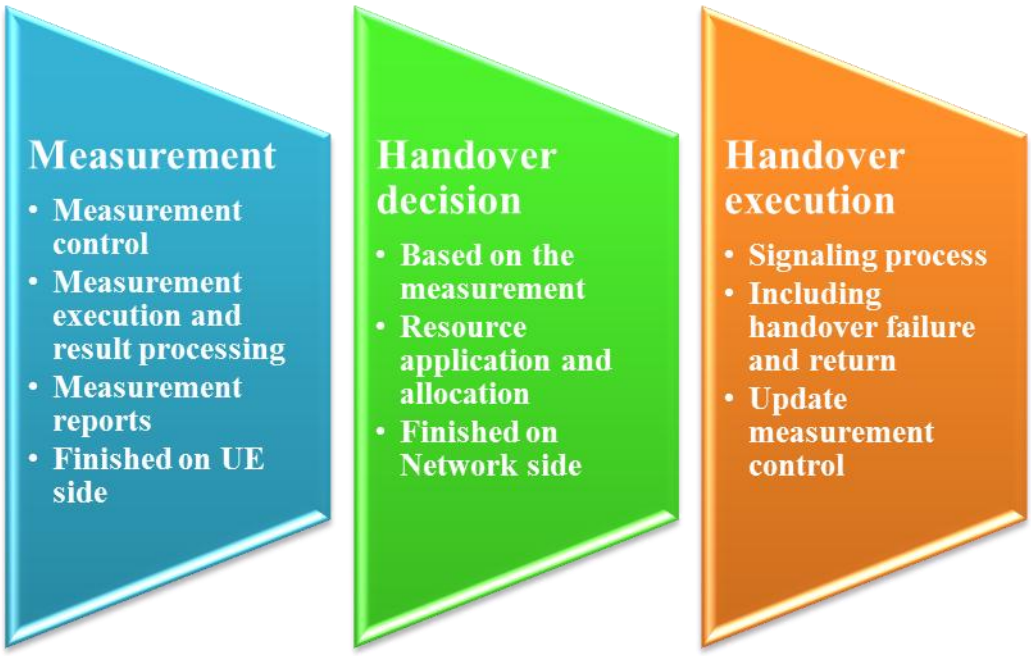

Figure 2-2 LTE handover.

When the UE is in active mode, there are two types of handover in LTE downlink: S1 and X2. Active mode refers to the UE transmitting or receiving data packets from the core networks. The X2 handover is typically used for network load balancing and interference prevention among eNBs, but if there is no X2 interface existing between two eNBs, or if the eNB is configured to perform a handover directly to a special target eNB through the S1 interface, the S1 handover will be triggered [28]. S1 handovers are normally performed for non-3GPP technologies, such as the CDMA2000/HRPD [29]. Table 2-2 shows the X2 handovers related to HeNBs that are allowed.

Table 2-2 X2-based handover support [23]**.**

Serving	Target	Notes
eNB or any HeNB	Open access HeNB	
eNB or any HeNB	Hybrid access HeNB	
Hybrid access HeNB or closed access HeNB	Closed access HeNB	Only applies for the same CSG ID and PLMN and

		if the UE is a member of the CSG cell.
Any HeNB	eNB	

In Table 2-2, we can see three different access control mechanisms. The first is open access HeNBs, which are normally deployed by the operators. All UEs can connect to the HeNBs for the offered data services. The second is the closed access HeNBs, which are normally deployed privately. These HeNBs are defined as the CSG cells and their access control is located in the GW. The last type is hybrid access HeNBs, which offer open access to all UE, but the subscribed UE gets priority over unsubscribed UE when utilizing the resources [30].

Three phases exist in the S1 and X2 handovers: preparation, execution, and completion [23]. During the preparation phase, measurement reports are sent to the serving eNB periodically by the UE [31], while the serving eNB will make the handover decision to determine which target eNB is suitable for the UE according to these reports. In addition to the measurement reports, other criteria are also considered before the handover control messages is sent to the target eNB. After receiving the handover control message from the serving eNB, the target eNB should prepare a buffer for the UE.

After completing the handover preparation phase, the handover execution phase starts. During this phase the serving eNB sends a handover command message to the UE to notify the UE that it is going to be forwarded to another eNB. Once the UE receives this message, the link between the serving eNB and the UE will be disconnected and a request for new connection establishment to the target eNB will be sent. The serving eNB will also send all data packets belonging to this UE to the target eNB simultaneously. The data packets are queued by the target eNB in the UE

buffer and are ready to be transmitted to the UE once the connection between the UE and the target eNB is successfully established. At the end of the execution phase, the UE sends a ‘handover complete’ message to the target eNB to confirm the handover is finished.

The final phase is the completion phase, which involves communication between the eNBs and the upper layers. These communications focus on the release of resources in the serving eNB and tell the upper layer to switch the following packets to the target eNB. As a result, the target eNB needs to notify the serving eNB to release the resources for the UE, and the MME needs to switch the path to the target eNB.

Figure 2-3 illustrates the detailed handover procedures in detail. The three handover phases with respect to handover preparation, handover execution, and handover completion are clearly displayed, and the handover procedures are divided into 18 steps. Detailed explanations can be found in [23], [32].

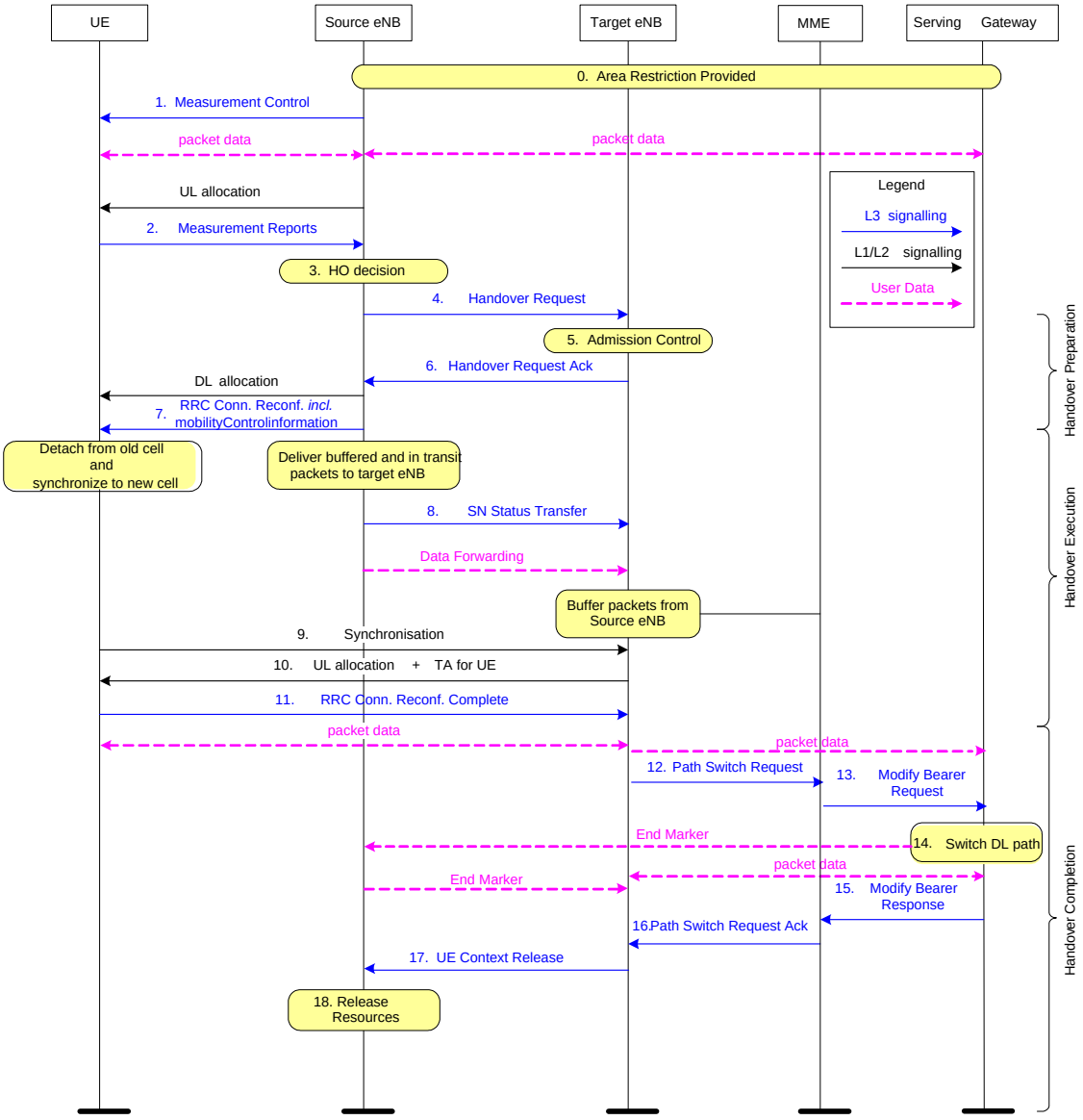

Figure 2-3 Intra-MME/Serving Gateway handover [23].

2.2.4. Handover Control Parameters

The LTE hard handover decision algorithm consists of two control parameters: HM and TTT. HM is a constant variable that represents the threshold of the difference in received signal strength between the serving and target base stations. TTT value is the time interval that is required for satisfying the HM conditions. A handover will be initiated if the two conditions are fulfilled: 1) if the RSS of a potential target cell is

greater than the RSS of the current serving cell plus the HM value, and 2) if condition 1 is satisfied for at least the time specified in the TTT parameter.

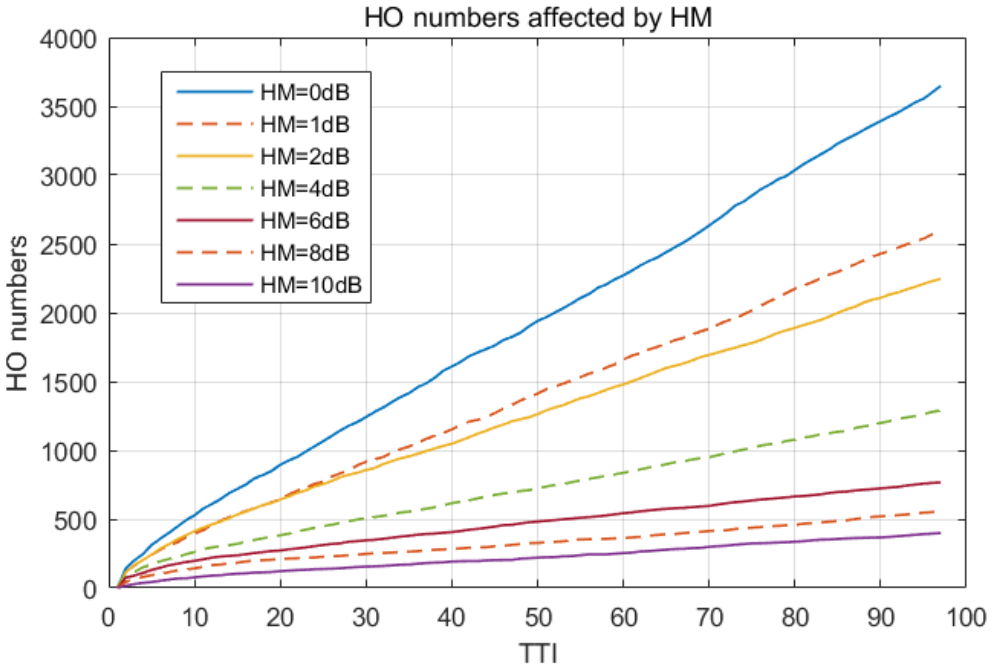

Figure 2-4 The handover variation trend according to different HM values.

Figure 2-4 shows the variation in handover numbers affected by different HM values and highlights the impact of HM on handover numbers. We did not choose the random UE moving model for this figure, but instead use the straight line moving model. As we can see from Figure 2-4, as the value of HM increases, the number of handovers decreases, e.g. when the HM is 0dB, over 3,600 handovers take place in the 100-transmission time interval (TTI). In contrast, when HM is 10dB, only 400 handovers happen in the same amount of time.

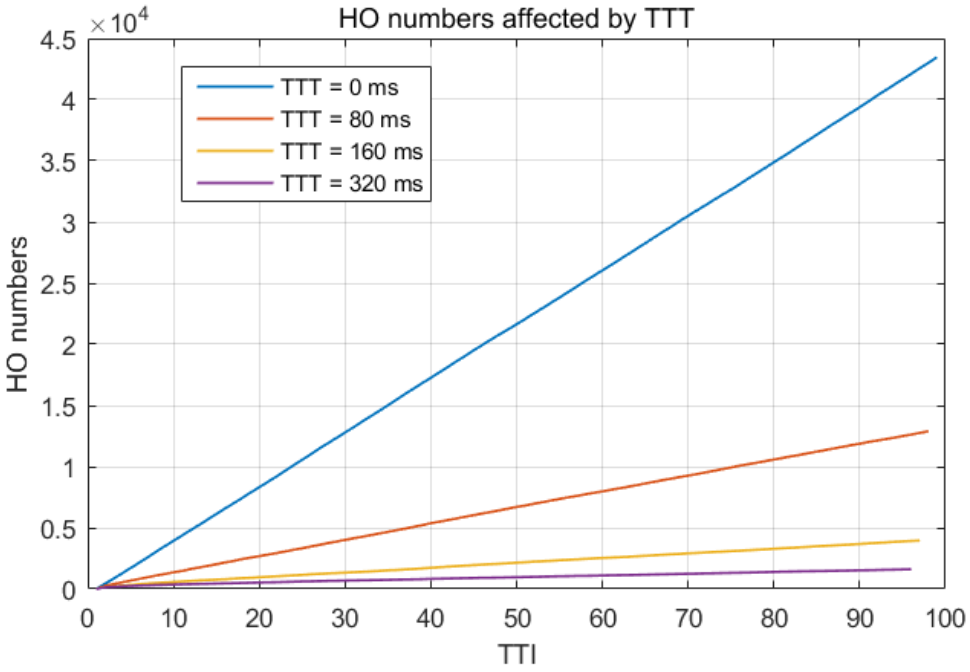

Figure 2-5 The handover variation trend according to different TTT values.

Figure 2-5 shows the number of handovers that happen in the 100 TTI and how this is affected by different selections of the TTT. Compared to the effect of HM, changing the TTT causes a much more severe reduction in handover numbers. When the TTT is set to 0ms, the handover will initiate whenever the RSS of the target cell exceeds that of the serving cell. If a 40ms period is added to the TTT, the number of handovers drops by more than 75%. As the TTT increases, the number of handovers decreases.

Various researches have been done by analysing handover performance in terms of HM and TTT. Work in [33] proposed a self optimisation mechanism based on the optimisation of handover parameter through the checking of network feedback. The system will automatically check the call drop ratio and ping-pong handover ratio in each optimisation step, through modification of HM and TTT, to dynamically control the network performance. However, the proposed algorithm is only tested in a

limited simulation scenario, in order to prove the advantages of this algorithm, it should be tested in a more general scenario.

A comprehensive analysis of handover control parameters was proposed in work [34]. The authors firstly analysed the sensitivity of HM and TTT under different cell loading circumstances, the result suggested that the HM is more efficient for the network performance controlling. Hence, secondly, a fuzzy logic adaptive HM selection scheme was proposed to optimise the system handover performance. The main reason that TTT was not suggested for this paper is caused by the network evaluation parameters selected by the authors. However, in the evaluation of handover quality, TTT is the main controller of ping-pong handover effect, if the TTT is ignored, a handover phase is incomplete. As a result, the combination of TTT and HM should both taken into consideration.

Through the handover performance evaluation in terms of radio link failure ratio and ping-pong handover ratio, work in [35] proposed a TTT selection scheme. In the condition of maintaining a certain radio link failure ratio, the optimal TTT value can be determined through curve fitting for UE with any speed. However, the same reason as above, the analyses of handover is suggested taken both HM and TTT into consideration, the second problem worth mentioning is the selection of TTT is unreliable as the detailed the curve fitting method is not introduced.

Theoretical analysis of handover failure and ping-pong handover ratio according to user velocity and TTT is introduced in detail in work [36], by taking HetNets into consideration, the ping-pong handover probability and handover failure probability are represented as a function of TTT and UE velocity under the assumptions that the small cell coverage and radio link failure areas are circular regions, and the UEs are moving as linear trajectories. Similar work is also

investigated in [37], among which, an adaptive TTT selection scheme is added into the theoretical analysis.

In [38][39], the authors focus on the evaluation of radio link failure, ping-pong handover ratio caused by inter-site distance, TTT and UE velocity. A closed form expressions for the handover performance probabilities were derived as a function of inter site distance and speed of the UEs. Although the expression is clearly, but the assumption that small cell coverage is a circular shape need to be discussed, because in a HetNet scenario, due to asymmetry transmit power of different tiers, the entry point of a handover condition is different when UE enter from different directions of a small cell.

2.3. Review of Handover Decision Algorithms

In this section, five different handover decision algorithms based on different parameters are discussed. As introduced in the previous section, the decision part of a handover referred to as the handover decision phase. In heterogeneous networks, the decision phase is always performed at the serving cell part. The vast majority of the discussed algorithms use a combination of different parameters to get the final decision. The main decision parameters for handovers between cells can be divided into five categories: 1) received-signal-strength-based, 2) speed-based, 3) cost-function-based, 4) interference aware, and 5) energy-efficient-based.

2.3.1. Received-Signal-Strength-Based Handover Decision Algorithms

The handover decision algorithms in this category are based on the RSS. The handover control parameter HM is used here to compare the RSS of the serving cell to the RSS of the target cells. The ping-pong handover ratio and handover probability

can be significantly improved by the system dynamically adjusting the HM. As shown in Figure 2.6, the cell range expansion (CRE) is always used in SCNs as a virtual bias to expand the small cell coverage. In handover decisions, it can also be understood as the cell individual offset (CIO) as introduced in the previous A3 handover event. Assuming the UE is moving from macrocell to small cell, when the received signal strength and HM meet the criteria, the handover will execute.

A new RSS-based handover decision algorithm was proposed in [40], [41]. The main idea of this work was to combine the RSS of macrocells and small cells to generate a new RSS criterion that compensates for the uneven RSS levels of macrocells and small cells. An exponential window function is utilised in the algorithm to mitigate the fluctuation of RSS. Through the combination of macrocell and small cell RSS, an adaptive cell offset is generated to perform a better handover performance. A further research of this handover decision is taken by work [42], based on the RSS and cell loading criterion, the authors proposed a new handover policy not only included the UE's perspective but also taken network load into consideration. However, the authors only take two parameters as the system performance evaluation, which are the number of handovers and UEs assignment probability to different cells. These two parameter is insufficient in system level evaluation.

Similar to the previous RSS-based handover decision algorithm, an RSS and pathloss-based handover decision algorithm was proposed in [43] where the analysis and simulation is also tested under a single macro-small cell scenario. Although the actual loss is added to the previous algorithm, this decision algorithm still got great difference in real life scenario. In heterogeneous network, the small cells are normally

dense deployed, not only macro-small cell scenario, but also small-small cell scenario should also take into consideration.

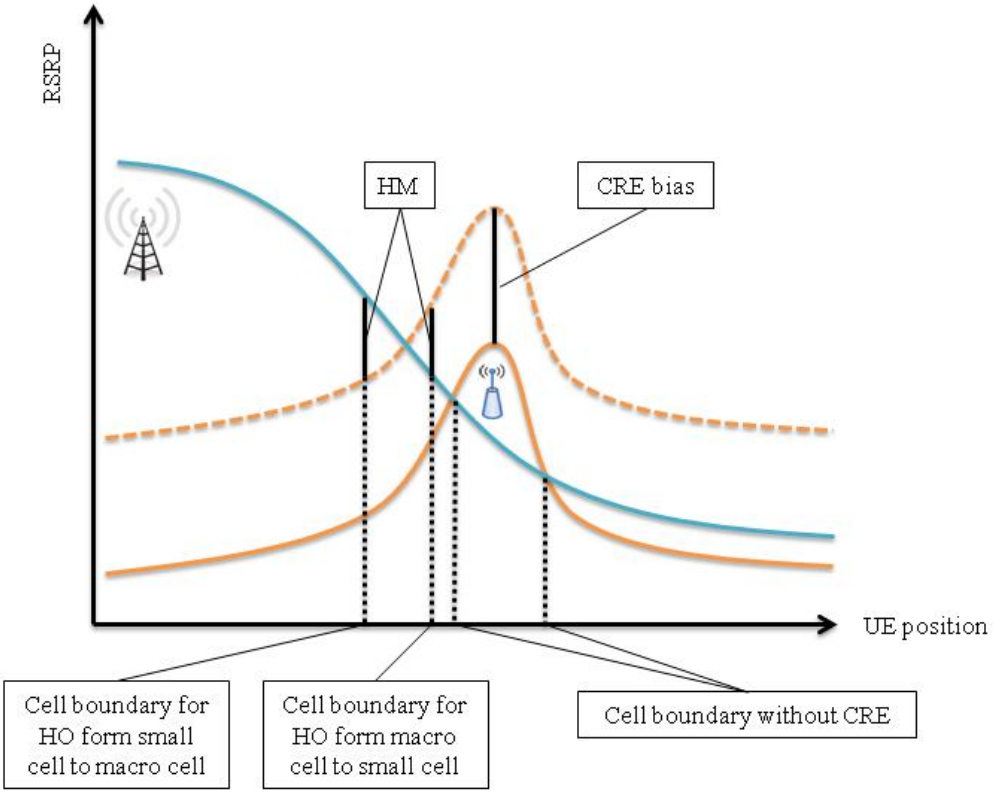

Figure 2-6 Received-signal-strength-based handover.

The authors of [44] proposed an intra-cell handover method that can be used for the handover between sub-channels. This handover decision criterion not only considers the avoidance of interference, but also takes the RSS handover decision into consideration. Further analysis of this approach is presented in the work of [45]. Through the detection of UE's cross tier interference, the algorithm will decide whether it should perform an intra-cell handover or initiate it in the small cell cell list.

Alexandris et al. [42] proposed an RSS based load aware handover decision algorithm. By considering both the UE and networks perspectives, the network load and RSS of UE are taken as the handover constraints. The proposed algorithm

outperforms the conventional RSS handover and distance-based handover in terms of user service delay and cell assignment probability. However, a more complex scenario should taken into consideration, the number of UEs need to be increased for the study of user distribution that will affect the system handover performance.

Kalbkhani et al. [46] proposed a handover algorithm based on the prediction of RSS and SINR. Through the prediction of future SINR performance, the candidate cell list effectively shortened, after the prediction, base station with highest throughput will be assigned for the UE in order to achieve a better system performance. Although this algorithm seems to provide the best solution of system performance, the authors haven't consider the time of stay for UEs , especial in small cells, since the small cell coverage is very limited.

2.3.2. Speed-Based Handover Algorithms

UE speed is used as the primary handover decision criterion in this class of algorithm. The handover decision is made by comparing the UE speed with an absolute threshold, which in most cases is arbitrarily picked. Speed-based algorithms are normally incorporated into other handover decision constraints, such as the RSS level constraint, the type of UE traffic, the available bandwidth on the target cells, and the UE membership status.

The work of Ulvan et al. [47] proposed a QoS and speed-based handover decision algorithm, with the authors dividing the speed into three categories: 0-15, 15-30, and >30km/h. Moreover, the traffic type is also divided into real-time traffic and non-real-time traffic. Through the comparison of the UE speed and the speed threshold, the algorithm will decide whether the UE should be handed over to a small cell or not. In addition, if the speed threshold is satisfied after the UE's traffic type

detection, a further handover decision will be made (i.e. proactive handover or reactive handover). However, they only consider the UE speed without the UE moving direction, which will significantly affect the accuracy of potential target cell selection. The authors expand their work into mobility prediction through the adoption of the Markov chain process in [48]. By predicting the UE's potential target cell, the performance of the proposed algorithm is better than normal handovers in terms of handover latency and the link establishment delay. Similarly, if they taken UE moving direction into consideration, a better performance should be expected.

In [49], the authors proposed a low complexity handover optimisation algorithm. Similar to the previous algorithm, this also uses speed as the constraint to decide whether the UE should handover to a small cell. The performance evaluation of the proposed algorithm is conducted by comparing the traditional handover algorithm in terms of the handover signalling overhead. The results show that with a higher proportion of high speed users, the proposed handover algorithm has a much lower signalling overhead than the traditional one. This paper only consider two kinds of UEs moving model, low speed and high speed, a more comprehensive UE moving model is needed when verifying the heterogeneous networks performance.

In [50], a more complicated speed-based handover decision algorithm is introduced. Several parameters are combined in this algorithm and the author takes the RSS, the UE speed, the UE type (CSG user or non-CSG user), and the interference level into consideration. However, in the interference detection phase, the authors didn't take co-layer interference in to consideration, which will result in the inaccuracy of interference management, meanwhile, the small-small cell handover is also neglected.

Work in [51] proposed a UE speed and traffic type based handover decision algorithm, by categorising the UEs into four categories, the handover control parameters is independently assigned for each category. The proposed algorithm outperforms the single category traditional handover algorithms. Although the idea of categorise handover control parameters into four kind is novelty, but two problems need to be considered. First is the selection scheme of handover parameters, since the combination of the parameters are varied, second is the UEs speed categorising, a standard need to be found or established to support this paper.

In [52], the authors proposed an unnecessary handover minimisation scheme based on monitoring the UE distance to the small cell, the moving speed and moving direction. Through the detection of these parameters, the candidate cell list is shortened, which effectively decreased the signalling cost and enhanced the system total capacity. However, in this paper, the assumption that small cell coverage is a circle need to be reconsidered, as the small cell coverage will significantly affected by its distance to macrocell.

By considering the location of candidate cells and the moving direction of UEs, Kishida et al. proposed a new cell selection mechanism aimed at reducing unnecessary handovers [53]. The authors examined the proposed mechanism in a metropolitan scenario through the comparison of conventional maximum SINR based scheme, 30% handovers decreased without any degradation in call flow time.

The work in [54] proposed a cell selection scheme based on the UE moving speed and interference signal level. Based on the neighbouring cell location information and UE moving status, the handover probability to each candidate cell can be formulated. However, the simulation taken place in a street scenario, which is very limited for small cell handover evaluation, in addition, the most important

variable in this paper is predefined by the authors, which seems to be not sufficient enough for this algorithm.

2.3.3. Cost-Function-Based Handover Algorithms

The aim of this type of handover decision algorithm is to integrate a wide range of different handover decision parameters, such as traffic type, battery lifetime, RSS, cell load, and UE speed, into one single cost function.

In the work of [55], a weighted performance handover decision algorithm was proposed. The main system performance indicator consists of three handover performance indicators: 1) the handover radio link failure ratio indicator, 2) the handover failure ratio indicator, and 3) the ping-pong handover ratio indicator.

By combining the parameters w_1, w_2, and w_3, the system will automatically optimize the handover control parameters HM and TTT in each time slot with handover performance parameter HP. The system handover performance significantly improves through this algorithm and several similar works also adopt this algorithm as the basic cost function [56], [57]. However, the selection of weight combination w_1, w_2 and w_3 is predefined by the authors, which is lacking of adequate proof that these combination is the optimised one.

$$HP = w_1 HPI_{rlf} + w_2 HPI_{hof} + w_3 HPI_{hopp} \qquad \textbf{Equation 2-1}$$

In [58], a cost-function-based adaptive HM algorithm is proposed to minimise the handover failure rate. This algorithm also uses different weightings, but each parameter in the weighted equation is a normalized function that consists of the load difference between the target and serving cells, the UE speed, and the service type. By comparing different combinations of weight parameters in the proposed algorithm, the

authors achieve an improved handover failure rate. Although the performance is optimised, the simulation only takes macrocells into consideration, whether this algorithm is suitable for heterogeneous networks is not testified.

Xu et al. [59] proposed a UE traffic type and SINR cost-function-based handover decision algorithm based on UE speed, UE traffic type, SINR performance of the serving and target cells, and the RSS level. The authors combined the UE traffic type and speed with a binary multiplication function by comparing the logical variable R_{ms} with a certain threshold in order to decide whether the UE should make a handover. The parameters $f(v)$ and $f(q)$ shown below represent the function of speed and the traffic type, respectively. Parameters v and v_{th} represent the UEs moving speed and system predefined handover speed threshold. Considering the simulation model, the authors need to consider the UEs moving direction, since the probability that a handover happened at small cell boundary is significantly different if the UEs are moving towards or away from the small cell.

$$R_{ms} = F\big(f(v), f(q)\big) = f(v) * f(q)$$

$$f(v) = \begin{cases} 1, v \le v_{th} \\ 0, v > v_{th} \end{cases}, f(q) = \begin{cases} 1, Class\ A \\ 0, Class\ B \end{cases}$$

Equation 2-2

Vondra and Becvar [60], [61] presented a new handover control parameters selection mechanism, the authors introduced a new parameter CINR to instead of the RSS compared with [62] to calculate the actual value for handover control parameters. The parameter CINR is based on the serving cell's transmitter power, path loss, noise power, and interference power. By simulating specific scenarios, optimal values for handover performance in terms of downlink throughput and handover amounts were achieved. However, if these papers need to improve, two main points are

nonnegligible. First, similar to the previous references, the authors didn't consider heterogeneous network environment, only macrocells are considered, the effectiveness of this algorithm with small cell included need to be testified. Second, the authors didn't takes TTT into consideration, as handover happened in a moving system, the time domain parameter TTT will also affect the handover probability.

2.3.4. Interference Aware Handover Algorithms

In the HetNet scenario, interference is a very important aspect that needs to be considered. The main parameters are the signal quality, e.g. the SINR performance, the received interference power level, the received signal quality, and the cell site interference constraints.

A double threshold handover decision algorithm is proposed by [63] that aims to reduce unnecessary handovers. The authors not only considered the RSS level of UE, but also the interference signal level and capacity. Similar work is proposed in [64], where the proposed call admission control mechanism effectively reduces the number of unnecessary handovers by checking the UE's quality of service. However, these two algorithms only checked by the unnecessary handover numbers, whether or not these reduction will decrease the system capacity is not stated.

Alhabo et al. [65] proposed an interference-based handover algorithm that aims to improve the system throughput and load balancing in small cells. The authors incorporated the interference level with the neighbor cell list to reduce the candidate cells by checking SINR and time of stay before making the handover decision. The optimal result is presented in terms of UE mean throughput and system throughput. Although the proposed algorithm outperformed the other handover mechanisms, the

assumption that small cell coverage is a circular maybe not rigorous, since the small cell coverage is an irregular ellipse that affected by its distance to macrocells.

Dionysis et al. [66] proposed an interference and energy efficiency-based handover decision for HetNet. The two main parameters in this algorithm are the UE transmitter power and an adapted HM. A wide range of constraints are introduced in this algorithm, including UE membership state, the transmitter power at both cell sites, the interference limitation, the bandwidth limitation, and the operating frequency. By measuring these parameters, an optimised result was achieved in terms of mean UE received interference power and mean UE consumed energy when delivering certain data bits. However, the high interference signal level typically affect the UEs that positioning at cell boundary or with high moving speed, the parameter mean interference power maybe not suitable for evaluate the network performance.

An interference mitigation and handover management scheme combined with cloud RAN (C-RAN) was proposed by Zhang et al. [67]. The interference and signalling overhead of cell boundary UEs effectively mitigated through the adoption of coordinated multiple points (CoMP) clustering scheme. Moreover, combining with self-optimisation mechanism, the interference power control and handover performance will be enhanced.

Antoro et al. [68] proposed an interference and distance-based handover decision algorithm. By combine the nearest small cell distance with the RSS of different tier cells, a pre-handover mechanism is proposed. An SINR threshold is set to mitigate the cross tier interference. However, the interference power level is also distance dependent, to simplify the proposed algorithm, the distance and interference should be consider into one constraint.

2.3.5. Energy Efficient-Based Handover Algorithms

This type of algorithm aims to increase the system's energy efficiency by utilizing small cells. Several criteria can be set as the primary constraints in this type of handover decision, such as the UE mean transmitter power, the UE power consumption, and the system's power consumption. As the power consumption of the UE and the network are both strongly dependent on the interference signal strength, energy efficiency-based handover decision algorithms are similar to interference-based handovers.

Compared with the four-decision criteria mentioned earlier, only limited literature can be found in this area. The work from Boujelben et al. [69] proposed a green handover algorithm that aimed to save system energy through the optimal selection of candidate cell lists based on the UE speed and the cell loads. A remarkable effect is gained from the offloading of macrocells. In addition, the authors didn't consider the interference power, to improve this algorithm, inter cell interference power level should be added as a constraint.

Araniti et al. [70] proposed a green handover algorithm based on the detection of UE moving speed and overall transmit power of small cells. Similar to the speed-based handover, any UE with high moving speed will be rejected to handover into the small cells, only the handovers that will not increase the overall base station transmit power will be accepted. Through the adoption of this algorithm, the number of unnecessary handovers and system energy efficiency improved. However, a possible solution to improve the proposed algorithm is to complicate the simulation environment, as the authors only consider single macrocell in their simulation.

In conclusion, various handover decision algorithms have been investigated in recent years. Based on different optimisation target, different criterion are set. The main aim when designing a handover decision algorithm is to optimize the handover control parameters to improve the system's handover performance.

2.4. Review of the Markov Chain Process

The Markov Chain Process (MCP) is a stochastic process that is widely used in wireless communication systems [71]. When a stochastic process is provided by its current state and past state, and its future state probability distribution is only dependent on its current state, it is said to satisfy the Markov property. In other words, when the present state is provided, the future state is independent of the past states [72]. Assuming $\{X_k\}$ is a stochastic process and $\{E\}$ is the state space, for any $I_n \in E$, its conditional probability represented by *Prob* can be expressed as the equation shown below:

$$Prob\left[X_n = I_n \middle| X_{n-1} = I_{n-1},\ X_{n-2} = I_{n-2,} X_{n-3} = I_{n-3}, \dots, X_1 = I_1\right] = Prob[X_n = I_n | X_{n-1} = I_{n-1},] \quad \textbf{Equation 2-3}$$

2.4.1. Discrete Time Markov Chain

The Discrete Time Markov Chain (DTMC) is used for heterogeneous network structures. If the transition probability of a DTMC from one state to another is independent of the time, it is called a stationary DTMC. Otherwise, it is a non-stationary DTMC.

2.4.2. Probability Transition Matrix

The probability transition matrix describes a Markov Chain in finite state space [73]. In a specific time-step, the probability of transfer from state I_n to I_j can be described as $Prob[\, j \mid n \,]$. This can be represented by the transition matrix in the *n*th row and *j*th column as shown in the following matrix:

$$Prob[\, j \mid n \,] = \begin{bmatrix} P_{1,1} & P_{1,2} & \cdots & P_{1,j} & \cdots & P_{1,E} \\ P_{2,1} & P_{2,2} & \cdots & P_{2,j} & \cdots & P_{2,E} \\ \vdots & \vdots & \ddots & \vdots & \ddots & \vdots \\ P_{n,1} & P_{n,2} & \cdots & P_{n,j} & \cdots & P_{n,E} \\ \vdots & \vdots & \cdots & \vdots & \ddots & \vdots \\ P_{E,1} & P_{E,2} & \cdots & P_{E,j} & \cdots & P_{E,E} \end{bmatrix} \qquad \textbf{Equation 2-4}$$

It should be noted that any $P_{n,j}$ appearing in the matrix should satisfy $1 \geq P_{n,j} \geq 0$ and the summation of each row should be equal to *1*, as for any given state *n* the next state must be one of the possible states.

$$\sum_{j \in E} P_{n,j} = 1 \qquad \textbf{Equation 2-5}$$

2.4.3. Related Works

As mentioned previously, MCP is widely adopted in the modelling of wireless communication networks, and the work of [74] proposed a UE mobility prediction model in the macro-small cell scenario using MCP. The authors set each state as the UE's potential target cell and the probability of the UE moving to the next cell is dependent on the UE's current location, direction, and speed. The unnecessary handover numbers are minimised by the prediction of UE movement.

Another Markov-based HetNet mobility modelling and analysis work is proposed in [75], [76]. The authors first build a UE trajectory model and derive the average UE capacity. Secondly, a DTMC handover model of a single macro-small cell scenario is built up. By using the proposed model, optimal system average capacity and cell load can be achieved. However, the detailed handover probability model is not accurate for small cell environment, since small cell normally assigned with a certain virtual bias to increase the UEs assignment to small cells. This bias will play an opposite role if the UE is served by different cells when handover happened.

2.5. Summary

In this chapter, SCNs, LTE handover procedures, handover decision algorithm classification, and the Markov Chain Process are reviewed.

As part of the review of SCNs, the history of small cell development is introduced, followed by the advantages and disadvantages of utilizing small cells. The two-tier E-UTRAN is introduced to explain how small cells connect to the core network.

In the overview of handover procedures, handover classification is introduced, followed by the handover entry events summary and the introduction of handover implementation. The handover control parameters are emphasized as the TTT and HM directly influence the system handover performance.

In the review of handover decision algorithms, five categories of algorithm are introduced. The current algorithms are summarized, and the lack of a system level energy efficiency algorithm is discussed.

Finally, in the review of the Markov Chain Process, the DTMC and probability transition matrix are introduced, followed by a literature review of MCP utilized in modelling the mobility of the HetNet scenario.

Chapter 3. Two Self-optimisation Handover Decision Algorithms

Overview

In this chapter, two handover decision algorithms are proposed. The first is based on the system SINR and ping-pong handover ratio, which can also be understood as a system self-optimisation mechanism, based on interference and ping-pong handover ratio. Similarly, the second optimisation mechanism is based on system energy efficiency and ping-pong handover ratio status, which also provides a self- optimisation mechanism. The main concept of the proposed algorithms is that they dynamically select two handover control parameters: TTT and HM, based on the current network performance in terms of SINR, energy efficiency states, energy reduction gain (ERG), and ping-pong handover ratio, the system will automatically modify the handover control parameters to yield better network performance.

3.1. Introduction

HetNets were first proposed in Release 10 of 3GPP [10]. Following the wide deployment of 4G, data rate was significantly increased. The upcoming 5G standard is expected to have between 10 and 50 Gbps data rates [77]. With such high demand in data traffic volume, the extremely high density of small cell deployment is inevitable [78]. With the wide adoption of small cells in networks, the user distance from base stations is much shorter compared to the one-tier macrocell only network, which strongly enhanced the network capacity. As stated in the previous chapter, another benefit that can be achieved by using small cells is good isolation, which can significantly improve the network spectrum reusing efficiency, by reusing radio spectrum indoors [7].

While we benefit from the convenience brought by utilising small cells, several unavoidable problems arise. The complicated network structure leads to a severely challenging situation for mobility management, particularly the handover decision part. The smaller coverage compared to a macrocell will result in frequent handovers. Among these handovers, a number of them will be unnecessary handovers. If we can reduce the number of these handovers, the UEs will benefit from better quality of experience (QoE), and network burdens will be decreased. The interference issue is an important problem when applying densification deployment of small cells, not only in the case of macro-small cell interference, but also for small-small cell interference. Another issue is the energy consumption problem; the increasing density of base stations significantly increased the energy consumption in a cellular network, since 57% energy is consumed by the base stations [79], [80]. At the same time,

mobile switching occupied 20% energy cost [81]. Network energy efficiency will be severe affected by unnecessary handovers.

In order to solve the first frequent handover issue, an algorithm that dynamically selects the handover control parameters TTT and HM is introduced. These two parameters are designed for the prevention of unnecessary handovers caused by sudden fluctuations in signal strength. As previously introduced, in order to perform a handover, both the HM and TTT constraints need to be satisfied [82]. For the purpose of solving system interference and energy efficiency issues, two self-optimisation mechanisms are proposed. In order to solve the interference problem, another performance evaluation parameter system average SINR indicator is added to determine the handover control parameters. The system will make the decision of changing control parameters through the monitoring of average SINR and ping-pong handover ratio state. On the other hand, the network energy efficiency issue is also challenging, but can be solved by reasonably establishing the system power consumption model and checking the system energy status when making a change in handover control parameters.

The detailed power consumption model for both base station and users are introduced in this chapter. It is worth mentioning that, in order to formulate a comprehensive model, when establishing the system power consumption model, we not only take base stations into consideration, but also mobile terminals. Many handover decision algorithms have been proposed to solve frequent handover problems, e.g., speed-based handover decisions, RSS-based, and interference aware-based [22]. In conventional handover decisions, different constrains have been used to make handover decisions, but an energy efficiency-based handover decision algorithm has not been proposed. In this chapter, we propose an energy efficiency-based

handover decision algorithm which aims at self-optimizing the network system energy efficiency and system total ping-pong handover ratio.

This chapter is organized as follows. In the first part, an SINR and ping-pong handover ratio-based self-optimisation handover decision algorithm is introduced, followed by simulation results and analysis. Part two introduces the three different power consumption models with respect to the UE, macro cell, and small cell, followed by three energy efficiency metrics. The proposed ping-pong handover ratio and system energy efficiency-based handover decision algorithm is described in detail, and simulation parameters and simulation results are presented.

3.2. An average SINR and ping-pong handover ratio-based handover decision optimisation algorithm

3.2.1. Downlink SINR calculation

Within the network, there are *J* macro cells and *N* small cells. Assume we have one UE, *x*, who is served by a macrocell, *m*; the distance between this user and the macrocell can be expressed as d_{mx}, if the UE is served by this macrocell, the downlink SINR of this UE can be calculated as Equation 3-1. In the following equation, α_m and α_f denote the path loss coefficient of the macrocell and small cell, respectively. P_{jx} and P_{kx} represent the transmit power from macrocell and small cell to this UE, P_{mx} denotes the transmit power of current serving macrocell, and *n* denotes the thermal noise.

$$SINR_{mx} = \frac{P_{mx}(d_{mx})^{-\alpha_m}}{\sum_{1,j\neq m}^{J} P_{jx}\,(d_{jx})^{-\alpha_m} + \sum_{1}^{N} P_{kx}\,(d_{kx})^{-\alpha_f} + n} \qquad \textbf{Equation 3-1}$$

Similarly, for a small cell serving user, we only need to change the serving cell, P_{fx} denotes the transmit power of current serving small cell, d_{fx} represents the distance to this small cell, which is shown as Equation 3-2.

$$SINR_{fx} = \frac{P_{fx}(d_{fx})^{-\alpha_f}}{\sum_1^J P_{jx}\,(d_{jx})^{-\alpha_m} + \sum_{1,k\neq f}^{N} P_{kx}\,(d_{kx})^{-\alpha_f} + n} \qquad \textbf{Equation 3-2}$$

As the handover decision algorithm proposed here is constrained by system average SINR and ping-pong handover ratio performance. The average SINR is calculated as:

$$\overline{SINR} = \frac{\sum_1^X SINRx}{X} \qquad \textbf{Equation 3-3}$$

$\overline{SINR}$ is the average SINR, which is calculated from the summation of each UE's SINR, divided by the total number of UEs, which is represented by X in the system.

3.2.2. Ping-pong handover ratio

Ping-pong handover can be interpreted as a call being handed over to a new cell and then handed back to the original cell in less than critical time (T_c). According to 3GPP TR36.839, the recommended T_c here is one second. Ping-pong handover ratio here is calculated using equation 3-4, inside the equation, N_{HOpp} denotes the ping-pong handover number, N_{HOtot} represents the total handover number, and HPP_{ratio} is the ping-pong handover ratio. The ratio calculated here is the number of ping-pong handovers divided by the total number of handovers.

$$HPP_{ratio} = \frac{N_{HOpp}}{N_{HOtot}} \qquad \textbf{Equation 3-4}$$

A special case of the first order auto regressive moving average (ARMA) filter is used in this instance to study the proposed handover decision algorithm.

$$HI_{sinr(t)} = (1-\beta) * HI_{sinr(t-1)} + \beta * \overline{SINR}_{(t)} \quad \textbf{Equation 3-5}$$

$$HI_{HPP(t)} = (1-\beta) * HI_{HPP(t-1)} + \beta * HPP_{(t)} \quad \textbf{Equation 3-6}$$

In the equations above, HI represent the handover indicator. $\mathrm{HI_{sinr(t)}}$ and $HI_{HPP(t)}$ are two parameters used here to indicate the system average SINR and ping-pong handover performance. $\overline{\mathrm{SINR}}_{(\mathrm{t})}$ is the average SINR value at time slot (t), $\mathrm{HI_{sinr(t)}}$ and $\mathrm{HI_{sinr(t-1)}}$ are the filtered $\overline{\mathrm{SINR}}$ value at time slot (t) and time slot $(\mathrm{t}-1)$. Similarly, $HPP_{(t)}$ represents the ping-pong handover ratio at time slot (t), and $\mathrm{HI_{HPP(t)}}$ and $\mathrm{HI_{HPP(t-1)}}$ are the filtered HPP value at time (t) and time $(\mathrm{t}-1)$, where $\mathrm{HI_{sinr(0)}}$ and $\mathrm{HI_{HPP(0)}}$ are set to $\overline{\mathrm{SINR}}_{(0)}$ and $\mathrm{HPP_{(0)}}$ when the first measurement results are received. Parameter β here is known as the forgetting factor and is used for deciding the weight given to current value and previous value ($0 < \beta < 1$). The closer the value of β gets to zero, the higher the proportion for which the current $\overline{\mathrm{SINR}}$ and HPP depend on the filtered value in the previous time interval. On the other hand, the closer the forgetting factor gets to one, the higher the proportion for which the current filtered $\overline{\mathrm{SINR}}$ and HPP depend on the current value. Figure 3-1 is a *200* ms simulation that shows the $HI_{sinr(t)}$ affected by forgetting factor β. From the figure, we can see when $\beta = 1$, the $\mathrm{HI_{sinr(t)}}$ is the instantaneous value of $\overline{\mathrm{SINR}}$; as β decreases, the $\mathrm{HI_{sinr(t)}}$becomes smooth. The set of β used here aims to prevent a sudden variation in variables.

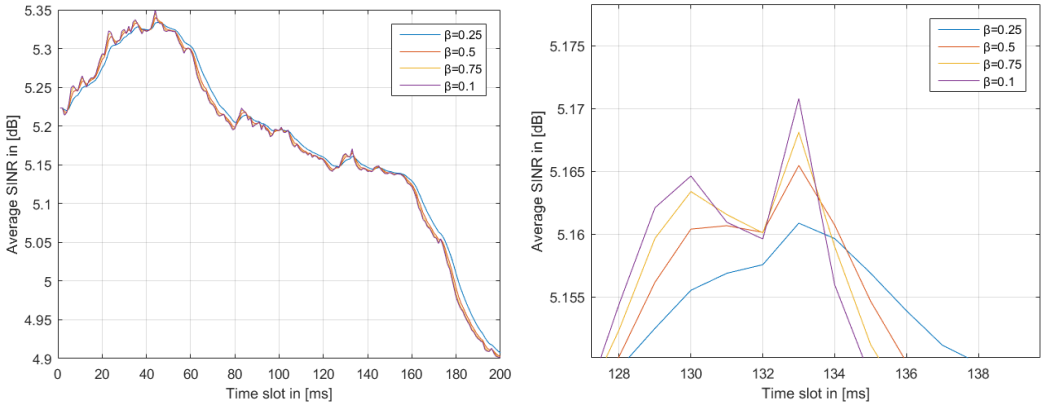

Figure 3-1 β variation vs $HI_{sinr(t)}$

3.2.3. System model

A 19-hexagonal macrocell closely deployed environment, in which the small cells are randomly distributed. Figure 3-2 (a) and (b) display the 3D view and top-down view of the entire simulation network system, which comprises a two-tier macro-small cell network SINR map. As stated in the previous, there are 19 macro cells and 91 small cells in the entire simulation system. In the top-down view of this map, we can see that the different signal strengths created differential BS coverage, different position of same type of BS result in a different coverage as well (as the two small orange windows displayed in the figure, the small cells are assigned with the same transmit power, but they are offering different SINR coverage).

Figure 3-2 (c) and (d) shows the interference map of the entire network system. It can clearly be seen that the denser the deployed cells, the higher the interference will be. The processes of SINR and interference maps calculated here are shown below. The entire map was divided into *100*100* pixels, note that, the *x* axis and *y* axis of these figures are represented by pixel numbers. RSS was used to determine the current serving cell in each pixel. The RSS of rest 109 BSs was considered to be interference power. The entire map was scanned to create the SINR and interference maps.

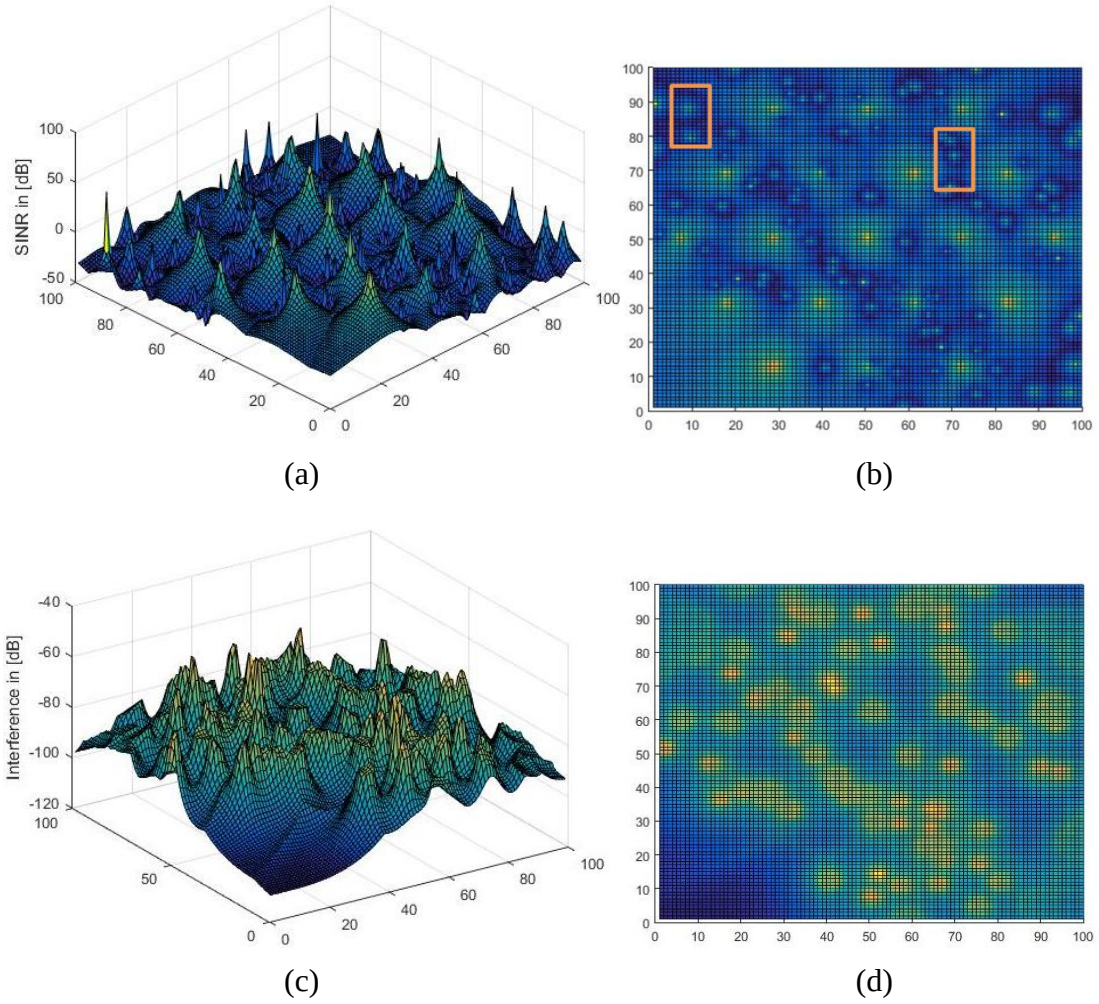

Figure 3-2. 3D view and top-down view of SINR map and interference map.

3.2.4. UE mobility

The SINR and interference maps that calculated in section 3.2.3 were created in a static process. The cell that provides the maximum RSS is considered as the serving cell, while the remaining RSS are considered as interference power. However, handover is a dynamic process, which means even if the user moved out of the cell serving region and the maximum RSS is from a different cell, it can still be served by the original cell.

The number of UEs in the simulation totalled 1,000. The UEs are initially randomly dropped onto the simulation map, and the direction for each UE is randomly

chosen from zero to 2π. Each UE moves in a straight line with a constant speed, which in this case ranged from 30km/h, 60km/h, and 120km/h. When the UE was almost outside of the simulation environment (4000m×4000m square area), the UE was set to change movement into the opposite direction.

3.2.5. SINR and ping-pong handover ratio optimisation mechanism

Figure 3-3 represents the flow chart for the detailed handover optimisation step, which was used in the proposed handover algorithm. Following the initial phase, data was collected from the network, six threshold values are represented as follows: $HI_{HPP\mathrm{th}}$, $HI_{HPP\mathrm{g}}$, $HI_{HPP\mathrm{b}}$, HI_{sinrth}, $HI_{sinr\mathrm{g}}$ and $HI_{sinr\mathrm{b}}$. Among these six values, the subscript ending with th refers to threshold, with g referring to good performance value, and b means bad performance value. Parameters starting with HI refers to handover indicators, while those starting with C_HI represents the current value of HI. The decision-making part can mainly be divided into four steps, as shown in Figure 3-3. The first two decisions are to check the HO ping-pong ratio; steps three and four are based on SINR judgment.

Step 1. Compare the C_HI_{HPP} and $HI_{HPP\mathrm{th}}$, if $C\_HI_{HPP} < HI_{HPP\mathrm{th}}$, the left branch, Step 2a, Step 3a and Step 4a will be executed, otherwise, execute Step 2b, Step 3b and Step 4b.

Step 2. a.(left branch) Compare the C_HI_{HPP} and $HI_{HPP\mathrm{g}}$, if $C\_HI_{HPP} < HI_{HPP\mathrm{g}}$, decrease the current threshold and good performance value, which means the current data is of good performance, the current threshold is not suitable for filtering. Step 2. b(right branch) Compare the C_HI_{HPP} and $HI_{HPP\mathrm{b}}$, if $C\_HI_{HPP} > HI_{HPP\mathrm{b}}$, similarly, increase the $HI_{HPP\mathrm{th}}$ and $HI_{HPP\mathrm{b}}$.

Step 3. a(left branch) Compare C_HI_{sinr} and $HI_{sinr\text{th}}$, if $C\_HI_{sinr} > HI_{sinr\text{th}}$, execute step 4. a, otherwise, go to next optimisation step. Step 3.b(right branch), if $C\_HI_{sinr} < HI_{sinr\text{th}}$ execute step 4. b, otherwise, go to next optimisation step.

Step 4. a(left branch) Compare the C_HI_{sinr} and $HI_{sinr\text{g}}$, if $C\_HI_{sinr} > HI_{sinr\text{g}}$ increase the HM and TTT. Step 4. b(right branch) if $C\_HI_{sinr} < HI_{sinr\text{b}}$, decrease the HM and TTT.

The main idea of this optimisation including two directions which shown as the two branches in the figure, in each direction, four steps are included. The first two steps are the checking of ping-pong handover performance, step 3 and step 4 are the SINR checking progress. Since ping-pong handover ratio is the priority issue that we concern, therefore, the SINR performance checking will start only when ping-pong ratio criterions are satisfied.

Left branch: The handover control parameters HM and TTT will be reset only when $C\_HI_{HPP} < HI_{HPP\text{g}}$, and $C\_HI_{sinr} > HI_{sinr\text{g}}$ are satisfied, which means current ping-pong handover ratio and SINR performance are both in very good condition, in order to have better system performance, the system will automatically decrease HM and TTT.

Right branch: similarly as left branch, the HM and TTT will be increased, only when both ping-pong handover ratio and SINR performance are in bad performance condition, which shown as the $C\_HI_{HPP} > HI_{HPP\text{b}}$ and $C\_HI_{sinr} < HI_{sinr\text{b}}$. The target of this branch is to decrease the ping-pong.

In step 2, 3 and 4, other six cases will also possibly happen, the reason that these cases happened is because the current system feedback value is better than the threshold value, but haven't reach the good or bad performance condition, under such

circumstance, the system will hold on and keep waiting for the next time slot feedback.

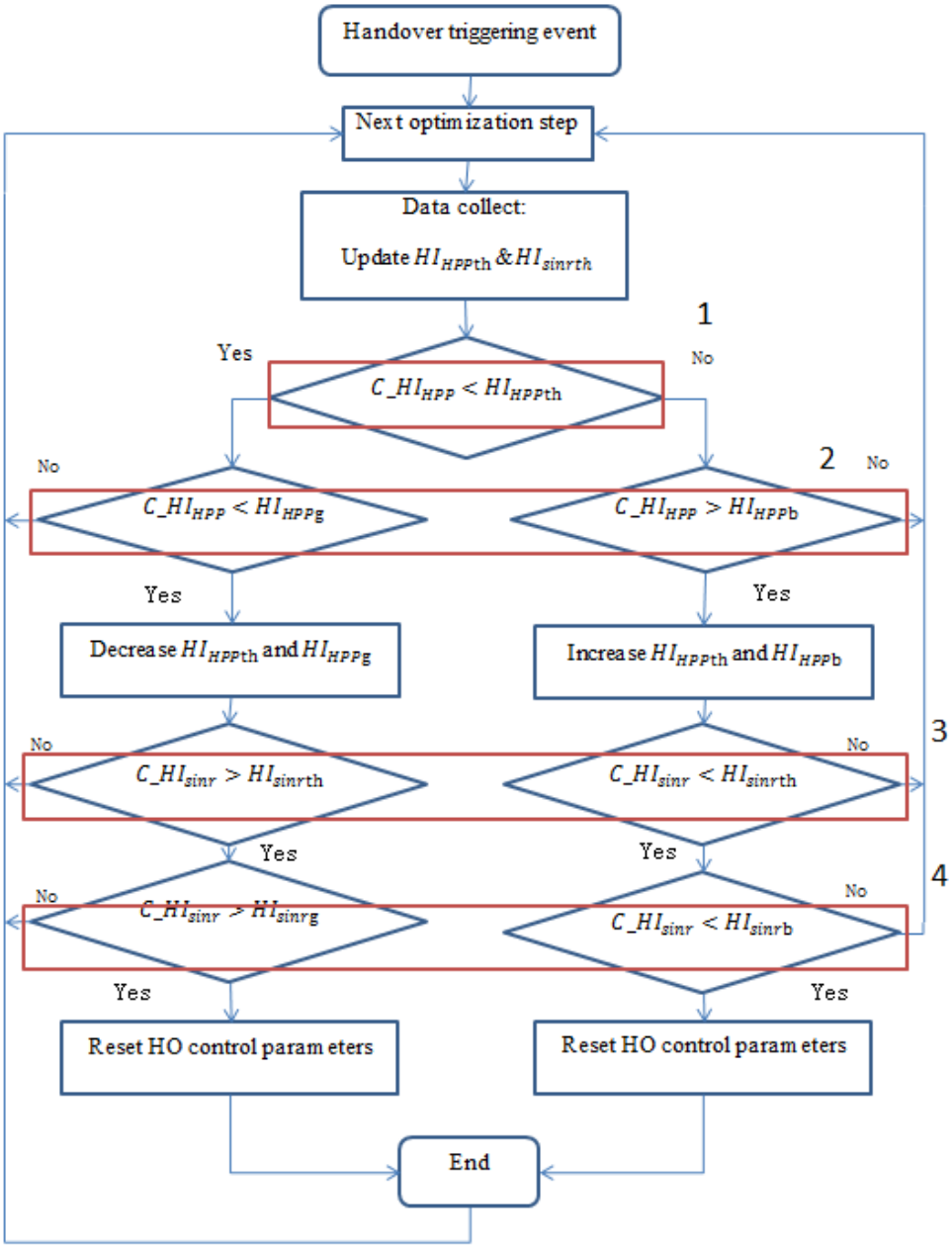

Figure 3-3 SINR and PPHO ratio self-optimisation flow chart

Figure 3-4 introduced the optimisation direction of the handover control parameters; 20 different possible parameter combinations were considered to assist in resetting HO control parameters when optimisation was undertaken. Figure 3-4 shows two optimisation directions (red arrows). The higher the step value, the lower the

handover ping-pong rate and SINR performance. Contrarily, a lower step value will result in a higher ping-ping ratio and better SINR performance.

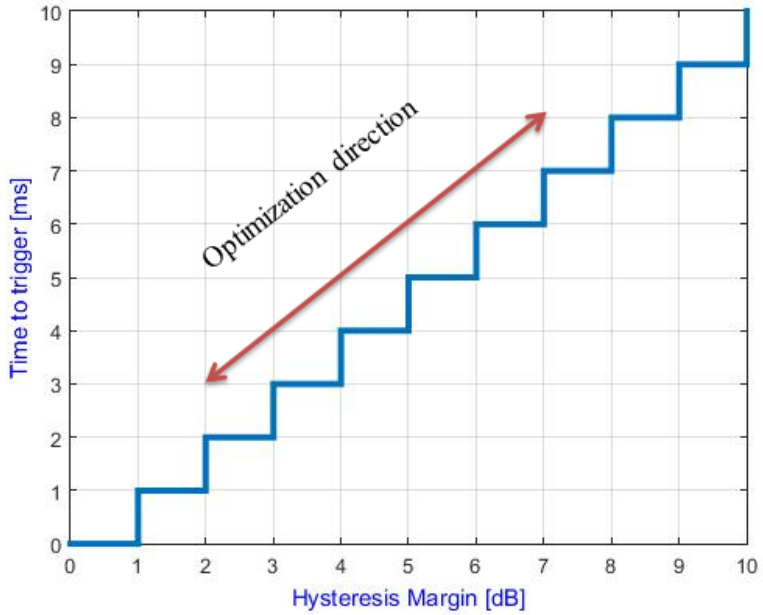

Figure 3-4 Optimisation direction of TTT and HM.

The parameters employed are listed in Table 3-1. Detailed network layout and user deployment are introduced in section 3.2.2. According to 3GPP TR 36.842 [83], we use two different path loss models for the macro and small cells.

Table 3-1 Simulation parameters.

Parameters	**Values**
Macrocell layout	19 Cells, hexagonal grid, wrap-around
Femtocell layout	91 cells randomly deployed
Carrier frequency	2 GHz
Bandwidth	10 MHz
Macrocell path loss	128.1+37.6*log10(d/1000) d in [m]
Femtocell path loss	147 + 36.7*log10(d/1000) d in [m]
Macrocell Tx power	46 dBm
Femtocell Tx power	20 dBm
User deployment	1000 Users randomly deployed
User velocity [km/h]	30/60/120

Simulation time	500TTI
TTI	10 ms
Forgetting factor β	0.25
TTT [ms]	0/40/64/80/100/128/160/256/320/480
HM [dB]	1/2/3/4/5/6/7/8/9/10

3.2.6. Simulation result

In this section, the performance evaluation of the proposed handover decision algorithm is discussed from a different perspective.

3.2.6.1 Optimisation under UE velocity v=120km/h

Figure 3-5 shows the overall ping-pong handover ratio variation in a 500 TTI simulation. The overall ping-pong handover ratio is calculated from the number of ping-pong handovers occurred, divided by the number of handovers occurring up to the current time slot. From the figure, it is clear that with more time spent in the simulation, the value of the no-optimisation-based curve (blue) turns out to be smooth at roughly 0.17. Similarly, the optimised ratio stabilized and fluctuated at roughly 0.14; 3% of ping-pong handover ratio was optimised in this condition. There is a crossover at roughly 190; prior to this time point, the ratio of the optimised algorithm is higher than the non-optimised algorithm. The reason for this can be observed in Figure 3-4. Following the check for the ping-pong handover ratio stage, the check for SINR performance resulted in the resetting of handover control parameters. According to Figure 3-5, bad SINR performance will cause optimisation direction to drop to a lower stage of control parameters, where the lower value of control parameters will function at a reduced ping-pong handover performance.

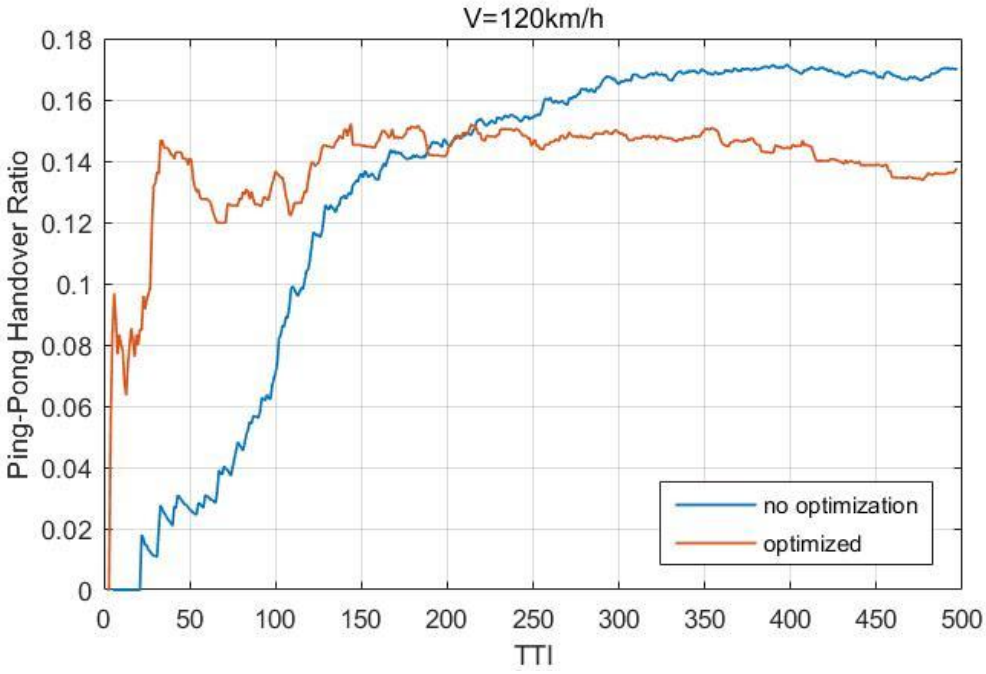

Figure 3-5 Overall ping-pong handover ratio v=120km/h.

3.2.6.1.Optimisation under UE velocity v=60km/h

Compared to Figure 3-6, no overlapping of two curves exist, and the value of the non-optimised-based curve stabilized at roughly 0.33; optimised curve was smooth at 0.285. The optimised ping-pong handover ratio was roughly 4.5%.

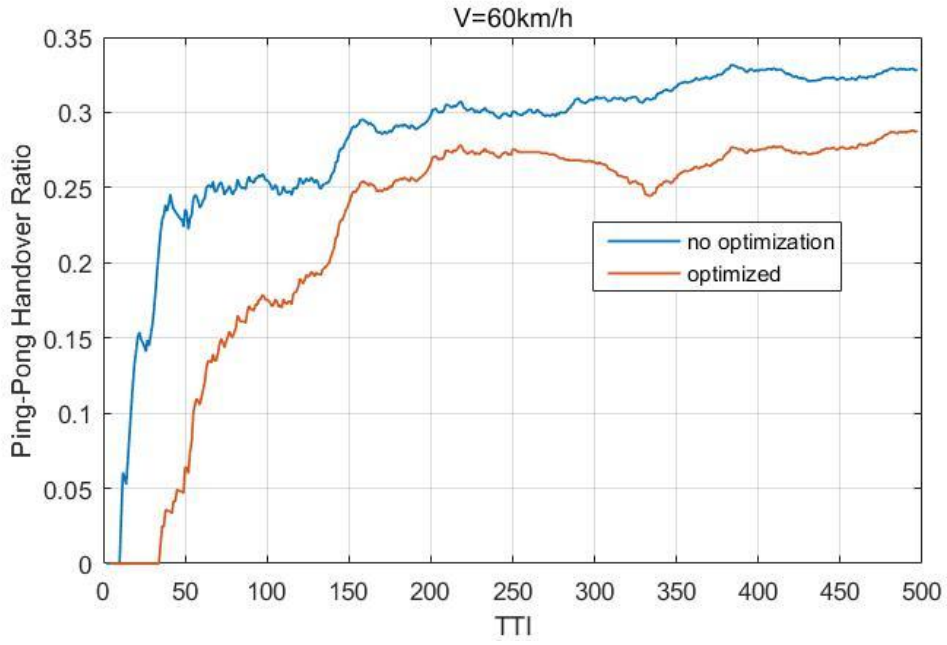

Figure 3-6 Overall ping-pong handover ratio v=60km/h.

3.2.6.2.Optimisation under UE velocity v=30km/h

From Figure 3-7, it is clear that no optimisation occurred from 0~80 TTI. Two reasons for this are the stable SINR and ping-pong handover ratio. After time slot 80, optimisation is clearly shown in the figure; the ratio of the non-optimised curve fluctuated at 0.34, and the optimised curve stabilized at 0.28; optimised ratio was roughly 6%. If we consider Figure 3-5, Figure 3-6, and Figure 3-7 together, it is not difficult to see that with a decrease in UE velocity, the ping-pong handover ratio became larger, and the optimised ratio increased.

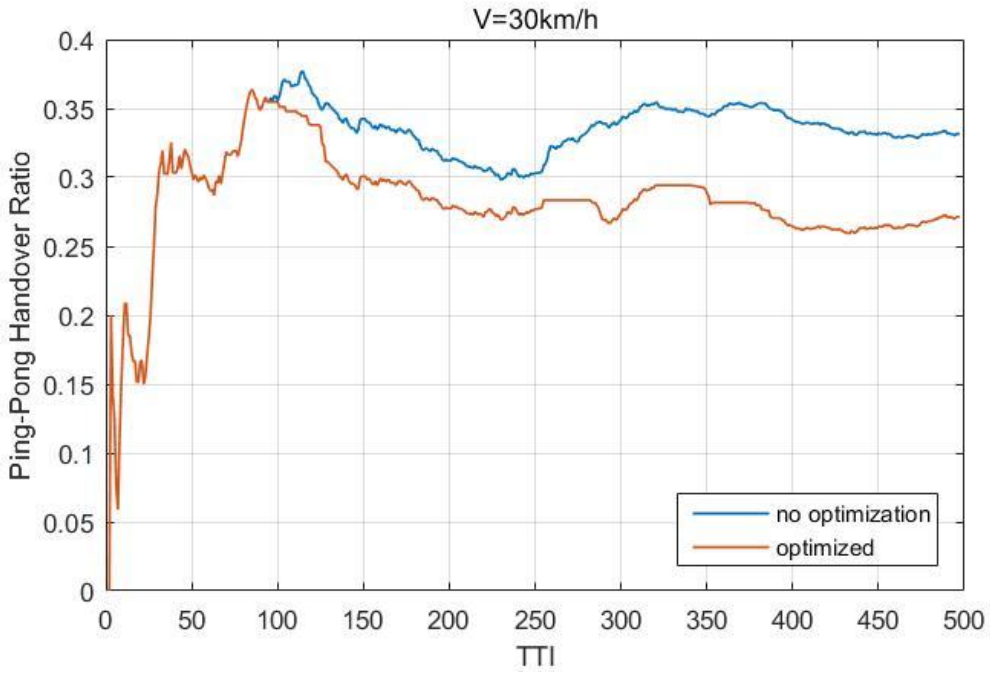

Figure 3-7 Overall ping-pong handover ratio v=30km/h.

3.2.6.3.Average SINR value optimisation

Table 3-2 lists the average SINR value for a comparison of the optimised and non-optimised algorithms. The average SINR is the mean value of $\overline{SINR}_{(t)}$.

Table 3-2 average SINR optimisation result.

UE velocity	Non-optimised average SINR [dB]	Optimised average SINR [dB]
120km/h	5.1090	5.4310
60km/h	5.3181	5.7880
30km/h	6.0531	6.4716

The optimisation for SINR is not significant compared with the optimisation of ping-pong handover ratio, with respect to 0.322, 0.4699, and 0.4185 dB.

3.3. An energy efficient and ping-pong handover ratio-based handover decision optimisation algorithm

3.3.1. Handover model

In a conventional cellular network, assuming the UE is moving away from its serving base station, if the RSS of the target base station exceeds that of the serving base station for a certain threshold, HM, and satisfies the TTT constraint, a handover will start. The handover decision is given by the following equation, where RSS_t represents the RSS of target base station and RSS_s represents the RSS of serving base station.

$$RSS_t > RSS_s + HM \qquad \textbf{Equation 3-7}$$

3.3.2. UE Power Consumption Model

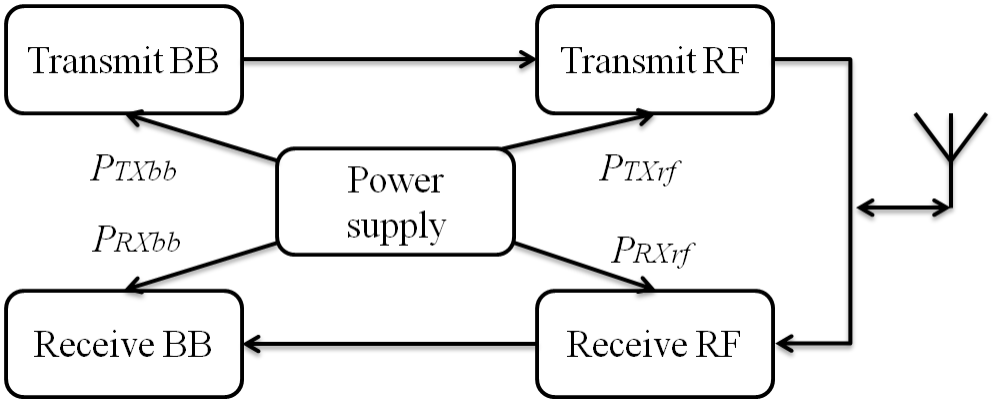

Figure 3-8 UE power consumption model.

In order to more effectively reflect the impact of LTE physical layer energy consumption, which affects the UE power consumption, a simplified energy efficiency model is adopted here [84], [85]. Figure 3-8 introduces the four power consumption parts following the simplification, which can be summarized as follows:

1). Transmit baseband part P_{TXbb}

2). Transmit radio frequency part P_{TXrf}

3). Receive baseband part P_{RXbb}

4). Receive radio frequency part P_{RXrf}

Assume that any user can be defined as being in one of two states, idle mode or busy mode; the four aforementioned power consumption parts are only considered for the user busy mode. Following these conditions, the UE power consumption model can be defined as:

$$P_{ue} = \alpha P_{idle} + (1 - \alpha) P_{busy} \qquad \textbf{Equation 3-8}$$

In the above equation, P_{ue} denotes the UE power consumption model, P_{idle} and P_{busy} represent the power consumption model when UE in idle or busy condition.

When the UE is in busy mode, the power consumption model can be further detailed as follows:

$$P_{busy} = \beta(P_{TX} + P_{TXrf} + P_{TXbb}) + (1-\beta)(P_{RX} + P_{RXrf} + P_{RXbb}) \quad \textbf{Equation 3-9}$$

Here, α and β are both logical variables that define the UE working state. The parameter, P, indicate different power consumption levels using different subscripts in each part, P_{TX} and P_{RX} represent the transmit power and receive power when the UE is in busy mode.

3.3.3. Base station power consumption model

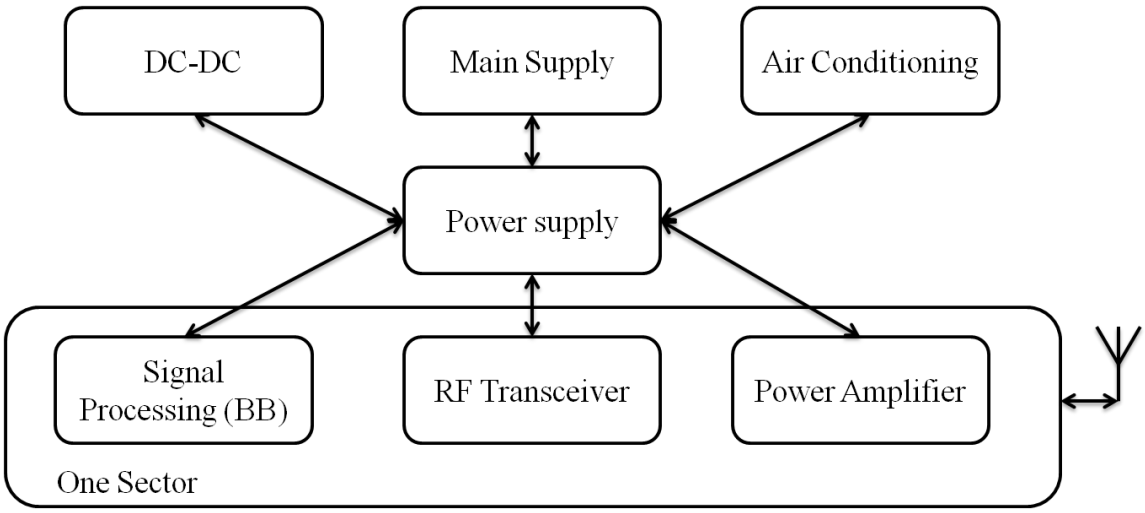

Figure 3-9 Macro cell power consumption model.

Two different power consumption models are adopted here to describe the macro and small cells in the HetNets system. For a typical macrocell [86]–[88], the main power consumption parts can be described as in Figure 3-9, which can be further derived as the following equation [89]:

$$P_{macro} = \frac{N_{sec}N_{PA/sec}\left(\frac{\gamma P_{PA}}{\mu_{PA}} + P_{RF} + P_{BB}\right)}{(1-\beta_{el/DC})(1-\beta_{el/M})(1-\beta_{el/CL})} \quad \textbf{Equation 3-10}$$

In the above equation, *Nsec* and *NPA/sec* represent the number of sectors in one base station, and the number of power amplifiers in each sector. The parameter, γ, is the load factor that represents the current loading of this cell; μ_{PA} denotes the power amplifier efficiency. The three power consumption factors in the molecular, which is represented by P_{PA}, P_{RF}, and P_{BB}, are the indicators of power consumption in the power amplifier, radio frequency, and baseband parts. The parameter, β, in the denominator, is a loss factor; three different loss factors are considered in this power consumption model: the DC converter factor, the mains electricity supply factor, and the cooling loss factor. Detailed small cell power consumption parts are shown in Figure 3-10.

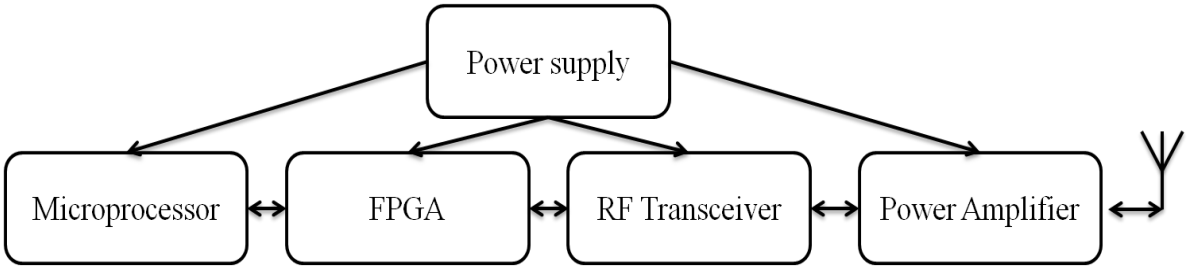

Figure 3-10 Small cell power consumption model.

Similarly, the small cell power consumption model [90] can be described as the equation shown below:

$$P_{small} = P_{tx} + P_{MP} + \frac{P_{PA}}{\mu_{PA}} + P_{FPGA} \qquad \textbf{Equation 3-11}$$

Compared to the macrocell power consumption model, the small cell model is simplified. Generally, the small cell is considered as having an omnidirectional antenna, which means only one sector is included. As the power consumption in the small cell is much lower than that of the macrocell, the cooling loss and DC-DC loss are not considered. The parameter, P_{MP}, is the power consumption of the microprocessor, which can also be regarded as the power consumed by the baseband

part. The only extra part here is the FPGA (field programmable gate array), which is used for authentication and encryption. A detailed power consumption model is shown in Figure 3-10.

3.3.4. Energy efficiency metrics

The energy consumption ratio (ECR), energy consumption gain (ECG), and energy reduction gain (ERG) are three metrics that are generally used for the evaluation of network system energy efficiency performance [91].

The ECR metric is used for the evaluation of energy consumed (E) when the system delivers (M) bits of data. This can be further derived as the ratio of system power consumption (P) over the system average throughput (R).

$$ECR = \frac{E}{M} = \frac{P \cdot T}{M} = \frac{P}{R} \qquad \textbf{Equation 3-12}$$

The ECG metric is generally used in the comparison of two different systems, which is represented by E1 and E2 in the equation below. When we substitute $E=M \cdot ECR$ into the ECG definition, the following function can be obtained:

$$ECG = \frac{E_1}{E_2} = \frac{M_1 \cdot ECR_1}{M_2 \cdot ECR_2} \qquad \textbf{Equation 3-13}$$

In order to compare two different systems more directly, the ERG metric was introduced, which can also reflect the gap in energy consumption between different systems in percentage. Both ECG and ERG was developed from the ECR metric.

$$ERG = \left(1 - \frac{1}{ECG}\right) \times 100\% \qquad \textbf{Equation 3-14}$$

The three models proposed in this section will be combined to evaluate system performance in the following section.

3.3.5. Energy efficiency and ping-pong handover self-optimisation algorithm

As handover occurs in a moving system, we can regard different time slots as different system states. Assuming the entire process comprising N time slots, which can be defined as N different systems, the energy variation of different time slots can be obtained. e.g., the energy consumption difference of time slot one to two can be expressed as $ERG_{timeslot1\text{-}2}$, which can be calculated as follows:

$$ERG_{timeslot1-2} = \frac{M_1 \cdot ECR_1 - M_2 \cdot ECR_2}{M_1 \cdot ECR_1} \times 100\% \quad \textbf{Equation 3-15}$$

The total energy consumed by the system is composed of the base station part and the UE part, which can be calculated as the summation of *Pue*, *Pmacro*, and *Psmall*, as follows:

$$P_{sum} = P_{ue} + P_{macro} + P_{small} \quad \textbf{Equation 3-16}$$

The core mechanism of the proposed algorithm can be described as follows: two threshold parameters can be obtained (system ERG and ping-pong handover ratio performance) through the sample of power consumption and SINR performance in each time slot. During each time slot, the network will feedback the conditions of ERG and ping-pong handover ratio, and compare them with the two threshold parameters. Following the comparison, the system will decide the optimisation directions of the next time slot (increase or decrease TTT and HM) to deliver better system performance.

Table 3-3 List of abbreviations.

Indicators	Explanations
HI_{HPPth}	The threshold of ping-pong handover ratio
HI_{ERGth}	The threshold of ERG value

C_HI_{HPP}	Current time slot ping-pong handover ratio indicator
HI_{HPPg}	Ping-pong handover ratio good performance indicator
HI_{HPPb}	Ping-pong handover ratio bad performance indicator
C_HI_{ERG}	Current time slot ERG value indicator
HI_{ERGb}	ERG value bad performance indicator
HI_{ERGg}	ERG value good performance indicator

Figure 3-11 presents a flow chart of the detailed handover optimisation step that is used in the proposed handover algorithm. Table 3-3 introduces the abbreviations of handover indicators that are used in the proposed algorithm. Following the initial phase, data are collected from the network to establish six threshold values as follows: HI_{HPPth}, HI_{HPPg}, HI_{HPPb}, HI_{ERGth}, HI_{ERGg}, and HI_{ERGb}. Among these six values, the subscript ending in *th* refers to threshold, *g* refers to good performance value, and *b* refers to bad performance value.

In Figure 3-11, parameters beginning in *HI* refers to a handover indicator, while those beginning in *C_HI* represent the current value of *HI*. The decision-making part can be divided primarily into four parts, as indicated in Figure 3-11. The first decision is the comparison of C_HI_{HPP} and HI_{HPPth}; then, the second part is carried out. If $C\_HI_{HPP} < HI_{HPPth}$, and $C\_HI_{HPP} < HI_{HPPg}$, we decreased the current threshold and good performance value, indicating that the current network status had good performance. The current threshold may not have been suitable for filtering; of this was not the case, the next optimisation step was initiated. Similarly, if $C\_HI_{HPP} > HI_{HPPth}$, and $C\_HI_{HPP} > HI_{HPPb}$, HI_{HPPth} and HI_{HPPb} were increased. The first two decisions checked ping-pong handover ratio; steps three and four decided system

energy efficiency, which was based on current system energy efficiency status. If both the condition $C\_HI_{ERG} > HI_{ERGth}$ and $C\_HI_{ERG} > HI_{ERGg}$ were fulfilled, we increased HM and TTT. On the contrary, if $C\_HI_{ERG} < HI_{ERGth}$, and $C\_HI_{ERG} < HI_{ERGb}$, TTT and HM needed to be decreased. After resetting the handover control parameters, the process moved to the next time slot.

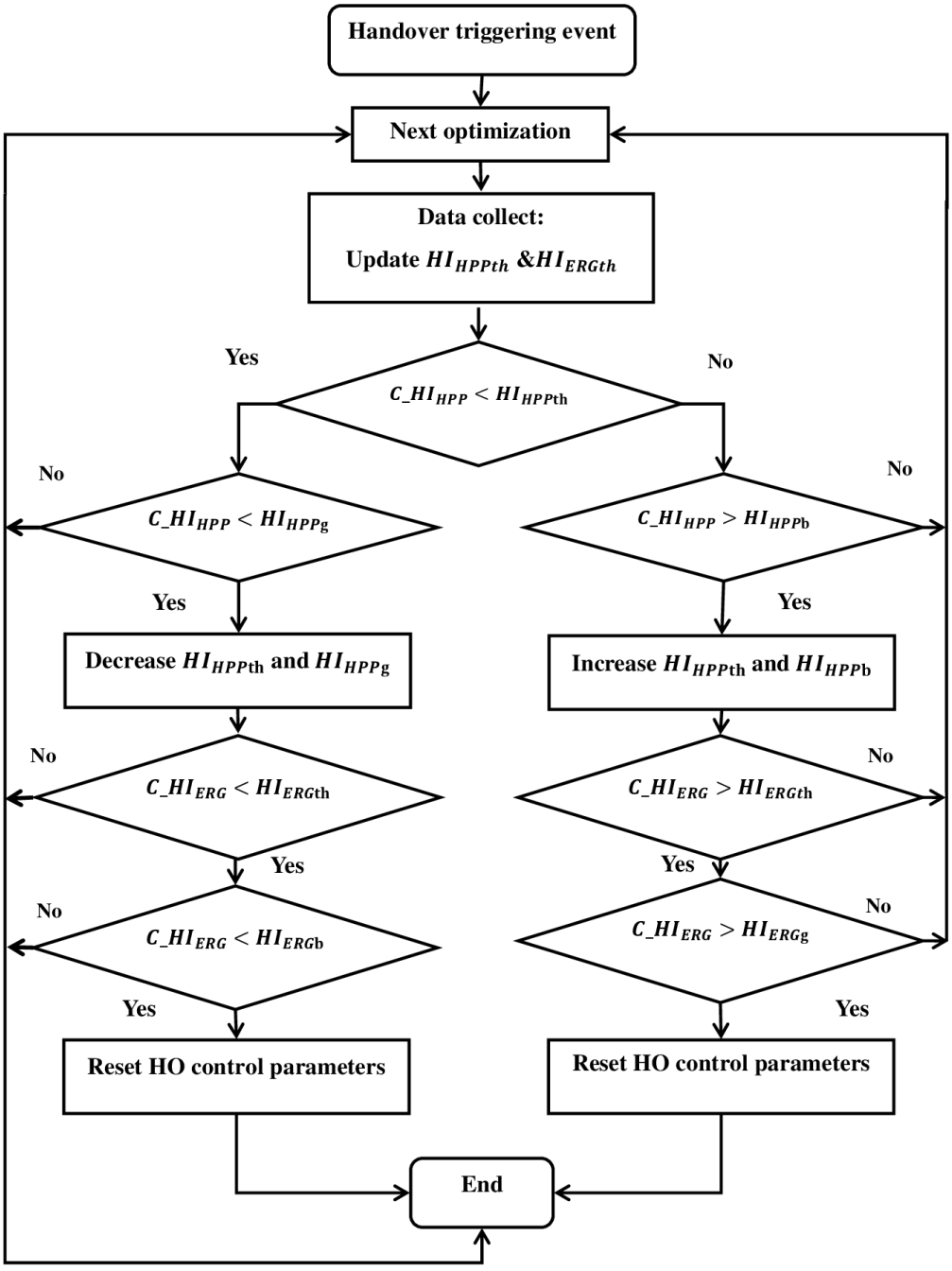

Figure 3-11 ERG and PPHO ratio self-optimisation flow chart.

3.3.6. Simulation and analysis

In this section, the simulation is analyzed to establish the proposed energy efficiency and ping-pong handover optimisation algorithm. The algorithm was tested in a 19-hexagonal macro base stations closely deployed environment, in which the small cells were randomly distributed. The detailed simulation parameters are listed in Table 3-4. the simulation environment was similar to that presented in section 3.2.3. 1000 UEs were randomly distributed in the scenario, and each UE assigned an initial speed and moving direction. At the start of each time slot, the UE will be randomly assigned a new moving speed and direction.

The entire simulation process comprised 200 TTIs, and each TTI lasts 10*ms*. In the initial phase, the system will collect basic data from network feedback, which included the system average SINR, system average throughput, system power consumption status, and the six handover performance indicators. Following data collection, the system will automatically check the system status and make comparisons with previous system feedback, following the proposed algorithm to make the decision of whether the system should change the handover control parameters for better system performance. After new parameters have been defined, the system will automatically enter a new optimisation step. The indicators will also be updated, which includes the most recent TTI information, the self-optimisation working mechanism is shown as this.

Figure 3-12 displays the ping-pong handover ratio optimisation results. In the beginning phase, there are nearly four TTI where no ping-pong handover occurs; this is because a ping-pong handover is defined as two separate handovers, during which the hand-in and hand-out cell must be the same serving cell. While the handover checking process waits for the TTT confirmation report, the two curves nearly

coincide, as previously noted; this is the data collection process. The first turning point appears near TTI 10, which is just about the first optimisation step working, both curves becoming stable in TTI 15. This happens because both UEs are becoming relatively stable. From TTI 15 to TTI 50, after the first reset of handover control parameters, the optimised curve moves gradually closer to the non-optimised curve; this is because according to the premise of ensuring the ping-pong handover ratio, the system will start optimizing system energy efficiency. At TTI 50 and TTI 70, two rapid decline points occur; however, tuning value differs slightly. This is caused by the self-optimisation mechanism of the system ping-pong handover threshold indicators. From a global perspective of the entire ping-pong handover ratio optimisation, the proposed algorithm provides an obvious optimisation effect.

Table 3-4 List of simulation parameters.

Parameters	**Values**
Macrocell transmit power P_{txm}	*46dBm*
Small cell transmit power P_{txf}	*24dBm*
Macrocell power amplifier efficiency μ_{PAm}	*31.1%*
Small cell power amplifier efficiency μ_{PAf}	*22.8%*
Macrocell power amplifier power P_{PAm}	*128.2W*
Small cell power amplifier power P_{PAs}	*2.4W*
DC-DC power supply loss $B_{el/DC}$	*7.5%*
Main supply loss $B_{el/M}$	*9%*
Cooling loss $B_{el/C}$	*10%*
Macrocell baseband power P_{BB}	*29.5W*
Macrocell RF power P_{RF}	*13W*
Microprocessor power consumption P_{MP}	*3.2W*
FPGA power consumption P_{FPGA}	*4.7W*

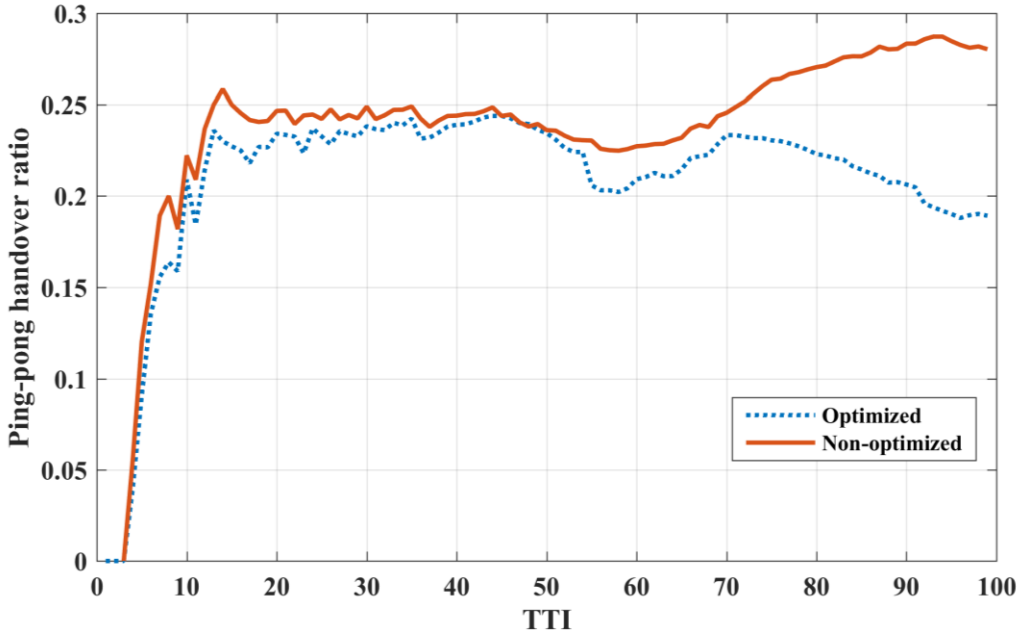

Figure 3-12 Ping-pong handover ratio optimisation result.

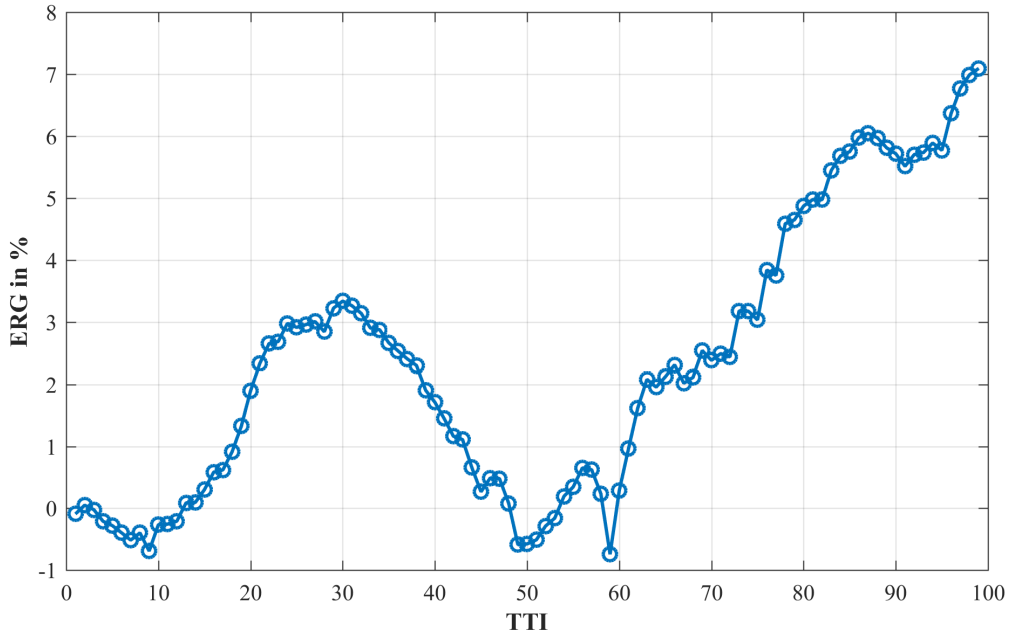

Figure 3-13 System energy efficiency optimisation result.

Figure 3-13 illustrates the optimisation result for system energy efficiency, which uses the ERG to create the result. As introduced in the previous section, the ERG is a comparison value of two different time slots (Equation 3-15). We considered the data collected from first TTI as the initial data. In TTI 0, the ERG

value is 0; from TTI 1 to 10, the ERG values are even negative; this is because the system is still in the data collecting phase. From TTI 10, when the first optimisation takes place, after checking the ping-pong handover ratio, when all conditions have been fulfilled, the resetting of system control parameters significantly increases the system energy efficiency in the next 40 TTI, and ERG value is positive. From the derivation in section two, it is easy to understand that when delivering the same bits, the optimisation system consumes much less energy. When system optimisation becomes stable, the value of ERG clearly approaches 0; when new optimisation steps start again at 50 and 60 TTI, the current system energy efficiency again increases significantly.

3.4. Summary

Two ping-pong handover ratio based control parameters self-optimisation mechanisms are proposed in this chapter. The process, from system setup to simulation results, was clearly introduced. The first algorithm aims to achieve optimisation of ping-pong handover ratio and the system average SINR performance. Various UE speeds were tested and via simulation, 3%, 4.5%, and 6% ping-pong handover optimised ratios were achieved, with respect to UE speeds of 120km/h, 60km/h, and 30km/h. The system average SINR also achieved improved performance. The second algorithm is an energy efficiency and ping-pong handover ratio self-optimisation algorithm. By applying this algorithm to the simulation, the system ping-pong handover ratio and energy efficiency was clearly optimised. The ping-pong handover ratio dropped nearly 5% and the system energy efficiency increased nearly 4%.

Chapter 4. An MCP-based performance evaluation of handover and load balancing in HetNets

Overview

HetNets have the advantage of assembling various cells into networks and enhancing users' QoS within the system. However, its development is constrained by two main issues: 1) load imbalance caused by different transmission powers for various tiers and 2) the unbalanced transmission power may result in unnecessary handovers. In order to solve the first issue, CRE can be applied to the system. This will benefit lower-tier cell range during the user association phase; while, the coordination of CRE, HM and TTT will be utilized to solve the second issue. However, the relationship of these parameters can be complicated and even reduce QoS if they are chosen incorrectly. This chapter evaluates the advantages and disadvantages of all three parameters and proposes an MCP based method in order to find optimal HM, CRE and TTT values. Subsequently, the simulations are carried out to obtain an optimal system total throughput.

4.1. Introduction

With the wide adoption of small cells, due to the shorter distance between the UE and the network, the weakening of signal strength due to path loss is improved. Another advantage of HetNets is that the data transfer rate is significantly increased, as spectrum reuse efficiency is improved [92]. However, HetNets come with a number of challenges as discussed in the following.

The first issue is load imbalance, which is caused by the different transmission powers of various tiers. Due to the structure of HetNets, UEs within the network may receive signals not only from the same tier, but also from higher tiers. Since UEs prefer to choose a signal with higher receiving power to obtain better user QoS, they may stick to higher tier cells and refuse to offload to lower tier cells. As a result, HetNets cannot operate efficiently if a higher tier cell is overloaded but there is a lower tier cell that is not being utilized [93]. The second issue is the handover problem. As mentioned earlier, different transmit power in different tiers may cause frequent handover, among which unnecessary handovers occupy a considerable proportion. System throughput is severely affected by unnecessary handovers.

In order to solve the first issue, 3GPP first introduced CRE in release 10. This parameter can be considered as a virtual bias that added to the actual UE received power part, which allows a UE to be served by a cell with lower received power, it is simple and typical one of alternative cell associations to enhance offloading, but on the other side, the adoption of CRE will cause downlink interference issue in not only data and also control channels. The CRE has became a practical power control technique in 3GPP standardization [94]. In a multi-tier network, most UEs are served by the macro cell due to its higher transmitting power and wider coverage area.

Compared to the macrocell, the transmitting power of a small cell is much lower; typically, the transmitting power of a macro and a small cell is 40 watts and 0.24 watts, respectively [95]. As a consequence, if traditional user association is adopted, most UEs will be allocated to the macrocell, which may lead to a macrocell overload and much worse QoS experience. With the utilization of CRE, the UEs' small cell receiving power strength is added with a CRE bias, which forces the UEs to be more likely to offload to small cells. This virtual bias limits macrocell load and stabilizes the UE when it travels around the cells' edges. At the same time, the unnecessary handover probability is also reduced, which increases network capacity [96]. However, CRE only focuses on the load balancing issue and does not take interference issues into consideration. Nevertheless, CRE will also change the UEs' handover position due to the coverage change by the small cells.

The second issue can be solved by the reasonable selection of different HM values to control the handover rate (HOR). As introduced in the previous section, the utilization of CRE will have a large impact on handover procedures. The determinant of CRE is normally based on cell load and network system performance and HOR is not considered when a CRE is chosen [32], [97]. As introduced in Chapter 2, a handover only occurs when the HM condition and TTT condition are both satisfied [98]. In a HetNets handover scenario, the two virtual biases, HM and CRE will each play a different role if the user is served by different cell types, namely a macrocell or a small cell. As introduced before, the HM parameter is permanently added on the serving cell side and as a result, when a UE is served by a small cell, the virtual bias that is added on the serving cell RSS should be HM + CRE and if a UE is served by a macro cell, the virtual bias should be HM - CRE. Figure 4-1 and Figure 4-2 depict the two virtual bias working mechanisms. In these two figures, the gray circle is the area

served by a small cell, which can be understood as where *RSSm* = *RSSs* happens. The blue circle represents the area served by a small cell plus CRE, which can be defined as *RSSm* = *RSSs* + *CRE*. The orange circle illustrates the HM bias added to the RSS of the cell providing service. As shown in the figure, when the UE moves from a macrocell to a small cell, the two virtual biases will cancel each other out. Whereas, if the UE is served by a small cell, when it is moving towards the macro cell serving area, the orange circle depicting the HM bias, which can be regarded as the real handover initializing position, greatly increases the area served by the small cell.

Both HM and CRE are virtual biases added to networks, but the directivity of these two parameters is different. A good combination of HM and CRE can not only increase system throughput, it can also reduce the HOR.

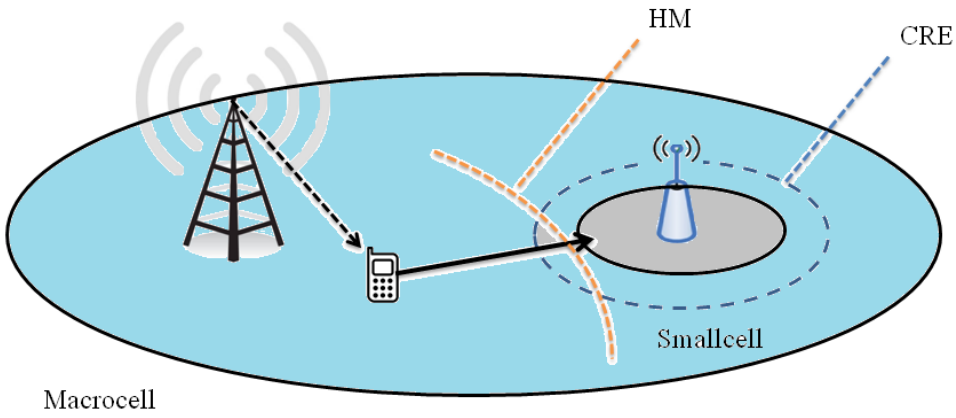

Figure 4-1 Handover from a macrocell to a small cell

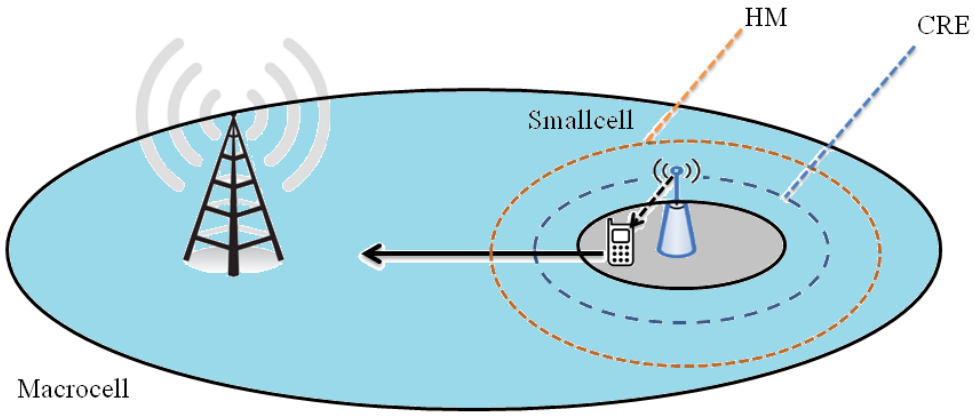

Figure 4-2 Handover from a small cell to a macrocell

The remainder of this chapter is organized as follows: in Section 4.2, the methodology of mapping HetNets into MCP is introduced, in Section 4.3, the system model is illustrated, after which the transition probability is calculated, and lastly, the simulation results are introduced in Section 4.4.

4.2. Methodology

4.2.1. Discrete Time Markov Chain (DTMC)

As introduced in Chapter 2, the DTMC is defined as a Markov stochastic process with countable states space, which only changes with the time step [99]. If the DTMC probability in state transfer process is not variable in accordance with a change of time, the DTMC is called stationary. However, if the transit probability is dependent on time variables, the MCP will have non- stationary transition probability, which is utilized in our modelling of a HetNets scenario.

4.2.2. Two-Tier HetNets Handover Model with MCP

The MCP is applied here for the model of the handover process and is further used to analyze the relationship of CRE, HM and TTT and their effects on UE

handover rate. Firstly, we applied DTMC to the model handover process so that all of the UEs' states could be represented by Markov States. TTT was divided into several TTIs and each TTI was defined as one step in the MCP. For each step, UEs will follow their mobility model and generate a new distance relationship to nearby cells, as with the transition matrix and status vector. According to the definition of TTT, a UE will not initiate the handover process unless its RSS is below the predefined threshold during the whole TTT. As a result, M states are considered as the status where UE is linked to a macrocell and S states are considered as the status where UE is linked to a small cell. Similarly, I and I' states represent the fact that an UE is undergoing the handover process, either from a macrocell to a small cell or from a small cell to a macrocell. Finally, this handover process loop can be transferred into an MCP, which is shown in Figure 4-3.

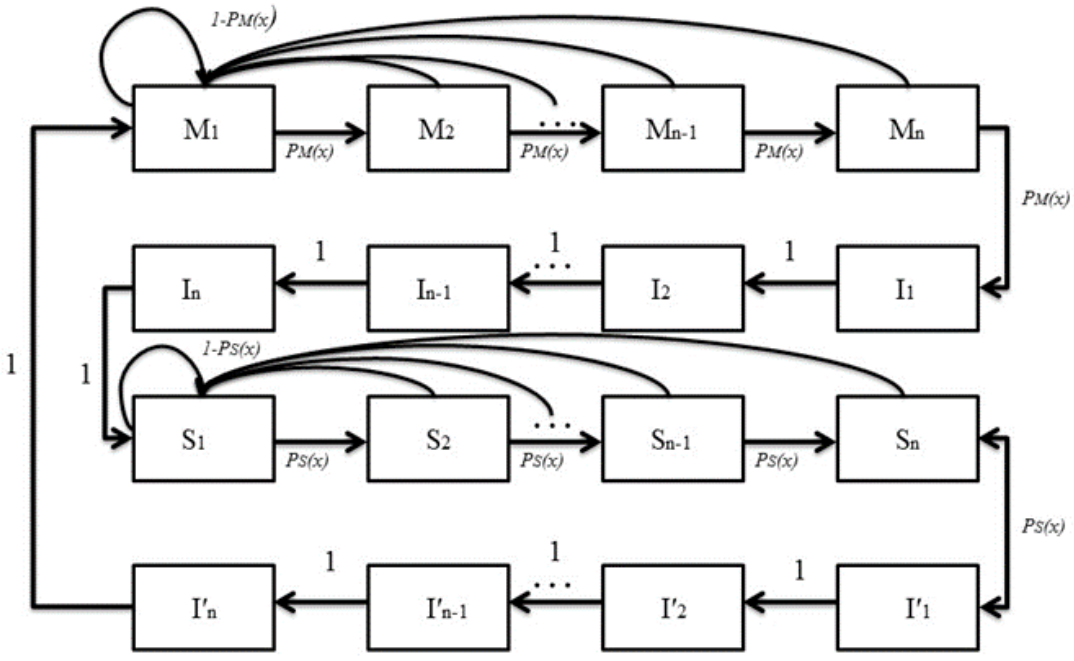

Figure 4-3 Markov Chain

In order to achieve the optimisation values for HetNets, the probability formula should be obtained using this MCP. Consider that an UE's initial state is M1,

which represents that it is bounded to a macro cell right now. Its probability of moving to the next state, M2 is PM(x); meanwhile, its probability of moving back to itself is 1 - PM(x). The same rule applies for all M states until Mn transfers to I1, which means that a handover is triggered. Within I states, there is a 100% chance that it will move to the next I state until the handover process is finished and the UE has been reallocated to a small cell that is in the S1 state. The rules for S and I' states are the same as for M and I states; thereby, the whole MCP loop is established. One important property for I and I' states is that traffic signals play a dominant part in guaranteeing the handover process during these phases. Consequently, an UE can barely receive an information signal during handover states and too many handover phases dramatically reduces an UE's QoS.

Transfer Matrix *T* can be obtained following the MC process after its transition probability has been defined. Table 4.1 lists the transition probability used for our simulation. It is a four-state transition matrix.

Table 4-1 Markov Transition matrix (T)

	M1	M2	M3	M4	I1	I2	I3	I4	S1
M1	$1-PM(x)$	$PM(x)$	0	0	0	0	0	0	0
M2	$1-PM(x)$	0	$PM(x)$	0	0	0	0	0	0
M3	$1-PM(x)$	0	0	$PM(x)$	0	0	0	0	0
M4	$1-PM(x)$	0	0	0	$PM(x)$	0	0	0	0
I1	0	0	0	0	0	1	0	0	0
I2	0	0	0	0	0	0	1	0	0
I3	0	0	0	0	0	0	0	1	0
I4	0	0	0	0	0	0	0	0	1

	S1	S2	S3	S4	I'1	I'2	I'3	I'4	M1
S1	$1-Ps(x)$	$Ps(x)$	0	0	0	0	0	0	0
S2	$1-Ps(x)$	0	$Ps(x)$	0	0	0	0	0	0
S3	$1-Ps(x)$	0	0	$Ps(x)$	0	0	0	0	0
S4	$1-Ps(x)$	0	0	0	$Ps(x)$	0	0	0	0
I'1	0	0	0	0	0	1	0	0	0
I'2	0	0	0	0	0	0	1	0	0
I'3	0	0	0	0	0	0	0	1	0
I'4	0	0	0	0	0	0	0	0	1

The transition matrix shown in Table 4-1 is the detailed transition probability, in which the leftmost column is the current state and the top row represents the next state. For example, in the matrix, the state S4 got a probability of 1- Ps(x) of moving back to S1 and a probability of Ps(x) of moving towards I'_1. The probability of moving to rest 14 state is 0. In the matrix, this is clearly displayed with a row and column value. The sum of each row equals 1. The two matrixes should be connected together to form a 16 by 16 state transition matrix.

After the setup of the probability transition matrix, the state probability vector *V* at *x-th* step can be calculated as Equation 4-1

$$V_x = V_1 \prod_{i=1}^{x} T_i \qquad \textbf{Equation 4-1}$$

In Equation 4-1, the *V1* is the probability of the UE's initial state, which is expressed as 1 in the vector. For example, if a macro cell's UE is in the state *M1* in time 1, then its initial probability vector will be expressed as *[1,0,0...0]*. When the TTI increases, the UE moves, which causes the probability of *Pmx* and *Psx* to change

in the Markov Transition matrix (*T*). According to Equation 4-1, the vector *V* will also change. As a result, the vector for any UE at any step *x* can be calculated, so that the HOR in each state is obtained.

4.3. System Model

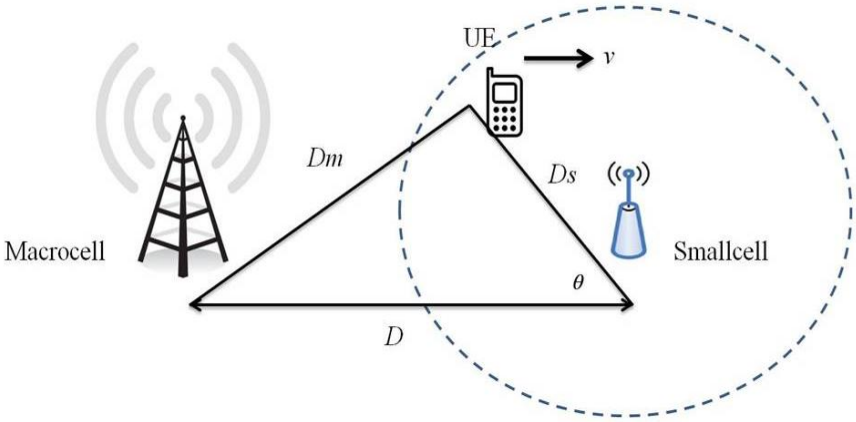

Figure 4-4 Two-Tier HetNets System Model

Figure 4-4 displays the system model used in this chapter. As we can see from it, a single macro-small cell scenario is adopted here. The cell radius of the macro cell is set to be 1 kilometer and the total simulation area is set to be a two by two square kilometer field. From the figure, it can be seen that a small cell is placed at a distance of D from the macro cell. For any UE inside the coverage, three parameters are assigned to it: the distance to the macro cell (*Dm*), the distance to the small cell (*Ds*), and an initial moving speed (*v*).

Using the aforementioned three parameters, the mobility model of the UE can be determined. The fact that each UE has an initial location information, moving speed and moving direction that is associated with the current serving cell from time slot 1, which is represented by TTI 1, is considered. The current serving cell at TTI 1 is decided by the receive signal strength (RSS) from different cells, *RSSm* and *RSSs*.

After TTI 1, the UEs will begin to move as its assigned mobility model until TTI reaches 100. Due to the change of locations, the UE's distance to the macrocell (Dm) and the small cell (Ds) will change accordingly. When the UE moves towards the small cell boundary and the RSS of the serving and target cells, represented by RSS_S and RSS_T, satisfy the Equation 4-2 concerning TTT time, a handover will occur.

$$RSS_{\text{Target}} \geq RSS_{Serving} + HM \qquad \textbf{Equation 4-2}$$

Note that, as mentioned before, the CRE is always added to the small cell side; therefore, the handover condition should change further to two different conditions, which can be described by the following equations: Equation 4-3, which represents the handover from small cell to macrocell, and Equation 4-4, which is the handover from macrocell to small cell.

$$RSS_{M\text{acro}} \geq RSS_{Small} + HM + CRE \qquad \textbf{Equation 4-3}$$

$$RSS_{Small} + CRE \geq RSS_{M\text{acro}} + HM \qquad \textbf{Equation 4-4}$$

Due to the HetNets scenario applied in this chapter, two different pathloss models were adopted for different tier UEs. The pathloss models for the macro cell and the small cell UEs can be expressed as Equation 4-5 and Equation 4-6, respectively. The distance (d) is in kilometers.

$$\delta_{M,t,k} = 128.1 + 37.6 log_{10}(D_{M,t,k}) \qquad \textbf{Equation 4-5}$$

$$\delta_{S,t,k} = 140.7 + 36.7 log_{10}(D_{S,t,k}) \quad \textbf{Equation 4-6}$$

The $\delta_{M,\,t,\,k}$ can be understood as the pathloss of k UE at time slot t with macro cell M. Similarly, the small cell pathloss is represented as $\delta_{S,\,t,\,k}$. Based on Equation 4-5 and Equation 4-6 (in dB scale), the $RSS_{i,t,k}$ of a certain UE allocated to a certain cell at each time slot can be calculated.

$$RSS_{i,t,k} = Pt_{i,t,k}\delta_{i,t,k}\xi_{i,t,k} \quad \textbf{Equation 4-7}$$

Note that, the above equation is calculated in linear scale, the Pt represents the base station transmit power, while $\xi_{M,\,t,\,k}$ and $\xi_{S,\,t,\,k}$ are the shadow fading components. As stated before, here, only single macrocells and single small cells are being considered. The SINR expression is as follows:

$$SINR_{i,t,k} = \frac{Pt_{i,t,k}\delta_{i,t,k}\xi_{i,t,k}}{Pt_{j,t,k}\delta_{j,t,k}\xi_{j,t,k} + \sigma^2} \quad \textbf{Equation 4-8}$$

In Equation 4-8 (linear scale), the numerator represents the receiving signal strength, which is affected by variables i, t, and k. Similarly, the interference is the summation of the surrounding cells' signal strength and is expressed by the first part of the denominator, while the second part, σ^2 is the thermal noise.

4.3.1. Defining the Transition Probability

Since all the states' physical meanings and the system model are understood, it is possible to establish a transition probability formula, which is *PM(x)* and *PS(x)* in

Figure 4.3 (x is the number of TTI). In MCP, this represents the chance to continue checking handover status. As long as a UE receives signals from both a macro cell and a small cell, the probability will move to the next state until the handover process. Therefore, the MCP transition probability is defined as follows: consider a small cell UE stays in the S state, it will receive signals not only from a macrocell ($RSS_{M,x,k}$), but also from a small cell ($RSS_{S,x,k}$). These two signal powers will compete to transfer the UE from the S state to the I' state. When RSS_M,x,k becomes greater than RSS_S,x,k plus the threshold, it will lead to a situation where the UE has the intention to initiate the handover process and is reluctant to stay in a small cell network. The opposite will occur if RSS_S,x,k is larger. At this time, HM bias, α and CRE bias, β will increase the weight of RSS_S,x,k and constrain the UE from moving back to the macrocell, which is depicted in Equation 4-12. In Equation 4-13, however, they may play the opposite role, as CRE has another function, namely offloading the UEs from the macrocell to the small one.

The condition for a handover from a macrocell to a small cell is defined in Equation 4-9, considering the transition matrix, which is also the transition probability for a UE to move from a current M state to the next states. The condition for handover is expressed by the following probability equation:

$$\begin{aligned} P_M[\alpha RSS_M < \beta RSS_S] &= P_M[\alpha Pt_M \delta_M \xi_M < \beta Pt_S \delta_S \xi_S] \\ &= P_M[\frac{\xi_M}{\xi_S} < \frac{\beta Pt_S \delta_S}{\alpha Pt_M \delta_M}] \\ &= 1 - P_M[\frac{\xi_M}{\xi_S} > \frac{\beta Pt_S \delta_S}{\alpha Pt_M \delta_M}] \end{aligned} \qquad \textbf{Equation 4-9}$$

In the system model, ξ_M and ξ_S are defined as the shadow fading, which follows the Rayleigh distribution with a unit mean and are independent, which are exponential

random variables. In Equation 4-9, the right side, $\frac{\beta Pt_S \delta_S}{\alpha Pt_M \delta_M}$ can be regarded as a constant whenever it is being mapped into a system, as the UE distance to a macrocell and a small cell is pre-defined as known variables, which are expressed as *Dm* and *Ds*. $\frac{\beta Pt_S \delta_S}{\alpha Pt_M \delta_M}$ is a constant, which when simplified, is expressed as *B*. $P_M[\frac{\xi_M}{\xi_S} > \frac{\beta Pt_S \delta_S}{\alpha Pt_M \delta_M}]$ can be expressed as:

$$
\begin{aligned}
P_M[\frac{\xi_M}{\xi_S} > \frac{\beta Pt_S \delta_S}{\alpha Pt_M \delta_M}] &= P_M[\frac{\xi_M}{\xi_S} > B] \\
&= P_M[\xi_M > B\xi_S] \\
&= \iint_{\xi_M > B\xi_S} f_{\xi_M,\ \xi_S}(u,v)dA_{u,v} \\
&= \int_0^\infty \int_{B\xi_S}^\infty f_{\xi_M}(u)\, f_{\xi_S}(v)dudv \\
&= \int_0^\infty f_{\xi_S}(v) \int_{B\xi_S}^\infty f_{\xi_M}(u)dudv \\
&= \int_0^\infty (e^{-Bva}) ae^{-va} dv \\
&= \frac{1}{1+B}
\end{aligned}
$$

Equation 4-10

Then, the probability of $P_M[\beta RSS_S < \alpha RSS_M]$ can be obtained, which is:

$$
P_M[\alpha RSS_M < \beta RSS_S] = 1 - \frac{1}{1+B} = \frac{B}{1+B}
$$

Equation 4-11

As we substitute $\frac{\beta Pt_S \delta_S}{\alpha Pt_M \delta_M} = B$ for PM, the transition probability of PM(x) to PM (x+1) can be calculated as follows:

$$P_M(x) = P_M[\alpha RSS_M < \beta RSS_S] = \frac{\beta Pt_S \delta_S}{\alpha Pt_M \delta_M + \beta Pt_S \delta_S} \quad \textbf{Equation 4-12}$$

Similarly, the transition probability of *Ps*(x) to *Ps*(x+1) is:

$$P_S(x) = P_S[\alpha\beta RSS_S < RSS_M] = \frac{Pt_M \delta_M}{Pt_M \delta_M + \alpha\beta Pt_S \delta_S} \quad \textbf{Equation 4-13}$$

After the two important transition probabilities of Transition matrix *T* are obtained, the model of UEs' handover process affected by HM and CRE is established.

4.4. Performance Evaluation

In this section, a simulation is completed to analyze the CRE, HM and TTT under different combinations. The simulated parameters are summarized in Table 4-2. All the simulations were performed by the MATLAB.

Table 4-2. List of Simulation Parameters

Parameters	Value
Carrier frequency	1800 MHz
Bandwidth	1 MHz
Cell layout	Single macro cell and small cell
Transmit power of macro cell	40 W/46 dBm
Transmit power of small cell	0.25 W/24 dBm
Noise power	-174 dBm
Number of TTI	100
CRE	1-10 dB
HM	1-10 dB
TTT	40, 60, 80, 100 ms

Firstly, the conventional user association combining with CRE to offload UEs scenario is tested. Whenever a macrocell UE satisfies the handover condition, it will

be directly offloaded to small cell without considering handover phases (there will be no 0 capacity during any TTI, but also no buffer time for UE, only result is focused). **Figure 4-5** displays how system total capacity affected by CRE when considering cross-tier interference. It is obvious that CRE has negative effect on system capacity, since it only focus on solving load balancing issues, and even increase the cross-tier interference. This effect is mild in the initial phase and will be severe with CRE value increases, especially after 9 dB. This shows that less macro UEs will be affected in low CRE value condition, and those remain in macrocell may ignore cross-tier interference due to high transmit power. However, more UEs are forced to offload towards small cell with CRE grows, and even central UEs of macrocell will be affected. These UEs are more vulnerable to cross-tier interference and will suffer huge QoS loss. The system total capacity for different CRE values are shown below, curve fitting is adopted to continuous plot, which can display the variation trend.

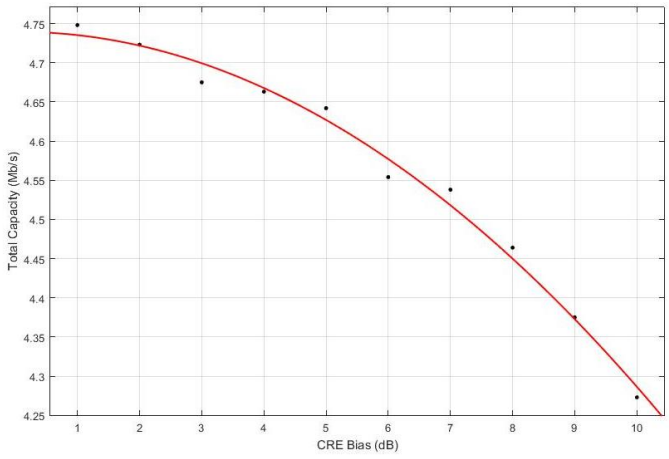

Figure 4-5 Total Capacity vs. CRE for conventional model

$$\mathbf{Y=-0.004561x^2+0.0002939x+4.739}$$

Secondly, the proposed MCP handover model is adopted to analyse how CRE affects handover rate for the system. Since the positive effect of CRE mainly reflects on the reduction of UE's HOR (which means less I or I' states during the process), we

keep the UE partition with 1 dB CRE to ignore its effects on offloading even if CRE bias increases. And then combine the capacity of each UE with its HOR obtained through MCP under current CRE (we suppose there is no data rate during I and I's states). Figure 4-6 displays the system total capacity changes with CRE when MCP is adopted. The result of MCP model is obviously opposite to the previous model, CRE will take positive effects on capacity due to its ability of controlling ping-pong handover. However, Figure 4-9 also shows its effect will fade with the increasing of CRE. This phenomenon is caused by the property of ping-pong handover. According to MCP, if CRE is large enough, the unnecessary handover probability will be significantly minimized, therefore less ping-pong handover will occur and the benefit of CRE will be diminished. The system total capacity for different CRE values when using MCP model is shown below, to display the variation trend, curve fitting also adopted to continuous plot.

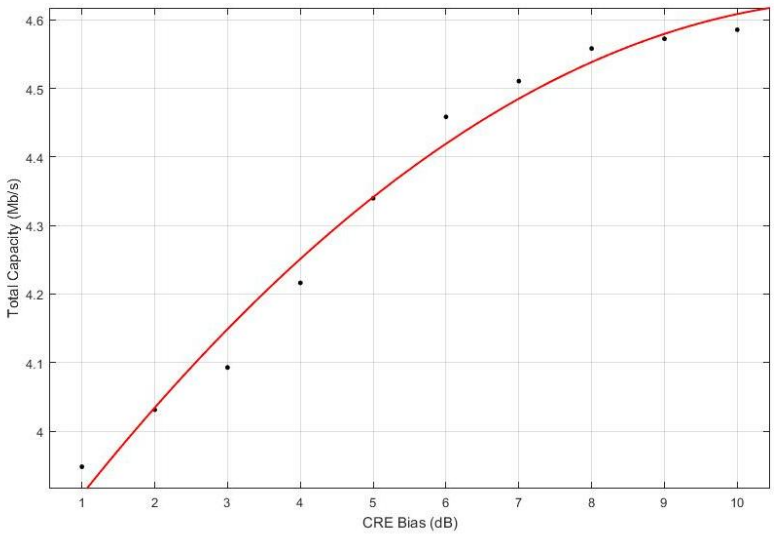

Figure 4-6 Total Capacity vs. CRE for MCP model

Therefore, the optimal CRE can be obtained with the help of the two curves. As we plot two curves according to their expression on the same graph, in Figure 4-7,

and the equilibrium point can be represented by the intersection of the HOR effect curve and the cross tier interference curve. Before the point, the positive effect of CRE is not fully exploited, after this point, the negative effects of CRE will be enlarged, since even core UEs may be affected. As a result, the point CRE *=7* is the nearest one to equilibrium point and is presumed to be the optimal CRE bias for offloading.

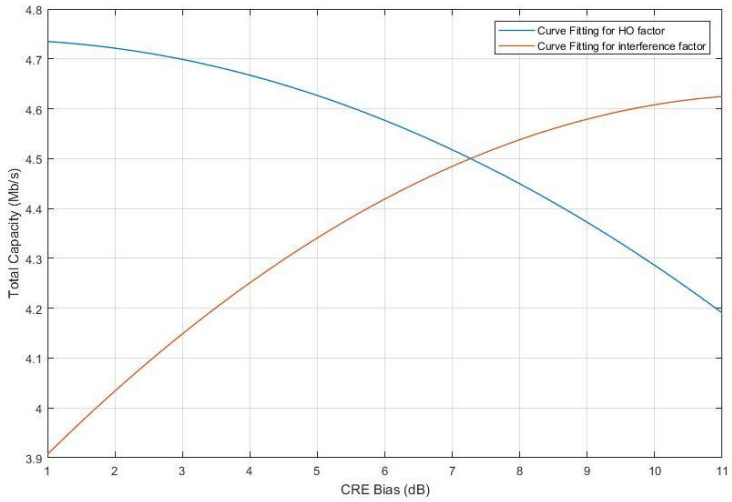

Figure 4-7 Combination of conventional model and MCP model curves

After the analysis of CRE effect for the system offloading performance, the handover performance is evaluated. Figure 4-8 and Figure 4-9 show how handover rates react to CRE and HM when TTT equals 60 ms.

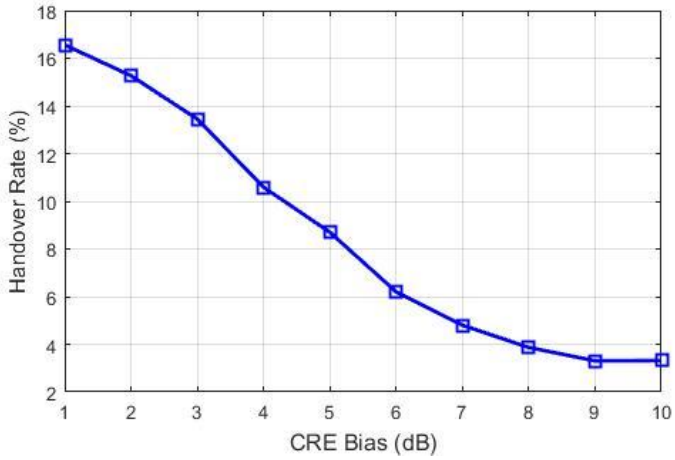

Figure 4-8 Handover Rate Versus CRE in TTT = 60 ms

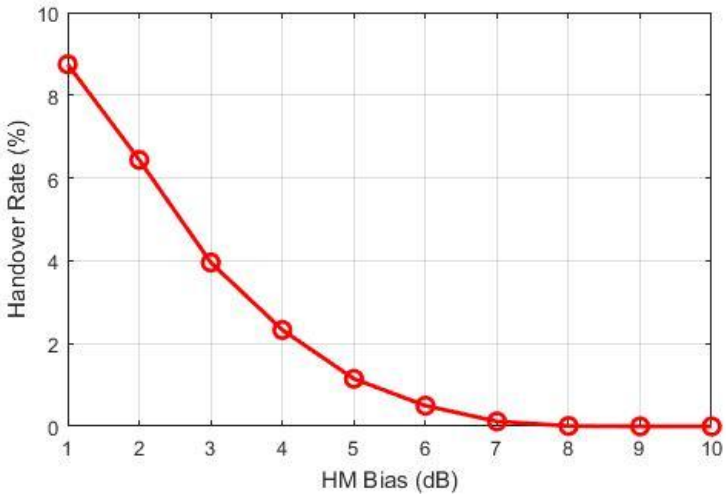

Figure 4-9 Handover Rate Versus HM in TTT = 60 ms

In general, it can be summarized as, the handover rate will decrease with the increasing in HM or CRE. However, their degree of influence may differ in many aspects. Firstly, the effect of CRE decreases rapidly and can be neglected when it reaches 9 dB, where handover rate stands still. While HM's effect on handover rate keeps increasing and achieves its limitation when HM reaches 7 dB. Secondly, the starting and ending point of CRE and HM is different. HM can reduce a handover rate from 9% to almost 0%, while CRE can only reduce it to around 3%. All of these phenomena display the superiority of HM in handover control and the reason can be

obtained from the MCP probability formula and the physical meaning of two parameters. As explained in the Section 4.1, the main target of HM is to bind the UE to its original serving cell, which includes both the handover from macrocell to small cell or from small cell to macrocell. On the other hand, the CRE has another function, namely offloading UE serving by macrocell to small cells, so that decent HetNets network efficiency can be maintained. As a consequence, the HM and CRE might have the counter influence in handover control when UE handover from a macrocell to a small cell. This also explains why the handover rate will remain 3% no matter what CRE value the network has. However, the HM's effect on the increasing total throughput is limited due to its lack of offloading effect on HetNets. Its rapid effect on handover control also restricts HM bias so that it may not reach a large value. Therefore, an optimal combination of CRE and HM value is required for HetNets.

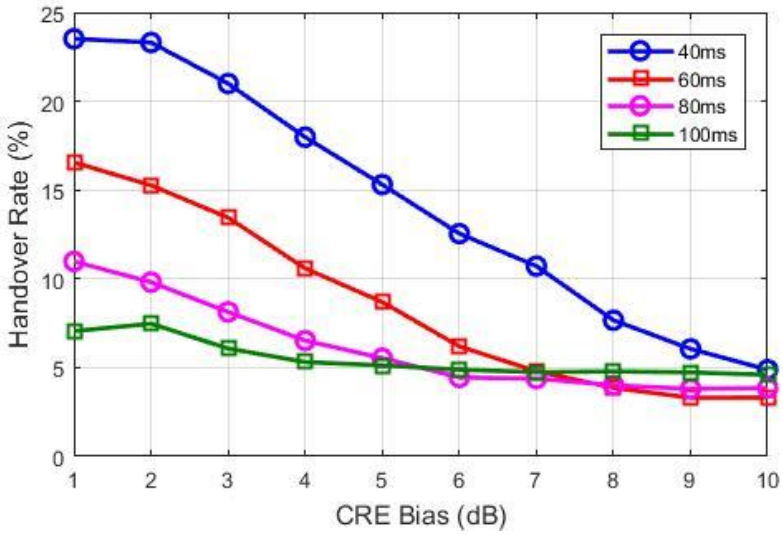

Figure 4-10 Handover Rate Versus CRE Under Different TTTs

Figure 4-10 presents the handover ratio variation trend according to different TTT values. It can be observed that four curves all have the same trend. With an increase in CRE bias, the handover ratio gradually decreases. The reason for this is that with the increase in CRE bias, the virtual coverage of the small cell grows as well

and the UEs originally at the small cell boundary are restrained to handing over from a small cell to a macrocell. With the increase in TTT value, the beginning handover ratio drops significantly from 24% to 7%. The suggestion of TTT that can effectively control the handover ratio is displayed. The end point of each curve nearly coincides, as the handover ratio controlled by CRE reaches a limit of around 5%. This can be explained by Equation 4-12, as the CRE can only affect the offloading from a macrocell to a small cell by increasing the weight in the equation.

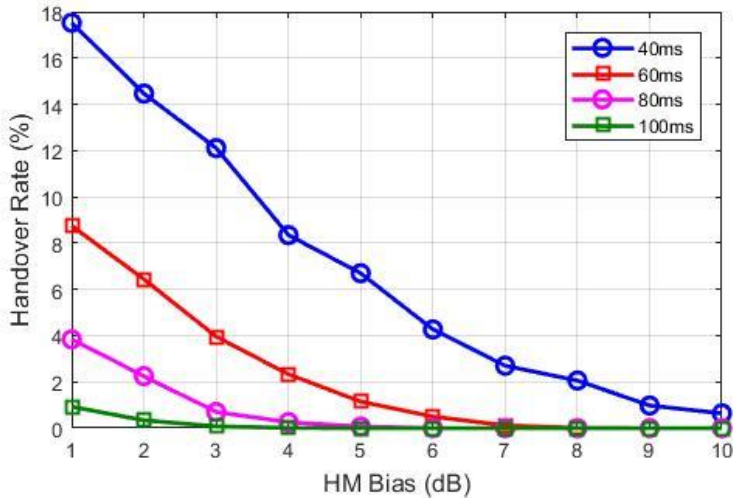

Figure 4-11 Handover Rate Versus HM Under Different TTTs

Figure 4-11 demonstrates how handover rate changes with HM Bias for different TTT values. It shows that TTT has a significant effect on handover rate control, which follows the prediction of MCP as well. It can be reflected by two aspects: initial point and reaching-zero bias. When TTT equals 40 ms, the handover rate's initial point is up to 18%, after which it drops rapidly to below 2% when the TTT is set to 100 ms. Besides this, HM's reaching-zero point is further limited as TTT increases. It is only 2 dB when the TTT is 100 ms. In other words, using a selected TTT value, HM's side effect on system total throughput may be mitigated. Compared to the influence in handover ratio affected by CRE (3.5% to 24%), the range of handover ratio variation is relatively narrow (0 to 18%).

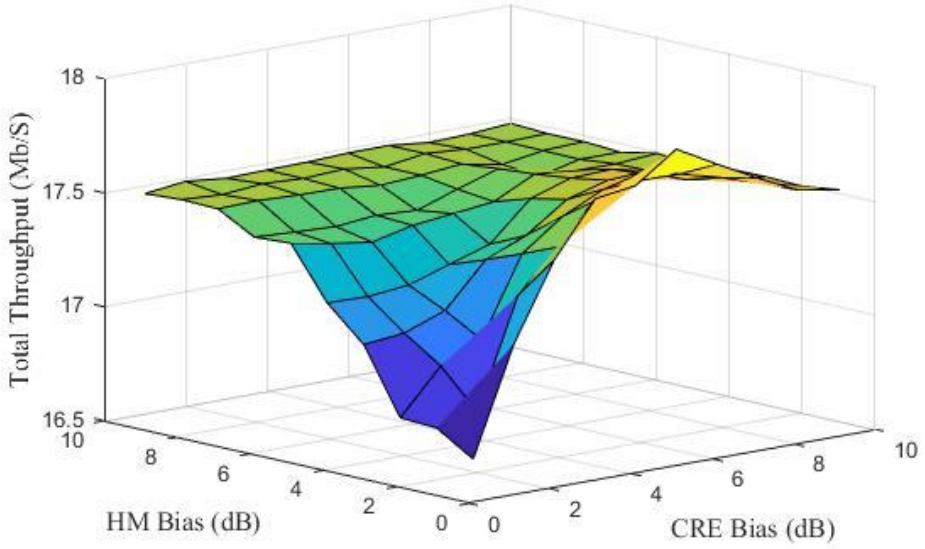

Figure 4-12 System Total Throughput Versus CRE and HM

By analyzing the relationship between CRE, HM and TTT, how the handover ratio is affected by the three parameters is identified. Figure 4-12 displays the influence that HM and CRE have on the system total throughput. The minimum point can be easy observed as the HM and CRE values equal 0. At this point, no vital biases are added to the serving cells and frequent unnecessary handovers significantly decrease system performance. In addition, the maximum value is not achieved by CRE and HM, which are both set at 10 dB. This is because a handover setting that is too large significantly constrains and affects system SINR performance; hence, the system total throughput is reduced. According to this figure, when HM and CRE are 1 dB and 6 dB, the optimal total throughput is obtained.

4.5. Summary

In this chapter, handover performance is evaluated by modelling the HetNets scenario into an MCP. With a combination of MCP, handover phases can be represented as a probability mode. As a result, the handover ratio and system total throughput can be realized and simulated. With a combination of CRE, HM and TTT, the handover performance index of the handover ratio is analyzed in detail. The relationship between CRE and HM is clearly identified and through the coordination of CRE and HM, optimal system total throughput is achieved.

Chapter 5. Adaptive HM and TTT selection scheme

Overview

Handover decisions and initiation depend on various situations, which mainly include the system parameters and environmental problems. The vast majority of these decisions are based on the RSS, and the HM plays a key role in mitigating unnecessary handovers. The decision of HM not only affects the handover performance in the system, but also significantly influences the serving cell coverage. In order to achieve a better coverage and handover probability, a dynamic HM selection scheme based on UE distance to serving cell is proposed. Another handover control parameter, the TTT, can effectively control the system's ping-pong handover performance but, in the meantime, larger value of TTT selection may result in radio link failure (RLF). In order to control the system RLF performance and provide a relative good ping-pong performance, an adaptive TTT selection scheme based on UE moving speed is proposed. By combining the two adaptive selection schemes, a new

system self-optimisation mechanism based on individual UE mobility status is proposed.

5.1. Introduction

In traditional systems, the HM and TTT are normally assigned a fixed value for all UEs, even if they are in different mobility states. Various studies have been carried out that focus on optimisation through dynamical controlling of the parameters [100]. In Chapter 3 and 4, fixed control parameters for all UEs have already been investigated for handover decisions and handover performance. However, fixed parameters for an arbitrary UE in the entire network is not reasonable, as different UEs have different mobility states. In this chapter, the aim is to generate a pair of proper HM and TTT for any UE at any time.

In order to make a decision about selecting the proper HM and TTT, it is important to define the UE moving states since, in modern networks, most cellular phones are already embedded in global positioning system (GPS) services. The status of the UE moving speed and that of the distance to each base station are easy to identify. Based on the UE's distance to its serving cell, the HM can be adaptively selected. The main idea behind the adaptive HM selection scheme is to formulate a function that is related to the distance between the UE and its serving cell; the further the UE is to the serving cell, the smaller the HM that is chosen. As this mechanism can efficiently control the handover probability within the cell serving area, the UE linked to its serving cell is strongly enhanced while the UE is inside the coverage.

It is hard to control the handover parameter TTT through detecting the UE's location, as TTT is a parameter related to the time domain. In order to formulate an adaptive TTT selection scheme, the UE moving velocities are taken into consideration. As the same TTT value will have a different effect according to different UE moving speeds, too small a TTT will result in frequent ping-pong handovers, but too large a

TTT can cause severe RLF [101]. In order to form a suitable TTT selection scheme, under the premise of maintaining certain RLF performance, the TTT is selected as the largest value to ensure the ping-pong handover performance.

Based on the adaptive HM and TTT selection mechanism, a network can simply decide the individual parameters for arbitrary UEs inside its coverage according to the mobility status of the UE.

The work in this chapter is organized as follows. In Section 5.2 an adaptive HM algorithm is proposed and verified in two scenarios. Section 5.3 introduces the adaptive TTT selection mechanism. Joint optimisation through a combination of adaptive HM and TTT is proposed in Section 5.4.

5.2. Adaptive HM selection scheme

5.2.1. Adaptive HM mechanism in macrocell only scenario

The definition of HM has been introduced in Chapter 2, and this is adopted for the minimisation of unnecessary handovers. In typical handover system models, the value of the HM is normally chosen as a constant for the entire system; however, this may be unreasonable for the actual scenario. For example, when a higher value of HM is chosen for the system, the mobility performance of UEs at the cell centre may not be affected, but the cell boundary UEs will be significantly influenced by the HM value. Even if the UEs have already moved into a good coverage of the neighbouring cells, it is still bound to the original serving cell.

The chosen of adaptive HM values are based on considering the UE's distance to its serving cell and the distance to the cell boundary. The purpose of the chosen HM mechanism is to bind the UE to its serving cell if it is inside the serving cell

coverage. In other words, the value of the HM should follow this principle: when the distance from the serving cell to the UE is increased, the HM value should decrease until the UE reaches the cell boundary, which leads to the minimum value when the UE is on the cell boundary or exceeds the cell serving region.

$$HM_{\text{adaptive}} = \max\left\{ HM_{\max}\left[1-\left[\frac{d_{serving}}{R_{cell}}\right]^{\alpha}\right],\ HM_{\min}\right\} \qquad \textbf{Equation 5-1}$$

The above equation interprets the HM chosen mechanism. In the equation, the indicators HM_{max} and HM_{min} determine the variation interval for the HM values; normally, the value of HM_{max} is *10*dB and HM_{min} is predefined as *0*. The distance between UE and its serving cell is represented by $d_{serving}$, and R_{cell} is the predefined cell serving distance, which will be clearly defined in the later simulation part.

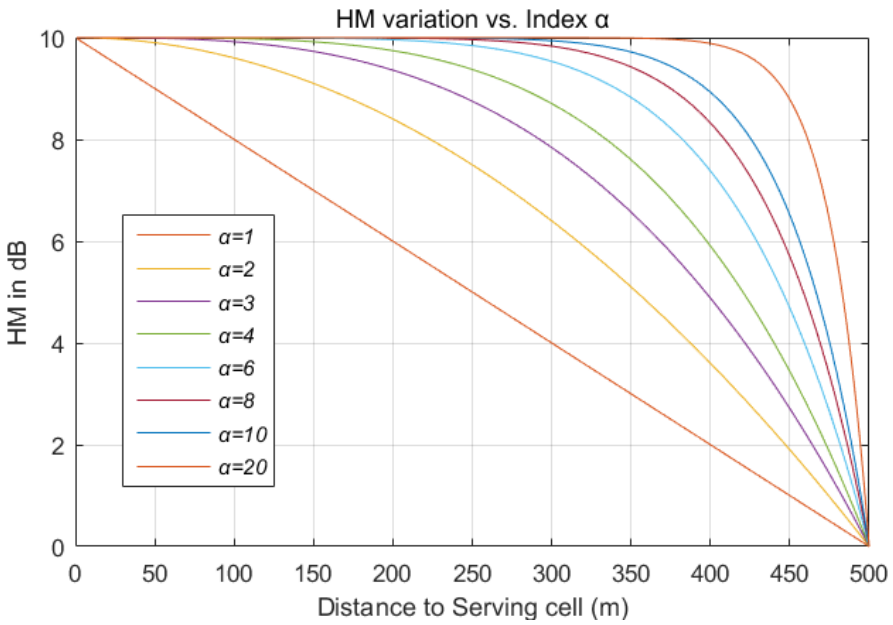

Figure 5-1 HM variation vs. *α*

The index α applied here is for deciding the trend for the HM variation. Figure 5-1 displayed the HM variation trend when index α with different values. We can see from figure that, with the increasing of UE distance to serving cell, the variation trend of HM is mild when the UE is near serving cell, and rapid decreasing will appear when UE approaching the serving cell boundary. with the increasing of α value, the rapid turning point of HM will getting closer and closer to the cell boundary. in order to easy calculate the handover probability, we set 4 as the default value of α. As the HM decrease progressively with the increasing of UE distance to serving cell, by applying this equation to an RSS-based handover decision, the effect of the adaptive HM mechanism can be achieved.

5.2.2. HO probability optimisation based on adaptive HM

5.2.2.1. RSS calculation

The handover here is regarded as being based on the received signal strength; as mentioned in the previous sections, the handover will be initiated if the RSS constraints are satisfied. The RSS (in dBm) is calculated using the following equation.

$$RSS_{i,j} = PT_i + \delta_{i,j} + \xi_{i,j} \qquad \textbf{Equation 5-2}$$

Here $RSS_{i,j}$ represents the received signal strength from the i*th* cell at place j, the index PT_i represents the transmit power from the i*th* cell and $\delta_{i,j}$ can be regarded as the path loss from the i*th* cell at place j, where shadowing is considered in the RSS calculation. The shadowing is represented as $\xi_{i,j}$, and the shadowing considered here follows a log-normal distribution with a zero mean and a standard deviation, σ, between 4 and 6 dB.

5.2.2.2. Handover probability calculation

Assuming the RSS of the serving cell is represented by RSS_1, the RSSs of other cells can be represented as RSS_i, $i \in \{2, 3 \ldots n\}$, in a certain place indexed by j; a handover will be initiated if the following equation is satisfied.

$$RSS_{i,j} \geq RSS_{1,j} + HM, \quad i \in 2,3,\ldots,n \qquad \textbf{Equation 5-3}$$

Therefore, the handover probability can be defined, for position j. If there exists an RSS_i that satisfies the handover equation, a handover will occur, which can be further calculated as the handover probability. In other words, the handover probability can be expressed as $1\text{-P}[\text{no handover occurs}]$, which is shown below.

$$\begin{aligned} P_{HO,\ j} &= 1\text{-P}[\text{no handover occurs}] \\ &= 1 - \prod_{2}^{n} \text{P}[RSS_{i,j} \leq RSS_{1,j} + HM], \quad i \in [2,3,\ldots,n] \end{aligned} \qquad \textbf{Equation 5-4}$$

In the above equation, capital P represents the probability indicator, and the calculation of $\text{P}[RSS_{i,j} \leq RSS_{1,j} + HM]$ can be detailed as follows.

$$P[RSS_{i,j} \leq RSS_{1,j} + HM] = E_{RSS_1}[\int_{-\infty}^{RSS_1+HM} f_{RSS1}(u)du] \qquad \textbf{Equation 5-5}$$

The E displayed in the above equation indicates the expectation, from which a double integral can be further derived.

$$E_{RSS_1}[\int_{-\infty}^{RSS_1+HM} f_{RSS1}(u)du] = \int_{-\infty}^{\infty} f_{RSS_1}(v) \int_{-\infty}^{v+HM} f_{RSS_i}(u)dudv \qquad \textbf{Equation 5-6}$$

$$\int_{-\infty}^{\infty} f_{RSS_1}(v) \int_{-\infty}^{v+HM} f_{RSS_i}(u)dudv = \int_{-\infty}^{\infty} \int_{-\infty}^{v+HM} f_{RSS_1}(v)\, f_{RSS_i}(u)dudv \qquad \textbf{Equation 5-7}$$

The $f_{RSS_1}(v)$ and $f_{RSS_i}(u)$ denote the probability density function (PDF) of *RSS1* and, where the $f_{RSS_i}(u)$ can be replaced by the cumulative distribution function (CDF) of RSS_i, as mentioned before, the shadowing follows the log-normal distribution.

$$CDF_v = \frac{1}{2}\left[1 + \text{erf}\left(\frac{v + HM - \mu_i}{\sigma\sqrt{2}}\right)\right] \qquad \textbf{Equation 5-8}$$

Here the erf shown in the above equation is the error function, which can be displayed as follows.

$$\text{erf}(x) = \frac{2}{\sqrt{\pi}}\int_0^x e^{-t^2}\,\text{d}t \qquad \textbf{Equation 5-9}$$

Finally, the handover probability for the i*th* cell can be expressed in the following equation.

$$\int_{-\infty}^{\infty}\int_{-\infty}^{v+HM} f_{RSS_1}(v)\, f_{RSS_i}(u)\,du\,dv = \int_{-\infty}^{\infty} \frac{1}{\sqrt{2\pi}} e^{-\frac{(v-\mu_1)^2}{\sigma\sqrt{2}}} \frac{1}{2}\left[1 + \text{erf}\left(\frac{v + HM - \mu_i}{\sigma\sqrt{2}}\right)\right] dv$$

Equation 5-10

The *E* displayed in the above equation indicates the expectation, from which can be further derived a double integral, then, P_{HO} can be calculated.

5.2.3. System model and simulation results

In order to clearly display the handover probability affected by the adaptive HM mechanism, a seven macrocell scenario is considered. The six cells are closely wrapped around the central cell, and the central cell handover probability situation is the main parameter that needs to be observed. The related simulation parameters are listed in Table 5-1.

Table 5-1 List of the simulation parameters

Parameters	Values
Macrocell Tx power:	46 dBm
Macrocell coverage:	1000m
Smallcell Tx power:	24dBm
Macrocell pathloss [3GPP TR 36.842]:	128.1+37.6*log10(d/1000) d in [m]
Femtocell pathloss [3GPP TR 36.842]:	147 + 36.7*log10(d/1000) d in [m]
$HM_{max:}$	10 dB
$HM_{mi:n:}$	0 dB
Fixed HM values used for simulation:	0 dB, 5dB and 10dB
Shadow fading stand derivation:	σ = 6dB

The whole simulation map is divided into 100*100 pixels and the handover probability for each pixel is calculated. Note that the handover probability calculation for the entire simulation map considers the central macro cell to be the serving cell, and the handover probability from the central cell to adjacent cells follows the calculation introduced in the previous section.

Figure 5-2, Figure 5-3, Figure 5-4,and,Figure 5-5 illustrate the variation in the handover probability according to different HM values, and the central macro cell is placed at position (50,50) in each figure. Figure 5-2, Figure 5-3 and Figure 5-4 display the impact of the HM value turning from 0dB to 10dB, which will severely influence how the handover probability changes in the cell boundary. As we define the probability from 0.3 to 0.7 as indicating that there is a high potential for a redundant handover to happen (which can be regarded as the region in the light blue to orange colour), as the HM value increases, the radius of the handover region also increases, but the width of the handover region circle does not show obvious changes. The width of this ring region significantly changes with the adoption of an adaptive HM system. If we compare Figure 5-5 with Figure 5-2, Figure 5-4, it is not hard to

make this inference. The peripheral area of the adaptive HM is similar to that of Figure 5-2, which is a dark red hexagonal region (formed by the handover probability = 0.9). On the other hand, the internal dark blue region (where the handover probability < 0.1) of an adaptive HM approaches the same area when the HM is fixed as 10dB. The width of the ring-shaped handover region is significantly reduced.

As a result, the effectiveness of an adaptive HM in terms of minimising the handover region is outstanding, which can be regarded as a reduction in unnecessary handovers, while, at the same time, an adaptive HM can increase the probability that the UE is bound to the cell, which provides the coverage.

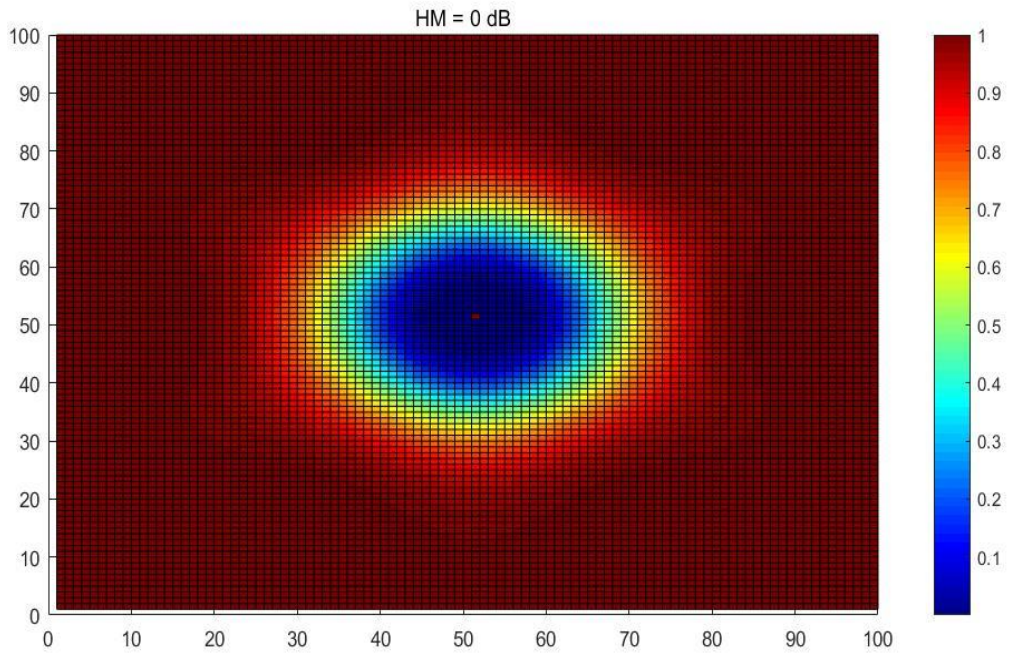

Figure 5-2 Handover probability in a macrocell scenario with HM = 0 dB

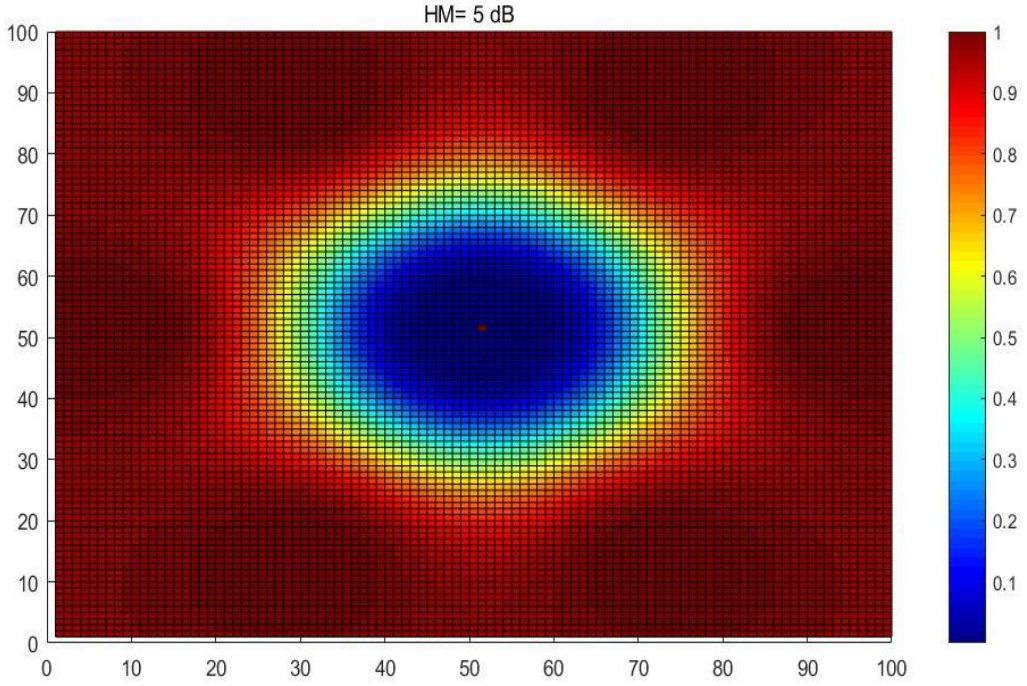

Figure 5-3 Handover probability in a macrocell scenario with HM = 5 dB

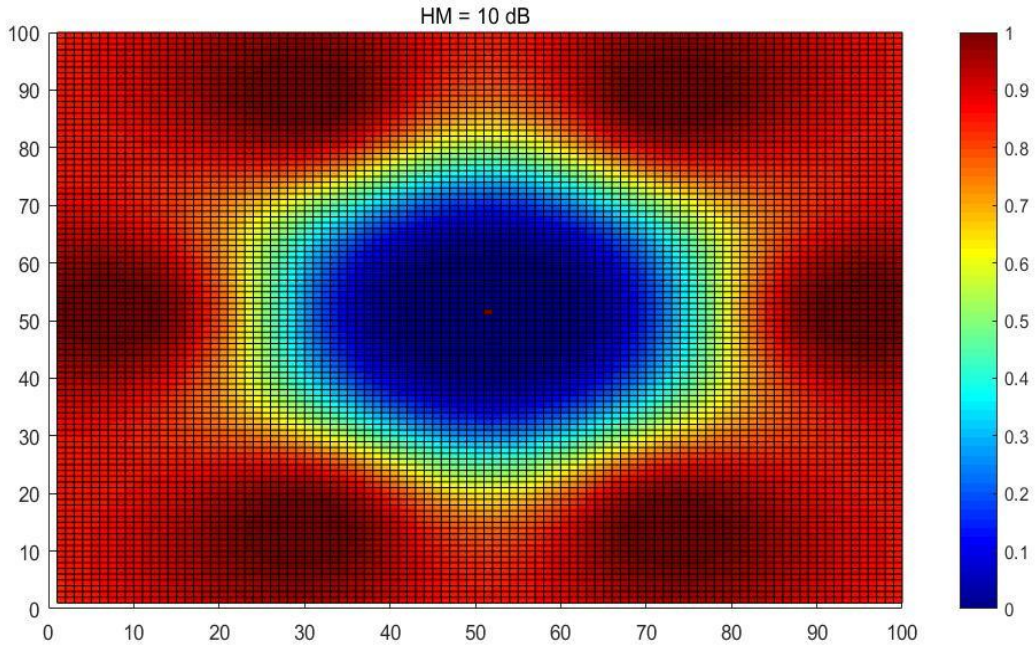

Figure 5-4 Handover probability in the macro cell scenario with HM = 10 dB

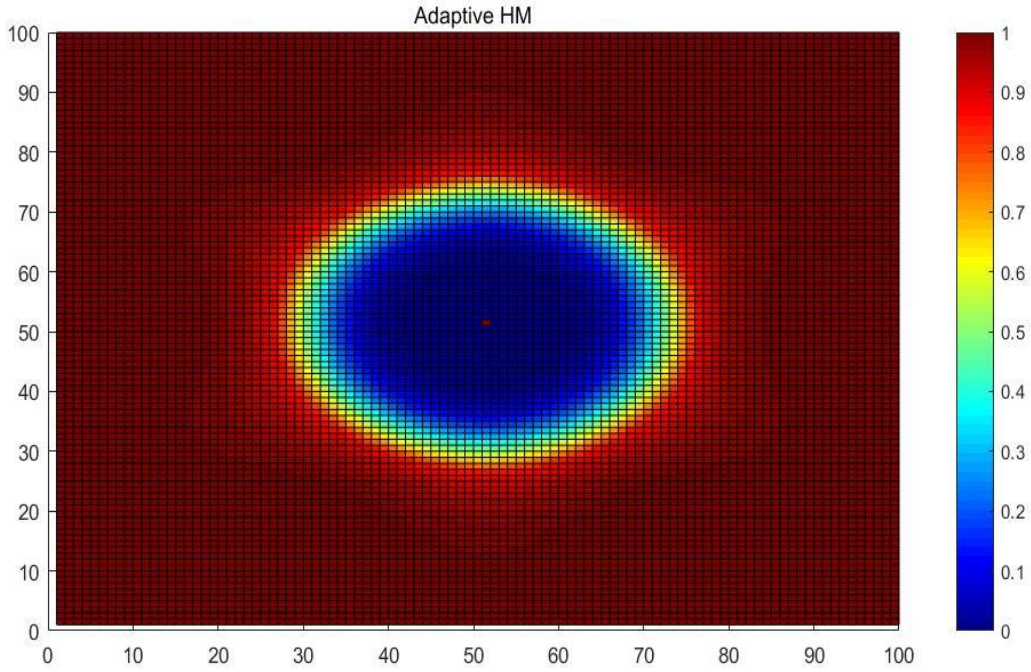

Figure 5-5 Handover probability in a macrocell scenario with the adaptive HM selected

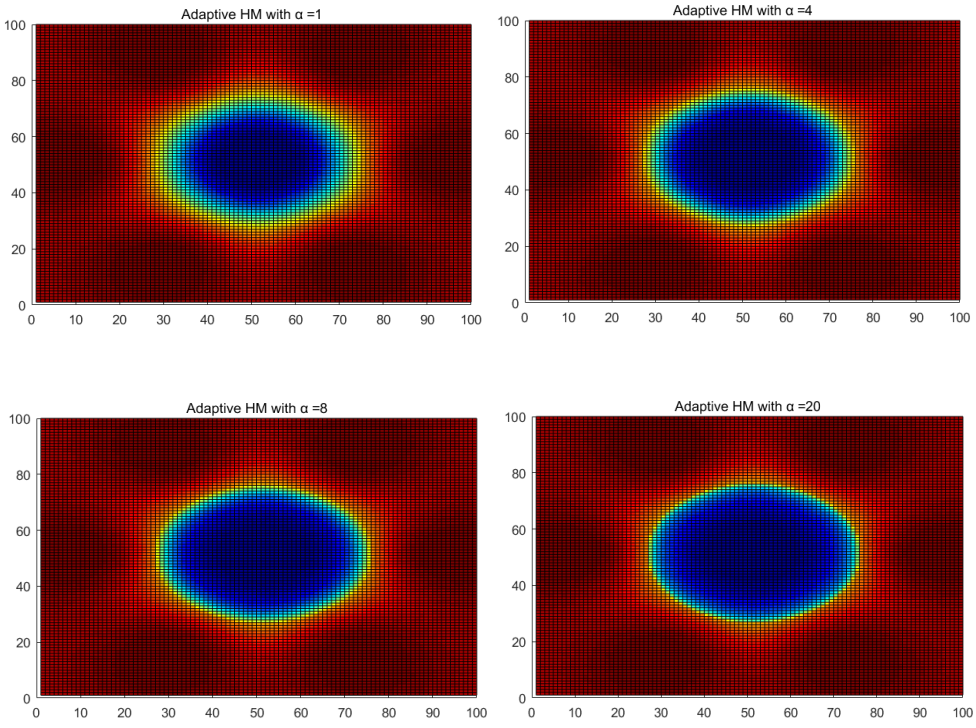

Figure 5-6 Handover probability with adaptive HM in different α value

Figure 5-6 displayed the handover probability when using different index α, we can see from figure that, with the increasing of α, the width handover circular ring become narrower and narrower. This phenomenon can be explained by the nature of α, with α increased, the turning point of sharp changing in HM value will getting closer to the cell boundary.

5.2.4. Adaptive HM mechanism in a macro-small cell scenario

In a one-tier macro cell scenario, the cell boundary is easy to define, while in the two-tier HetNet scenario, the small cells are normally deployed in the existing macro cells, and it is hard to decide the cell coverage. As a result, the set of cell radius R in the Equation 5-1 is not suitable for this scenario. Under these conditions, the decision to have an adaptive HM value should result in some changes.

The RSS is a distance-based variable, as shown in Equation 5-2. The main idea of an adaptive HM is to let the HM achieve a minimum value when the UE is approaching the cell boundary. In a small cell, the so-called cell boundary can be defined as the RSS of a small cell and a macro cell are of the same value and, as a consequence, the distance-based adaptive HM can be rewritten as follows.

$$HM_{\text{adaptive}} = \max\left\{ HM_{\max}\left[1-\left[\frac{RSS_{\text{ser}}}{RSS_{\text{tar}}}\right]^{4}\right]; HM_{\min}\right\} \qquad \textbf{Equation 5-11}$$

Assuming an UE is moving from the serving macro cell to the target small cell, the HM will reach a minimum value when the RSS of the target and small cell is the same. The simulation scenario is shown as follows: the original serving cell is considered to be a macrocell, which is placed at (50,50) in each figure. Six small cells are placed as two columns. Out of these, the two mid small cells are placed 250

meters away from the macro cell, and the other four small cells in the corners are at a distance of 353.55 meters away.

Figure 5-7, Figure 5-8 and Figure 5-9display the handover probability when the HM is picked as a fixed value. As the HM values vary, the potential handover region significantly changes, as stated in the previous section. A handover probability from 0.3 to 0.7 suggests there is a high potential for a redundant handover region to occur. In the HetNet scenario, the region is no longer displayed as a regular shape, which is due to the asymmetry in the macro cell RSS in each direction around the small cells. In order to clearly display the different handover probability regions, another color combination is chosen; the redundant handover region is in green and light yellow. As the HM value increases the small cell coverage significantly drops, and the central region (which can be regarded as the blue circle) is also reduced.

By applying the adaptive HM system, nearly the same result can be achieved compared with in the macrocell scenario. Under the conditions that maintain the handover probability for the small cell central region, the redundant handover region significantly decreased. Figure 5-10 displays the variation in the handover probability through adopting an adaptive HM. Figure 5-11 illustrates the trend in the HM variation in this simulation scenario. It is obvious that the macrocell centre UEs are given a higher HM value. With movement towards the small cells, the HM value decreases, and in the small cell central coverage region, the HM equals zero, which strongly binds the small cell covered UE to this cell.

In order to verify the adaptive HM, Monte Carlo simulation is adopted, as we divide the simulation map into 100*100 pixels. In each pixel, 10000 samples of the RSSs from seven cells are generated. For each sample. if there exists one RSS from the small cells that exceeds the macro cell RSS, it is thought that a handover would

take place. After 10000 samples are taken, the summation of the handover occurs, and if this is divided by the number of samples, a handover probability of one pixel can be calculated. Figure 5-12 displays the results for the Monte Carlo simulation. In order to clearly display the deviation between Figure 5-10 and Figure 5-12 a 3D deviation map is build, which is calculated using the difference between the two maps; most of the deviation is under 0.2% but, when approaching the small cell boundary, the maximum deviation reaches 1.5%, which can be considered acceptable.

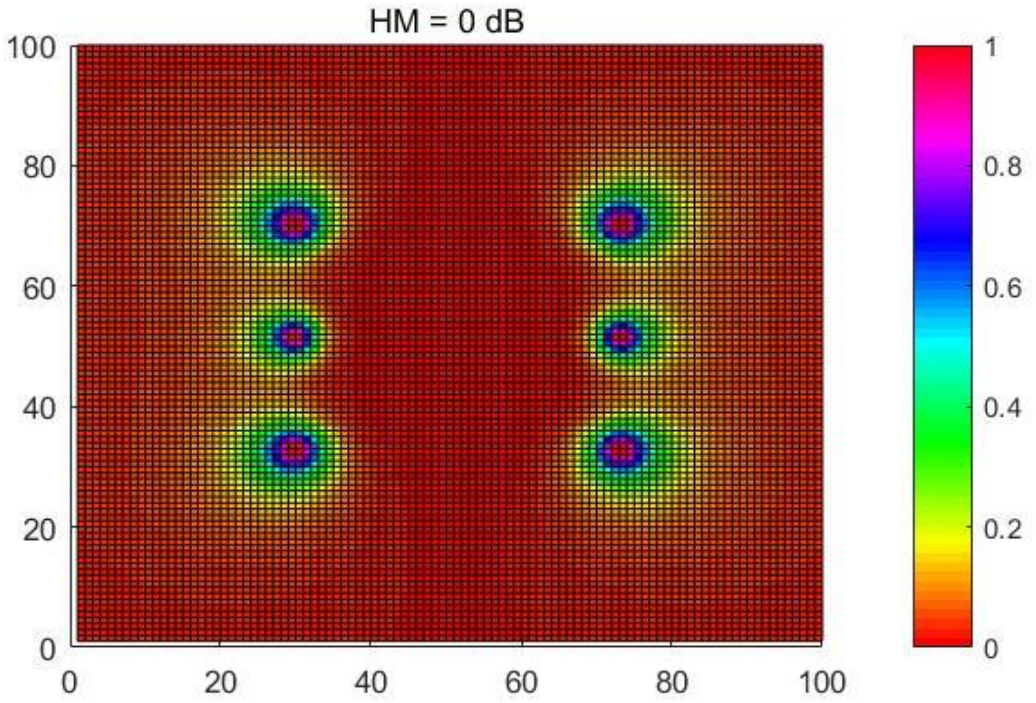

Figure 5-7 Handover probability in a macro-small cell scenario with HM = 0 dB

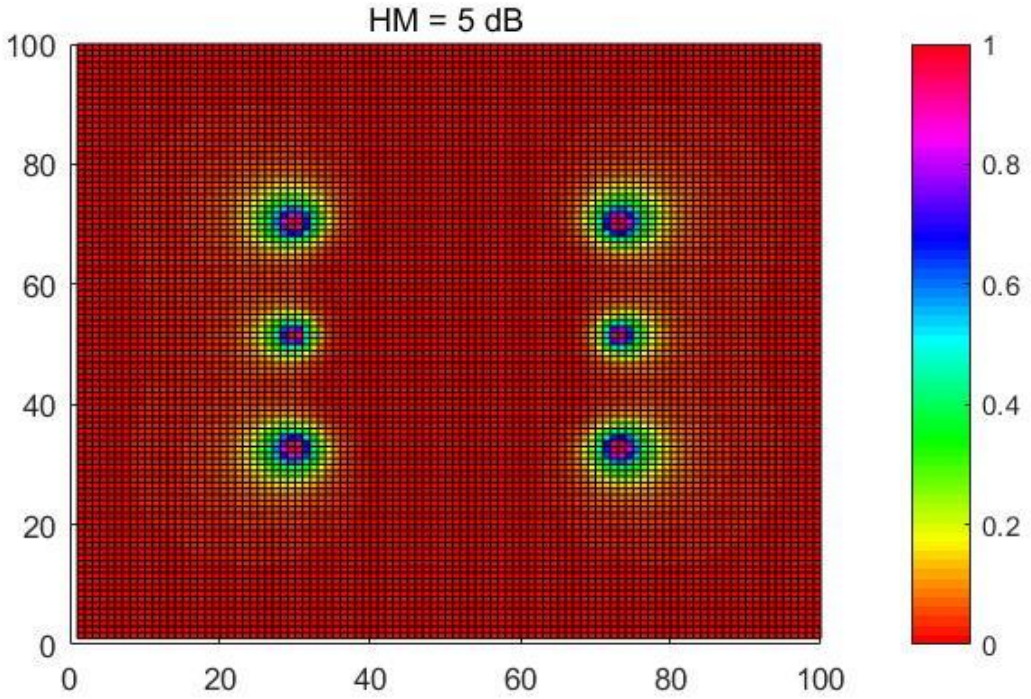

Figure 5-8 Handover probability in a macro-small cell scenario with HM = 5 dB

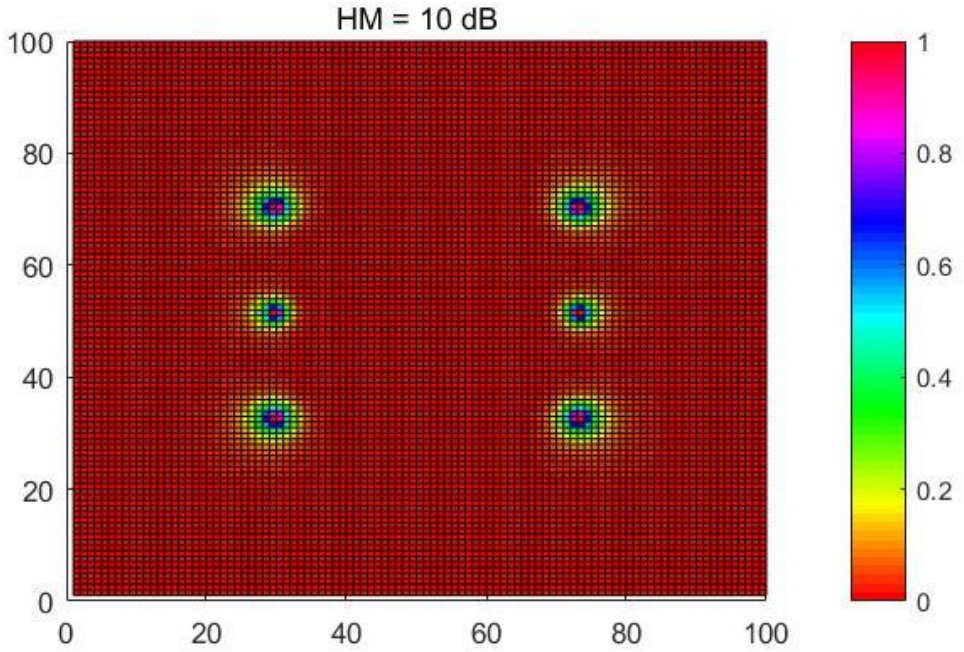

Figure 5-9 Handover probability in a macro-small cell scenario with HM = 10 dB

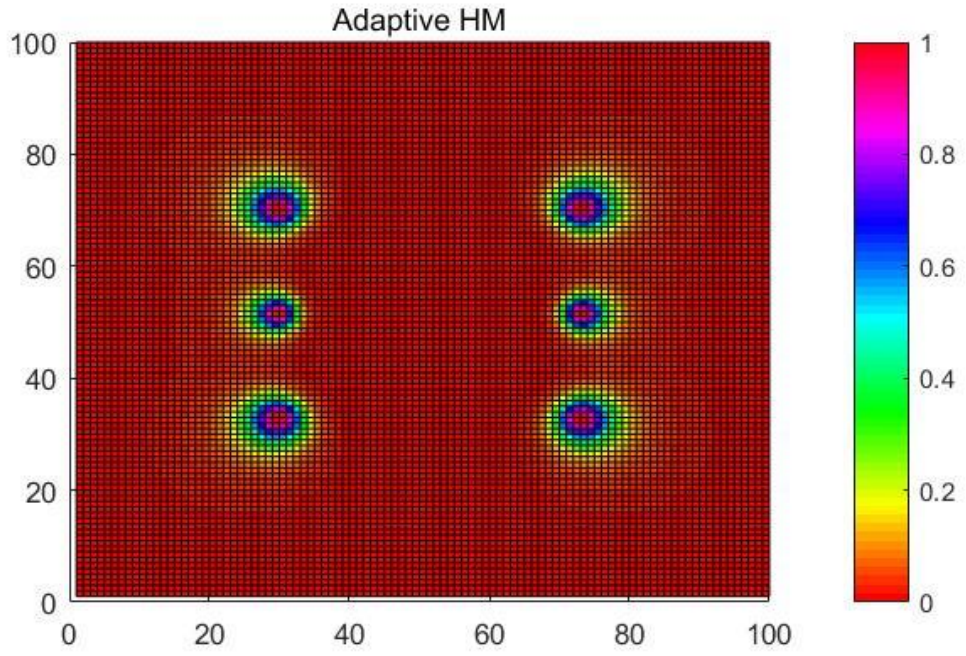

Figure 5-10 Handover probability in a macro-small cell scenario with an adaptive HM selected

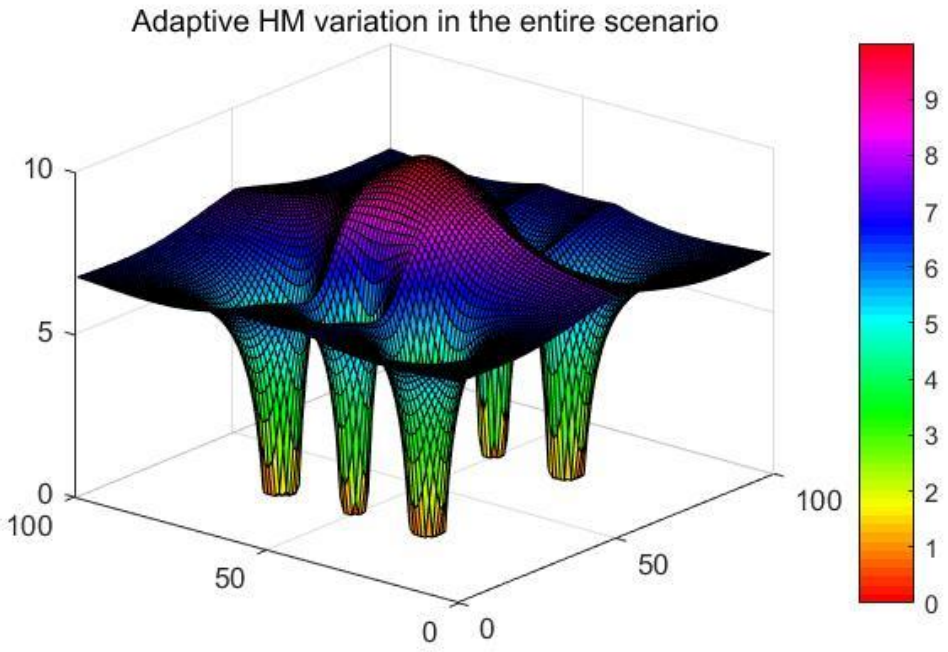

Figure 5-11 Trend in the variation in an adaptive HM system

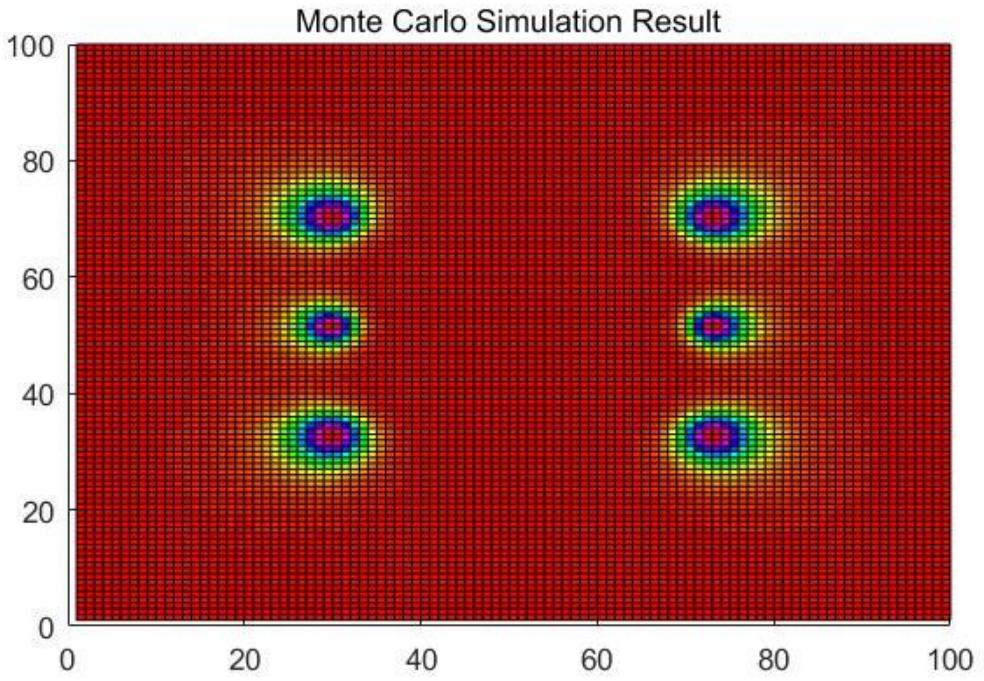

Figure 5-12 Adaptive HM using Monte Carlo simulation

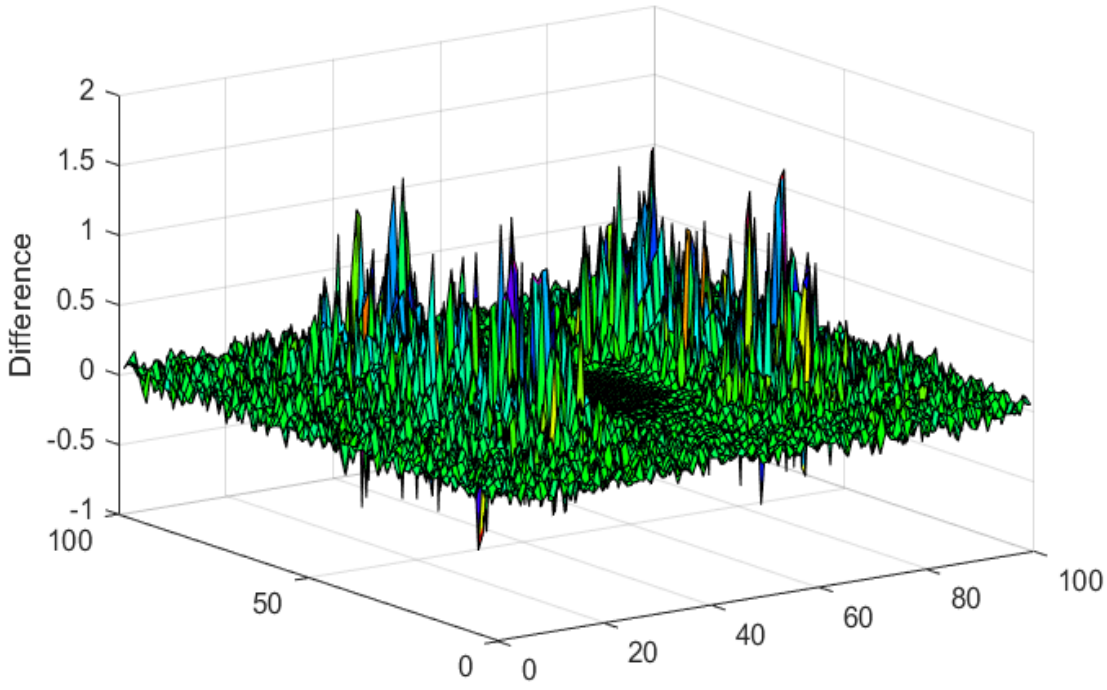

Figure 5-13 Deviation between theoretical and Monte Carlo simulation

5.3. Adaptive TTT selection scheme

For any UE inside a network, the main characteristics for its mobility are the distance to the base stations and its moving velocity. In the previous section, the UE distance related to the HM has been discussed and optimised. In this section the UE velocity related handover decision parameter TTT will be discussed. As the handover is related to a moving scenario, in order to evaluate the TTT we need to first build a time-varying system.

Assuming an UE is at the serving cell boundary with velocity *V* and it is moving away, when the handover triggering event A3 (Table 2-1) is satisfied, the TTT timer starts to count. After the TTT condition is satisfied, the distance that the UE moves is *V**TTT, as the TTT is given for 16 values, as 3GPP specifies (0, 40, 64, 80, 100, 128, 160, 256, 320, 480, 512, 640, 1024, 1280, 2560 and 5120 in [ms]), which will result in 16 different distances. This will hence cause different SINR variations. Figure 5-14 displays the effect of selecting different TTTs and how it may result in different SINRs after the TTT timer expires. As the UE with a longer TTT may run deep into the target cell, which will lead to a bad SINR situation, an RLF may occur. Although a large TTT value will result in a bad RLF performance, if the TTT is too small the system ping-pong handover probability will increase significantly, which will lead to a decrease in system performance.

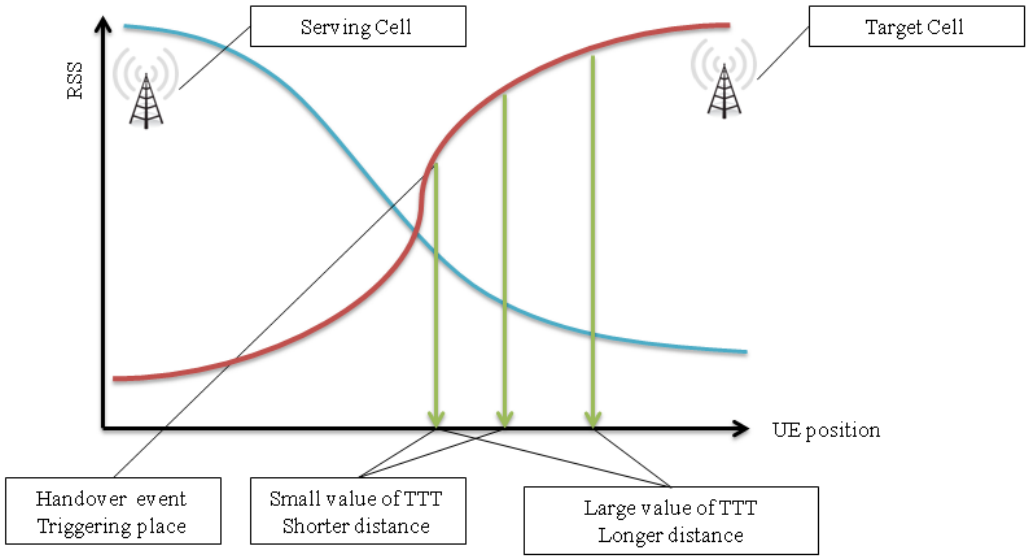

Figure 5-14 SINR affected by TTT

5.3.1. Simulation scenario

In order to evaluate the handover performance parameters, the ping-pong handover probability and the RLF affected by TTT is presented in the simulation scenario. A two-tier HetNet is adopted here: the central macrocell is surrounded by six other macro cells, and the distance between the central macro cell and the other macro cells is 1000 meters. Inside the central macro cells, there are six small cells, located at a distance of 250 meters and 353.55 meters away, which is illustrated in Figure 5-7. The UEs are randomly distributed in the central cells, which will suffer two-tier interference. In order to discover how the UE velocities affects the handover performance, the UE velocities are divided into five categories (5km/h, 15km/h, 30km/h, 60km/h and 120km/h). The rest of the simulation parameters are the same as those listed in Table 5-1.

5.3.2. Ping-pong handover performance evaluation using TTT and UE velocity

Figure 5-15 illustrates how the ping-pong handover probability is affected by the TTT. Four different TTT values are tested in the scenario, 40ms, 80ms, 160ms and

320ms respectively. It is obvious that the ping-pong handover probability would be significantly affected by a change in the TTT settings. In order to achieve a precise TTT comparison, the HM is set as 0. The same group of UEs is utilized here, and is assigned a fixed moving speed of 30km/h. When the TTT = 40ms, which is the minimum value that can be set, the ping-pong probability reaches a stable value at TTI around 40, and 40% of the handovers are ping-pong handovers. As the TTT increases, the ping-pong handover probability is significantly decreased when the TTT = 320ms, and the ping-pong handover proportion drops to nearly 8%. It is not hard to predict that, when the TTT is assigned a higher value, the ping-pong handover ratio will drop to zero.

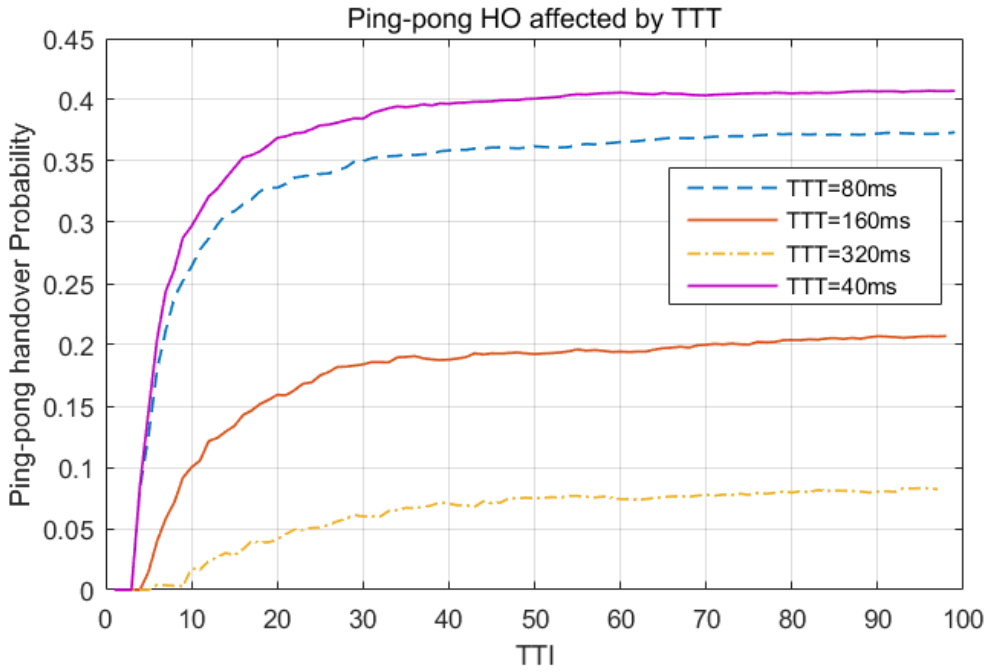

Figure 5-15 Ping-pong HO probability vs. TTT

Figure 5-16 displays how the ping-pong handover ratio is affected by different UE velocities. In this comparison, the HM is considered to be 0 and the TTT is set at 80ms. The same group of UEs is tested using different moving speeds. It can be concluded that, as the UE velocity increases, the ping-pong handover probability also

shows a decreasing trend but, compared with the influence of the TTT, the impact that the UE velocity has on the ping-pong probability is much lower. 120km/h is normally considered to be a highway speed but, even when the highest velocity is tested, the probability of a ping-pong handover only decreases by around 5%.

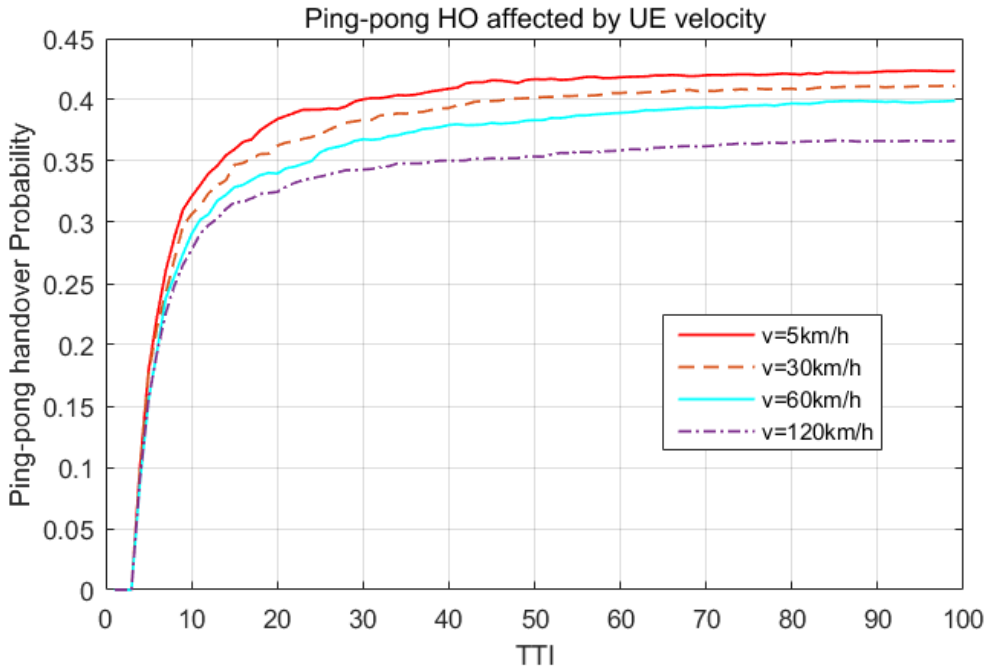

Figure 5-16 Ping-pong HO probability vs. UE velocity

5.3.3. RLF performance evaluation according to the TTT and UE velocity

Figure 5-17 displays the RLF affected by different TTT values and UE velocities. From the perspective of UE velocity, it is not hard to find that, for the same TTT values, a higher moving speed will result in a higher RLF percentage. As explained before, the UEs with a higher speed will experience a longer distance when moving inside the TTT timer, which might cause a large amount of degradation in the SINR and result in a RLF. Similarly, from the TTT perspective, the UE with the same moving speed will achieve a higher RLF potential as it is assigned higher TTT values. When the UE is assigned a lower moving speed (5km/h, 15km/h and 30km/h), the variation trend in the RLF is very slow for lower TTT values (TTT < 640ms). At the

same time, a higher speed for the UE (60km/h and 120km/h) will lead to a relative stable RLF, but only before TTT < 256. Each curve obtains a significant turning point; the higher the velocity, the earlier the RLF turning points appear. For instance, when the TTT changes from 640ms to 1024ms, the RLF of an UE with a speed of 5km/h only increases from 27.18% to 27.44%, while the RLF of an UE with a speed of 120km/h grows significantly from 37.28% to 46.16%.

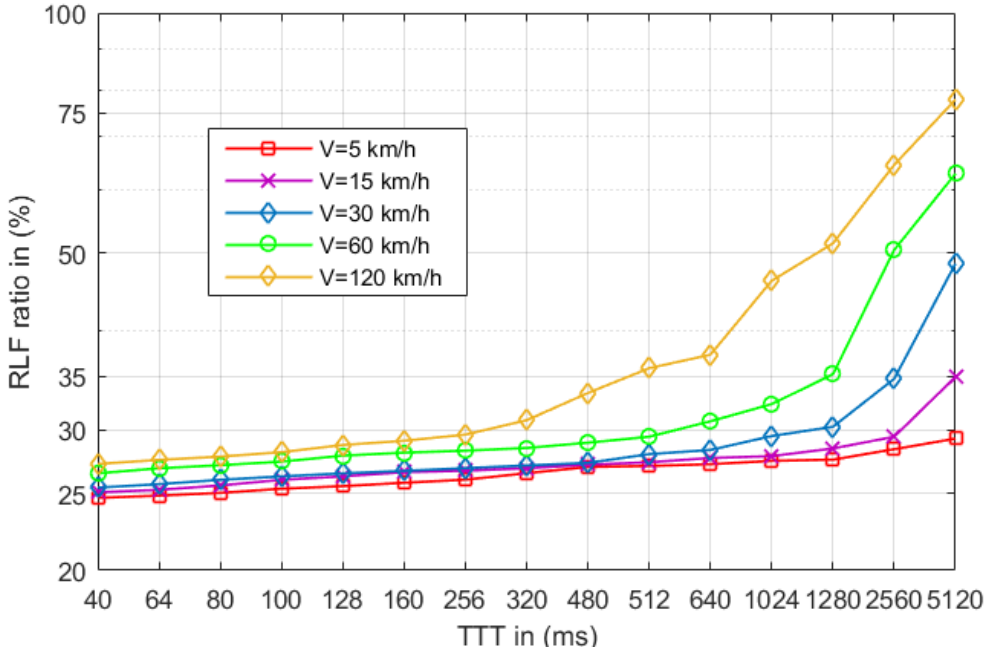

Figure 5-17 RLF affected by TTT and UE velocity

5.3.4. Adaptive TTT selection scheme

Based on the ping-pong handover and RLF analysis, the adaptive TTT selection scheme can be applied, as the ping-pong handover ratio is only affected by the lower TTT values. The decision about RLF can take all the TTT values into consideration. We take RLF as a constraint to selecting the optimal TTT values based on the UE velocity. If we set RLF to be < 27%, how the TTT satisfies the RLF condition can be seen in Table 5-2.

Table 5-2 TTT selections under the condition RLF < 27%

UE velocity	TTT [ms]
V = 5 km/h	40/ 64/ 80/ 100/ 128/ 160/ 256/ 320/ 480
V = 15 km/h	40/ 64/ 80/ 100/ 128/ 160/ 256/ 320
V = 30 km/h	40/ 64/ 80/ 100/ 128/ 160/ 256
V = 60 km/h	40/ 64/ 80
V = 120 km/h	40

As introduced in Chapter 2, the TTT seems to have great impact on handover probability control: the higher the TTT values chosen, the lower the handover probability that will be displayed. In order to minimise unnecessary handovers, when the RLF condition is satisfied, we select the largest TTT so as to apply the TTT selection scheme.

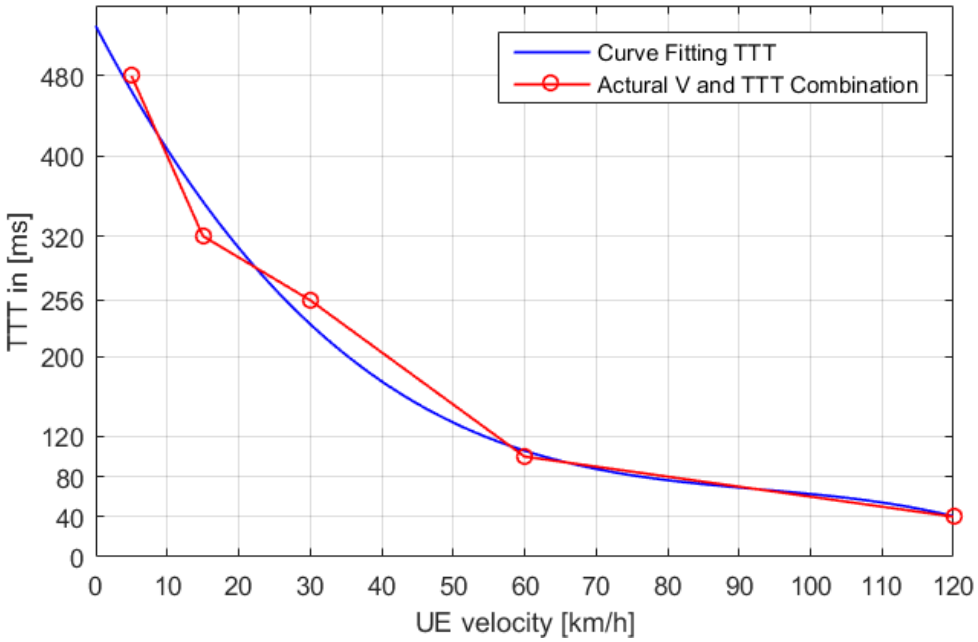

Figure 5-18 Adaptive TTT selection based on UE velocity

Figure 5-18 displays the TTT selection scheme based on RLF being < 27%. The actual TTT and V are shown as the red curve. By applying curve fitting, the TTT can be formulated as a function of the UE velocity. As a result, a proper TTT value for an arbitrary UE can be determined.

5.4. Joint handover optimisation based on the optimisation of adaptive control parameters

After defining adaptive HM and adaptive TTT selection schemes, joint optimisation can be initiated to optimize the system handover performance.

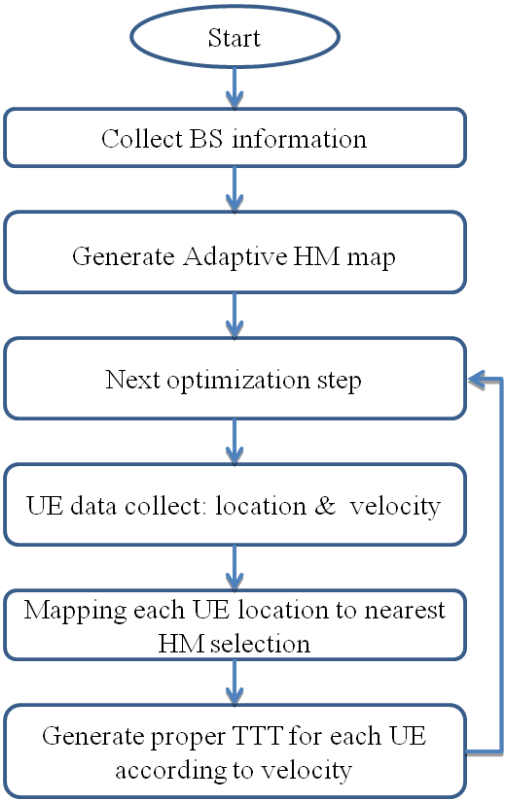

Figure 5-19 Adaptive TTT selection based on UE velocity

Figure 5-19 illustrates the optimisation mechanism. In a certain network, the deployment position for the base station should be fixed. Under such conditions, the distance between the base stations is considered to be fixed. As discussed in section 5.2, when the locations of the base stations are known, the adaptive HM assigned for each location can be calculated. According to the adaptive TTT selection scheme, when a UE is dropped into the network, and assigned a certain speed, a proper TTT

value can be calculated for this UE. Each UE inside the network is assigned an individual HM and TTT combination.

Simulations are taken in order to verify the proposed selection mecahnism for the handover control parameters. The handover probability (calculated as the handover numbers/all UE numbers) is considered to be the evaluation metric. 1000 UEs are uniformly dropped into the network (the same simulation scenario as in section 5.3), and assigned a random moving speed ranging from 0~120 km/h. Six cases are considered to compare the handover probability: 1) HM = 0 dB, TTT = 40ms, 2) HM = 5 dB, TTT = 40 ms, 3)HM = 10 dB, TTT = 40 ms, 4) HM = 0 dB , TTT = 480 ms, 5) HM = 5 dB, TTT = 480ms and 6) HM = 10 dB, TT = 480ms.

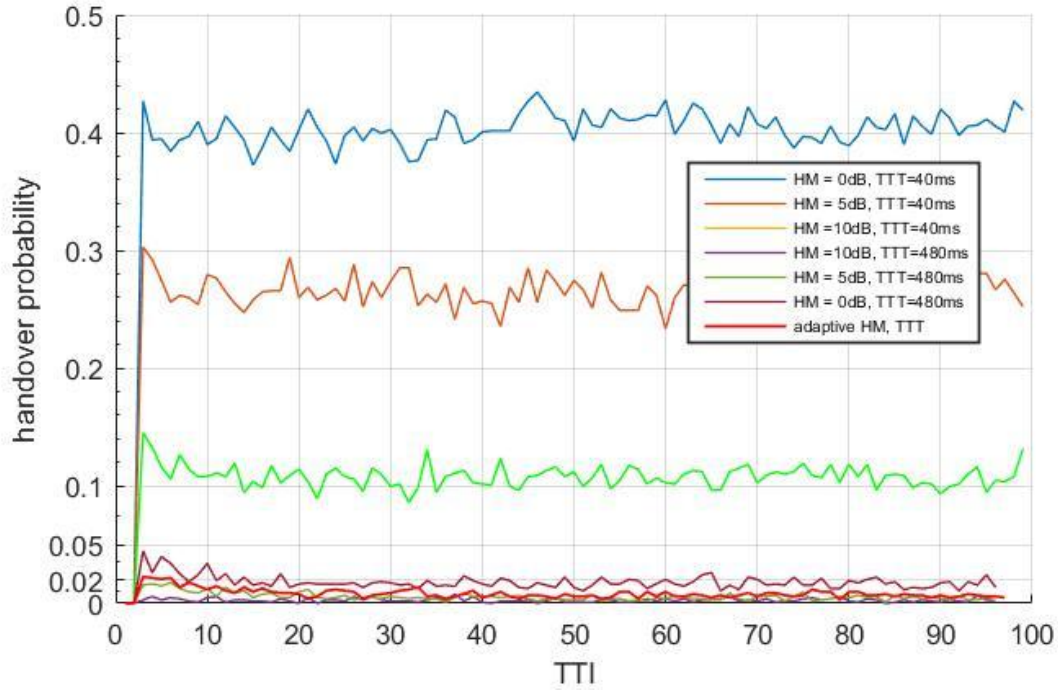

Figure 5-20 Handover probability in different cases

Figure 5-20 displays the handover probability variation in 100 TTI simulation time. When TTTs are chosen with a minimum value of 40ms, the handover probability can reach a minimum value, around 0.1, as HM = 10. When the TTT is

fixed as 480ms, the effect of changing HM is not significant, as the range is from 0.01 to 0.04. This can be considered a very low handover probability, as the 480ms setting for a small cell scenario is high enough. As we apply the adaptive HM and TTT selection scheme, a handover probability of roughly a curve of 0.02 can be found. In the figure, the handover probability curve is between case 4 and case 6, and the handover probability is significantly controlled. Although the minimum handover probability is achieved in this figure with case 6 (approaching zero), this is based on the suppression of all handover conditions, which will seriously affect the system's performance.

5.5. Summary

In this chapter, an adaptive selection scheme in HM and TTT is introduced. The main target of this chapter is to find suitable handover control parameters based on the UE mobility situation, and the mobility states in this chapter are defined as the distance and the UE moving speed. Based on the UE distance to different cells the adaptive HM scheme is chosen, and the main purpose of the selection method is to let UE bind to its original serving cell if it is inside the cell coverage. Through an analysis of two different scenarios, the chosen adaptive mechanism in the macrocell only and two-tier HetNet scenarios is analyzed. At the same time, the other mobility parameter, UE velocity, can be decided by selecting reasonable TTT values. The TTT selection scheme is based on ensuring the RLF rate. Under such conditions, the highest TTT are considered to be the most suitable ones. Through curve fitting, a proper TTT can be found for arbitrary UEs. After the TTT and HM are selected, we propose a self-optimisation mechanism, which is only based on the UE mobility states.

Chapter 6. Conclusion and Future Works

6.1. Conclusion

In this thesis, the handover control parameters in LTE HetNets were mainly investigated under three aspects. First, two self-optimisation handover decision algorithms were proposed in order to achieve better system performance. Then, a model of a HetNets scenario, which used MCP to analyze the handover performance affected by HM, TTT, and CRE, was introduced. Finally, the adaptive HM and TTT selection scheme was investigated, in order to create a new selection scheme for handover control parameters for individual UE.

In the first part of this research, two handover decision algorithms were proposed. The first algorithm is in the category of interference-aware handover decision algorithms, which aims to optimize the overall system's average SINR and ping-pong handover ratio. Based on the current network states for SINR and ping-pong ratio, the system will automatically change the control parameters HM and TTT to facilitate the system achieving better handover performance. UE of different velocities were tested, and the ping-pong handover ratio was significantly optimised. When UEs with high moving speed at *v=120km/h*, *3%* ping-pong handover ratio is optimised, *4.5%* optimisation is achieved at the *v=60km/h* condition, and *6%* optimisation at *v=30km/h*. At the same time, the system's average SINR performance was also improved compared with a non-optimised system, the optimisation for SINR is not significant compared with the optimisation of ping-pong handover ratio, with respect to *0.322dB, 0.4699dB,* and *0.4185dB.* The second handover decision

algorithm is in the category of energy-efficiency-aware algorithms, and the proposed optimisation algorithm for energy efficiency and the ping-pong handover ratio has the same working mechanism as the previous algorithm. Through modelling the macro cell, small cell, and UE power consumption model, with the analysis of power consumption both on UE and BS, the dynamic power consumption of network can be obtained, hence, the entire network power consumption model is established. The adoption of ERG metric clearly reflected the network energy efficiency states in terms of percentage. By monitoring the network's energy efficiency states and ping-pong handover ratio performance, the network dynamically chose the HM and TTT values for whole network to achieve system-level optimisation. The ping-pong handover ratio dropped nearly *5%* and the system energy efficiency increased nearly *4%*.

In the second part of this research, an MCP-based model of the HetNets handover process was generated. By mapping the handover process into an MCP, the handover probability of each state was clearly identified. By establishing a mathematical method to model the handover procedures, the coordination of the working mechanism of HM, CRE, and TTT was realized and evaluated. Thus far, investigations of the handover process in a HetNets scenario has hardly taken CRE into consideration; however, the work in this thesis not only took traditional handover parameters HM and TTT into consideration but also included CRE to evaluate the handover performance. From the analysis, two result have been achieved. Firstly, from the load balancing perspective, by using curve fitting through comparison between traditional model and the MCP model, the optimal CRE value by *7dB* is presumed to be the optimal CRE bias for offloading. Secondly, from the handover perspective, the result shows that CRE works as a similar mechanism to HM, or even has a stronger effect on the handover ratio. The handover ratio will change

significantly as a result of adjusting the CRE and HM, A good combination of CRE and HM will minimise the number of unnecessary handovers and will optimize the system's total throughput. when HM and CRE pick *1dB* and *6dB*, the optimal total throughput is obtained.

In the last part of this research, an adaptive HM and TTT selection scheme was proposed. The main purpose of this work was to find the most suitable pair of handover control parameters for any UE with any mobility state. Based on the distance from the UE to the serving cell boundary, the adaptive HM decision is made, which aims to bind the UE to its serving cell if it is inside the serving cell's coverage. In a HetNets scenario, the cell edge is not easy to identify, so to solve this problem an evolved adaptive HM decision was made, which was based on the RSS comparison of a macro cell and small cell. After defining the adaptive HM selection method, an adaptive TTT was proposed. By analyzing the UE's moving speed and the RLF variation caused by various TTT values, the deterministic condition of TTT was found. On the premise of guaranteeing the system's RLF, the TTT was chosen as its maximum value to minimise the potential for unnecessary handovers. Based on the adaptive selection scheme for HM and TTT, a new handover self-optimisation mechanism was generated. In traditional networks, the UE is always assigned a fixed value of HM or TTT, even if they are in different locations or have varied velocities; however, the new mechanism will automatically assign a pair with the most suitable HM and TTT, which can significantly minimise the probability of unnecessary handovers in the system.

6.2. Future works

As can be seen from chapter 3, the SINR, energy efficiency, and ping-pong handover ratio are optimised in the proposed handover decision algorithm. In the HetNets scenario, other handover metrics can also be taken into consideration, such as the handover failure ratio, RLF ratio, and handover probability. It is very complicated to include all handover metrics inside one optimisation algorithm, since the inner cooperation among handover metrics will significantly affect each other. The trade off based on different handover metrics needs to be studied in future analysis. Taking the nature of small cell networks into consideration, the other constraints can also be set as the handover decision algorithm constraints. For example, the handover decision can be made based on the minimum time of stay in a particular cell, through modelling or historical-data analysis based on UE behaviour.

In chapter 4, an MCP was utilized to analyze the HetNets handover procedure. As MCP is a mathematical method widely adopted in wireless communications, it also can be used in other modelling from the perspective of handovers. For example, in modelling UE mobility prediction, which is because UE has a probability of moving in each direction, and, based on establishing the probability transition matrix for the UE movement model, the potential location of the UE after several moves can be predicted. From the load balancing perspective, the MCP model is more realistic in reflecting the UEs assignment probability to each cell, especially combining with the handover process and the CRE bias. Another future research direction can be combined with the chapter 3 energy efficiency perspective, as we know, each equipment inside the network has different energy consumption states, if using MCP model, we don't need to build up the detailed power consumption model for each

equipment, through the statistic analysis of historical data, the probability that each kind of equipments stay in each state can be easy calculated, by modelling these MCP models, an MCP model for network energy efficiency can be easy established, which should be much more efficient in simplify the network energy efficiency model.

The research work presented in chapter 5 mainly investigated the UE's individual mobility states depending on the selection scheme for handover control parameters, in which the location and UE movement speed were taken into consideration. However, there is another parameter that has not been investigated, which is the UE movement direction. By considering the UE movement direction, the adaptive HM selection needs further constraints. For instance, the HM assigned to a UE at a cell boundary might be different: if the UE is moving toward the outside area of the serving cell coverage, the HM value might be zero; on the contrary, UE moving toward the centre of the serving cell might be assigned a higher value, which binds the UE to the serving cell. From the perspective of the adaptive TTT selection scheme, through a combination of the UE movement direction and velocity, there should be existing a trade off between the UE's handover potential to a certain target cell and the TTT adjustment; through this trade off, it can be decided to assign a specific TTT for a certain UE.

Additionally, other recent technologies can be adopted in the handover decision area. For instance, by applying big data to the handover decision, based on a reasonable analysis of the historical data, the system can automatically make a handover decision. By adopting machine learning, the UE behaviour can be more realistic displayed, which is helpful in establishing simulation scenarios.

Reference

[1] T. Teixeira, “Meet Marty Cooper-the inventor of the mobile phone,” *BBC News*, vol. 78, 2010.

[2] C. V. N. Index, “Cisco visual networking index: global mobile data traffic forecast update, 2014–2019,” *Tech. Rep*, 2015.

[3] T. Nakamura, S. Nagata, A. Benjebbour, Y. Kishiyama, T. Hai, S. Xiaodong, Y. Ning, and L. Nan, “Trends in small cell enhancements in LTE advanced,” *IEEE Commun. Mag.*, vol. 51, no. 2, pp. 98–105, 2013.

[4] D. López-Pérez, A. Valcarce, G. De La Roche, and J. Zhang, “OFDMA femtocells: A roadmap on interference avoidance,” *IEEE Commun. Mag.*, vol. 47, no. 9, 2009.

[5] T. Zahir, K. Arshad, A. Nakata, and K. Moessner, “Interference management in femtocells,” *IEEE Commun. Surv. tutorials*, vol. 15, no. 1, pp. 293–311, 2013.

[6] Y. Li, B. Cao, and C. Wang, “Handover schemes in heterogeneous LTE networks: challenges and opportunities,” *IEEE Wirel. Commun.*, vol. 23, no. 2, pp. 112–117, 2016.

[7] J. Zhang and G. De la Roche, *Femtocells: technologies and deployment*. John Wiley & Sons, 2011.

[8] J. G. Andrews, H. Claussen, M. Dohler, S. Rangan, and M. C. Reed, “Femtocells: Past, present, and future,” *IEEE J. Sel. Areas Commun.*, vol. 30, no. 3, pp. 497–508, 2012.

[9] J. Hoydis, M. Kobayashi, and M. Debbah, “Green small-cell networks,” *IEEE Veh. Technol. Mag.*, vol. 6, no. 1, pp. 37–43, 2011.

[10] 3GPP, “Group Radio Access Network: "Service requirements for Home Node B (HNB) and Home eNode B (HeNB),” 2011.

[11] V. Chandrasekhar, J. G. Andrews, and A. Gatherer, “Femtocell networks: a survey,” *IEEE Commun. Mag.*, vol. 46, no. 9, 2008.

[12] D. Lopez-Perez, I. Guvenc, and X. Chu, “Mobility management challenges in 3GPP heterogeneous networks,” *IEEE Commun. Mag.*, vol. 50, no. 12, 2012.

[13] 3GPP, “3rd Generation Partnership Project; Technical Specification Group Services and System Aspects; Vocabulary for 3GPP Specifications (Release 10),” 2011.

[14] A. Merwaday and I. Güvenç, “Handover count based velocity estimation and mobility state detection in dense HetNets,” *IEEE Trans. Wirel. Commun.*, vol. 15, no. 7, pp. 4673–4688, 2016.

[15] 3GPP TS 25.367 V8.1.0, “Universal Mobile Telecommunications System (UMTS);Mobility procedures for Home Node B (HNB);Overall description;(Release 8),” 2009.

[16] 3GPP TS 25.367 V9.5.0, “Universal Mobile Telecommunications System (UMTS);Mobility procedures for Home Node B (HNB);Overall description;(Release 9),” 2011.

[17] 3GPP TS 25.367 V12.0.0, “Universal Mobile Telecommunications System (UMTS);Mobility procedures for Home Node B (HNB);Overall description;(Release 12),” 2014.

[18] 3GPP, “Service accessibility,V9.1.0, Release 9.”

[19] 3GPP TS 25.467, “3rd Generation Partnership Project, Technical Specification Group Radio Access Network, UTRAN architecture for 3G Home Node B (HNB), Stage 2 (Release 11),” 2012.

[20] C.-C. Lin, K. Sandrasegaran, H. A. M. Ramli, R. Basukala, R. Patachaianand, L. Chen, and T. S. Afrin, “Optimization of handover algorithms in 3GPP long term evolution system,” in *Modeling, Simulation and Applied Optimization (ICMSAO), 2011 4th International Conference on*, 2011, pp. 1–5.

[21] Ericsson, “Long Term Evolution (LTE): an introduction,” *Access*, no. October, p. 19, 2007.

[22] D. Xenakis, N. Passas, L. Merakos, and C. Verikoukis, “Mobility management for femtocells in LTE-advanced: key aspects and survey of handover decision algorithms,” *IEEE Commun. Surv. Tutorials*, vol. 16, no. 1, pp. 64–91, 2014.

[23] 3Gpp, “Evolved Universal Terrestrial Radio Access (E-UTRA)and Evolved Universal Terrestrial Radio Access Network (E-UTRAN), Overall description, Stage 2 (Release 9),” 2010.

[24] M. Rahnema, “Power Control and Handover Procedures and Optimization,” *UMTS Netw. Planning, Optim. Inter-Operation with GSM*, pp. 137–157.

[25] Y. Lin, A. Pang, and H. C. Rao, “Impact of mobility on mobile telecommunications networks,” *Wirel. Commun. Mob. Comput.*, vol. 5, no. 7, pp. 713–732, 2005.

[26] 3GPP, “3rd Generation Partnership Project; Technical Specification Group Services and System Aspects;Vocabulary for 3GPP Specifications (Release

10),” 2011.

[27] B. Herman, N. Baldo, M. Miozzo, M. Requena, and J. Ferragut, “Extensions to LTE mobility functions for ns-3,” in *Proceedings of the 2014 Workshop on ns-3*, 2014, p. 2.

[28] E. Dahlman, S. Parkvall, J. Skold, and P. Beming, *3G evolution: HSPA and LTE for mobile broadband*. Academic press, 2010.

[29] A. K. Salkintzis, M. Hammer, I. Tanaka, and C. Wong, “Voice call handover mechanisms in next-generation 3GPP systems,” *IEEE Commun. Mag.*, vol. 47, no. 2, pp. 46–56, 2009.

[30] E. Seidel and E. Saad, “LTE Home Node Bs and its enhancements in Release 9,” *Nomor Res.*, pp. 1–5, 2010.

[31] J. Han and B. Wu, “Handover in the 3GPP long term evolution (LTE) systems,” in *Mobile Congress (GMC), 2010 Global*, 2010, pp. 1–6.

[32] X. Chu, D. López-Pérez, Y. Yang, and F. Gunnarsson, *Heterogeneous Cellular Networks: Theory, Simulation and Deployment*. Cambridge University Press, 2013.

[33] T. Jansen, I. Balan, J. Turk, I. Moerman, and T. Kurner, “Handover parameter optimization in LTE self-organizing networks,” in *Vehicular Technology Conference Fall (VTC 2010-Fall), 2010 IEEE 72nd*, 2010, pp. 1–5.

[34] P. Muñoz, R. Barco, and I. de la Bandera, “On the potential of handover parameter optimization for self-organizing networks,” *IEEE Trans. Veh. Technol.*, vol. 62, no. 5, pp. 1895–1905, 2013.

[35] Y. Lee, B. Shin, J. Lim, and D. Hong, “Effects of time-to-trigger parameter on

handover performance in SON-based LTE systems," in *Communications (APCC), 2010 16th Asia-Pacific Conference on*, 2010, pp. 492–496.

[36] D. López-Pérez, I. Guvenc, and X. Chu, "Theoretical analysis of handover failure and ping-pong rates for heterogeneous networks," in *Communications (ICC), 2012 IEEE International Conference on*, 2012, pp. 6774–6779.

[37] L. Tang, D. Wang, and Q. Chen, "An adaptive scaling scheme for TTT in small cell," 2013.

[38] G. Kollias, F. Adelantado, and C. Verikoukis, "The impact of inter-site distance and time-to-trigger on handover performance in LTE-A HetNets," in *Communications (ICC), 2015 IEEE International Conference on*, 2015, pp. 3969–3974.

[39] G. Kollias, F. Adelantado, J. Vardakas, and K. Ramantas, "Handover performance in LTE-A HetNets through inter-site distance differentiation," in *Computer Aided Modeling and Design of Communication Links and Networks (CAMAD), 2014 IEEE 19th International Workshop on*, 2014, pp. 280–284.

[40] J.-M. Moon and D.-H. Cho, "Efficient handoff algorithm for inbound mobility in hierarchical macro/femto cell networks," *IEEE Commun. Lett.*, vol. 13, no. 10, 2009.

[41] J.-M. Moon and D.-H. Cho, "Novel handoff decision algorithm in hierarchical macro/femto-cell networks," in *Wireless Communications and Networking Conference (WCNC), 2010 IEEE*, 2010, pp. 1–6.

[42] K. Alexandris, N. Sapountzis, N. Nikaein, and T. Spyropoulos, "Load-aware handover decision algorithm in next-generation HetNets," in *Wireless*

Communications and Networking Conference (WCNC), 2016 IEEE, 2016, pp. 1–6.

[43] P. Xu, X. Fang, R. He, and Z. Xiang, "An efficient handoff algorithm based on received signal strength and wireless transmission loss in hierarchical cell networks," *Telecommun. Syst.*, vol. 52, no. 1, pp. 317–325, 2013.

[44] D. López-Pérez, A. Ladányi, A. Juttner, and J. Zhang, "OFDMA femtocells: Intracell handover for interference and handover mitigation in two-tier networks," in *Wireless Communications and Networking Conference (WCNC), 2010 IEEE*, 2010, pp. 1–6.

[45] D. López-Pérez, A. Valcarce, Á. Ladányi, G. de la Roche, and J. Zhang, "Intracell handover for interference and handover mitigation in OFDMA two-tier macrocell-femtocell networks," *EURASIP J. Wirel. Commun. Netw.*, vol. 2010, no. 1, p. 142629, 2010.

[46] H. Kalbkhani, S. Yousefi, and M. G. Shayesteh, "Adaptive handover algorithm in heterogeneous femtocellular networks based on received signal strength and signal-to-interference-plus-noise ratio prediction," *IET Commun.*, vol. 8, no. 17, pp. 3061–3071, 2014.

[47] A. Ulvan, R. Bestak, and M. Ulvan, "The study of handover procedure in LTE-based femtocell network," in *Wireless and Mobile Networking Conference (WMNC), 2010 Third Joint IFIP*, 2010, pp. 1–6.

[48] A. Ulvan, R. Bestak, and M. Ulvan, "Handover procedure and decision strategy in LTE-based femtocell network," *Telecommun. Syst.*, vol. 52, no. 4, pp. 2733–2748, 2013.

[49] H. Zhang, W. Ma, W. Li, W. Zheng, X. Wen, and C. Jiang, "Signalling cost evaluation of handover management schemes in LTE-advanced femtocell," in *Vehicular Technology Conference (VTC Spring), 2011 IEEE 73rd*, 2011, pp. 1–5.

[50] S.-J. Wu, "Handover Strategy in HIP-based LTE Femtocells Networks with Hybrid Access Mode," in *Genetic and Evolutionary Computing (ICGEC), 2012 Sixth International Conference on*, 2012, pp. 571–576.

[51] R. D. Hegazy and O. A. Nasr, "A user behavior based handover optimization algorithm for LTE networks," in *Wireless Communications and Networking Conference (WCNC), 2015 IEEE*, 2015, pp. 1255–1260.

[52] M. Alhabo and L. Zhang, "Unnecessary handover minimization in two-tier heterogeneous networks," in *Wireless On-demand Network Systems and Services (WONS), 2017 13th Annual Conference on*, 2017, pp. 160–164.

[53] A. Kishida, Y. Morihiro, T. Asai, and Y. Okumura, "Cell selection scheme for handover reduction based on moving direction and velocity of UEs for 5G multi-layered radio access networks," in *Information Networking (ICOIN), 2018 International Conference on*, 2018, pp. 362–367.

[54] S. Kapoor, D. Grace, and T. Clarke, "A base station selection scheme for handover in a mobility-aware ultra-dense small cell urban vehicular environment," in *Personal, Indoor, and Mobile Radio Communications (PIMRC), 2017 IEEE 28th Annual International Symposium on*, 2017, pp. 1–5.

[55] T. Jansen, I. Balan, S. Stefanski, I. Moerman, and T. Kurner, "Weighted performance based handover parameter optimization in LTE," in *Vehicular*

Technology Conference (VTC Spring), 2011 IEEE 73rd, 2011, pp. 1–5.

[56] M. S. I. Khan, M. M. Rahman, K. Raahemifar, J. Misic, and V. B. Misic, "Self-optimizing control parameters for minimizing ping-pong handover in Long Term Evolution (LTE)," in *Communications (QBSC), 2014 27th Biennial Symposium on*, 2014, pp. 118–122.

[57] N. Hassan, K. Elkhazeen, K. Raahemiafar, and X. Fernando, "Optimization of control parameters using averaging of handover indicator and received power for minimizing ping-pong handover in LTE," in *Electrical and Computer Engineering (CCECE), 2015 IEEE 28th Canadian Conference on*, 2015, pp. 92–97.

[58] D.-W. Lee, G.-T. Gil, and D.-H. Kim, "A cost-based adaptive handover hysteresis scheme to minimize the handover failure rate in 3GPP LTE system," *EURASIP J. Wirel. Commun. Netw.*, vol. 2010, no. 1, p. 750173, 2010.

[59] P. Xu, X. Fang, J. Yang, and Y. Cui, "A User's State and SINR -Based Handoff Algorithm in Hierarchical Cell Networks," in *2010 6th International Conference on Wireless Communications Networking and Mobile Computing (WiCOM)*, 2010, pp. 1–4.

[60] M. Vondra and Z. Becvar, "Connection cost based handover decision for offloading macrocells by femtocells," in *International Conference on Wired/Wireless Internet Communications*, 2012, pp. 208–219.

[61] Z. Becvar and P. Mach, "Adaptive hysteresis margin for handover in femtocell networks," in *Wireless and Mobile Communications (ICWMC), 2010 6th International Conference on*, 2010, pp. 256–261.

[62] S. Lal and D. K. Panwar, "Coverage analysis of handoff algorithm with adaptive hysteresis margin," in *Information Technology,(ICIT 2007). 10th International Conference on*, 2007, pp. 133–138.

[63] G. Yang, X. Wang, and X. Chen, "Handover control for LTE femtocell networks," in *Electronics, Communications and Control (ICECC), 2011 International Conference on*, 2011, pp. 2670–2673.

[64] M. Z. Chowdhury, W. Ryu, E. Rhee, and Y. M. Jang, "Handover between macrocell and femtocell for UMTS based networks," in *Advanced Communication Technology, 2009. ICACT 2009. 11th International Conference on*, 2009, vol. 1, pp. 237–241.

[65] M. D. J. Alhabo, L. Zhang, and O. Oguejiofor, "Inbound Handover Interference-Based Margin for Load Balancing in Heterogeneous Networks," in *2017 International Symposium on Wireless Communication Systems (ISWCS)*, 2017.

[66] D. Xenakis, N. Passas, L. Merakos, and C. Verikoukis, "Energy-efficient and interference-aware handover decision for the LTE-Advanced femtocell network," in *Communications (ICC), 2013 IEEE International Conference on*, 2013, pp. 2464–2468.

[67] H. Zhang, C. Jiang, J. Cheng, and V. C. M. Leung, "Cooperative interference mitigation and handover management for heterogeneous cloud small cell networks," *IEEE Wirel. Commun.*, vol. 22, no. 3, pp. 92–99, 2015.

[68] A. D. Antoro, I. W. Mustika, and S. B. Wibowo, "Downlink cross-tier interference mitigation for macrocell user in open access femtocell using

handover scenario," in *Electrical Engineering and Informatics (ICEEI), 2015 International Conference on*, 2015, pp. 656–660.

[69] M. Boujelben, S. Ben Rejeb, and S. Tabbane, "A novel green handover self-optimization algorithm for LTE-A/5G HetNets," in *Wireless Communications and Mobile Computing Conference (IWCMC), 2015 International*, 2015, pp. 413–418.

[70] G. Araniti, J. Cosmas, A. Iera, A. Molinaro, A. Orsino, and P. Scopelliti, "Energy efficient handover algorithm for green radio networks," in *Broadband Multimedia Systems and Broadcasting (BMSB), 2014 IEEE International Symposium on*, 2014, pp. 1–6.

[71] D. Katsaros and Y. Manolopoulos, "Prediction in wireless networks by Markov chains," *IEEE Wirel. Commun.*, vol. 16, no. 2, 2009.

[72] C.-C. Huang, "Non-homogeneous Markov chains and their applications," 1977.

[73] H. Pishro-Nik, "Introduction to probability, statistics, and random processes," 2016.

[74] S. H. S. Ariffin, N. N. N. Abd, and N. E. Ghazali, "Mobility prediction via Markov model in LTE femtocell," *Int. J. Comput. Appl.*, vol. 65, no. 18, 2013.

[75] F. Guidolin, I. Pappalardo, A. Zanella, and M. Zorzi, "A Markov-based framework for handover optimization in HetNets," in *Ad Hoc Networking Workshop (MED-HOC-NET), 2014 13th Annual Mediterranean*, 2014, pp. 134–139.

[76] F. Guidolin, I. Pappalardo, A. Zanella, and M. Zorzi, "Context-aware handover policies in HetNets," *IEEE Trans. Wirel. Commun.*, vol. 15, no. 3, pp. 1895–

1906, 2016.

[77] J. G. Andrews, S. Buzzi, W. Choi, S. V Hanly, A. Lozano, A. C. K. Soong, and J. C. Zhang, "What will 5G be?," *IEEE J. Sel. areas Commun.*, vol. 32, no. 6, pp. 1065–1082, 2014.

[78] A. Gupta and R. K. Jha, "A survey of 5G network: Architecture and emerging technologies," *IEEE access*, vol. 3, pp. 1206–1232, 2015.

[79] J. Wu, Y. Zhang, M. Zukerman, and E. K.-N. Yung, "Energy-efficient base-stations sleep-mode techniques in green cellular networks: A survey," *IEEE Commun. Surv. tutorials*, vol. 17, no. 2, pp. 803–826, 2015.

[80] M. H. Alsharif, J. Kim, and J. H. Kim, "Green and sustainable cellular base stations: an overview and future research directions," *Energies*, vol. 10, no. 5, p. 587, 2017.

[81] C. Han, T. Harrold, S. Armour, I. Krikidis, S. Videv, P. M. Grant, H. Haas, J. S. Thompson, I. Ku, and C.-X. Wang, "Green radio: radio techniques to enable energy-efficient wireless networks," *IEEE Commun. Mag.*, vol. 49, no. 6, 2011.

[82] B. Zhang, W. Qi, and J. Zhang, "A Markov Based Performance Analysis of Handover and Load Balancing in HetNets," *Int. J. Commun. Netw. Syst. Sci.*, vol. 10, no. 10, p. 223, 2017.

[83] 3GPP, "Study on Small Cell Enhancements for E-UTRA and E-UTRAN–Higher layer aspects,3GPP TR 36.842," 2013.

[84] A. R. Jensen, M. Lauridsen, P. Mogensen, T. B. Sørensen, and P. Jensen, "LTE UE power consumption model: For system level energy and performance optimization," in *Vehicular Technology Conference (VTC Fall), 2012 IEEE*,

2012, pp. 1–5.

[85] B. Dusza, C. Ide, L. Cheng, and C. Wietfeld, “An accurate measurement-based power consumption model for LTE uplink transmissions,” in *Computer Communications Workshops (INFOCOM WKSHPS), 2013 IEEE Conference on*, 2013, pp. 49–50.

[86] M. Deruyck, W. Joseph, and L. Martens, “Power consumption model for macrocell and microcell base stations,” *Trans. Emerg. Telecommun. Technol.*, vol. 25, no. 3, pp. 320–333, 2014.

[87] M. Deruyck, W. Vereecken, W. Joseph, B. Lannoo, M. Pickavet, and L. Martens, “Reducing the power consumption in wireless access networks: Overview and recommendations,” *Prog. Electromagn. Res.*, vol. 132, pp. 255–274, 2012.

[88] M. Deruyck, D. De Vulder, W. Joseph, and L. Martens, “Modelling the power consumption in femtocell networks,” in *Wireless Communications and Networking Conference Workshops (WCNCW), 2012 IEEE*, 2012, pp. 30–35.

[89] G. Auer, V. Giannini, I. Gódor, P. Skillermark, M. Olsson, M. A. Imran, D. Sabella, M. J. Gonzalez, C. Desset, and O. Blume, “Cellular energy efficiency evaluation framework,” in *Vehicular Technology Conference (VTC Spring), 2011 IEEE 73rd*, 2011, pp. 1–6.

[90] I. Ashraf, L. T. W. Ho, and H. Claussen, “Improving energy efficiency of femtocell base stations via user activity detection,” in *Wireless Communications and Networking Conference (WCNC), 2010 IEEE*, 2010, pp. 1–5.

[91] K. Samdanis, P. Rost, A. Maeder, M. Meo, and C. Verikoukis, *Green Communications: Principles, Concepts and Practice*. John Wiley & Sons, 2015.

[92] D. Lopez-Perez, I. Guvenc, G. De la Roche, M. Kountouris, T. Q. S. Quek, and J. Zhang, "Enhanced intercell interference coordination challenges in heterogeneous networks," *IEEE Wirel. Commun.*, vol. 18, no. 3, 2011.

[93] J. Oh and Y. Han, "Cell selection for range expansion with almost blank subframe in heterogeneous networks," in *Personal Indoor and Mobile Radio Communications (PIMRC), 2012 IEEE 23rd International Symposium on*, 2012, pp. 653–657.

[94] K. Okino, T. Nakayama, C. Yamazaki, H. Sato, and Y. Kusano, "Pico cell range expansion with interference mitigation toward LTE-Advanced heterogeneous networks," in *Communications Workshops (ICC), 2011 IEEE International Conference on*, 2011, pp. 1–5.

[95] K. R. Krishnan and H. Luss, "Power selection for maximizing SINR in femtocells for specified SINR in macrocell," in *Wireless Communications and Networking Conference (WCNC), 2011 IEEE*, 2011, pp. 563–568.

[96] J. G. Andrews, S. Singh, Q. Ye, X. Lin, and H. S. Dhillon, "An overview of load balancing in HetNets: Old myths and open problems," *IEEE Wirel. Commun.*, vol. 21, no. 2, pp. 18–25, 2014.

[97] R. P. Ray and L. Tang, "Hysteresis Margin and Load Balancing for Handover in Heterogeneous Network," *Int. J. Futur. Comput. Commun.*, vol. 4, no. 4, p. 231, 2015.

[98] J. Kim, G. Lee, and H. P. In, "Adaptive time-to-trigger scheme for optimizing

LTE handover," *IEEE Wirel. Commun.*, vol. 7, no. 4, pp. 35–44, 2014.

[99] S. Karlin, *A first course in stochastic processes*. Academic press, 2014.

[100] I. N. M. Isa, M. D. Baba, A. L. Yusof, and R. Ab Rahman, "Handover parameter optimization for self-organizing LTE networks," in *Computer Applications & Industrial Electronics (ISCAIE), 2015 IEEE Symposium on*, 2015, pp. 1–6.

[101] M. Mehta, N. Akhtar, and A. Karandikar, "Impact of handover parameters on mobility performance in LTE HetNets," in *Communications (NCC), 2015 Twenty First National Conference on*, 2015, pp. 1–6.